ALFRED-WEGENER-INSTITUT
HELMHOLTZ-ZENTRUM FÜR POLAR- UND MEERESFORSCHUNG

803
2025

Berichte
zur Polar- und Meeresforschung
Reports on Polar and Marine Research

The Expedition PS148 of the Research Vessel POLARSTERN to the Arctic Ocean in 2025

Edited by

Jennifer Dannheim
with contributions of the participants

HELMHOLTZ

Die Berichte zur Polar- und Meeresforschung werden vom Alfred-Wegener-Institut, Helmholtz-Zentrum für Polar- und Meeresforschung (AWI) in Bremerhaven, Deutschland, in Fortsetzung der vormaligen Berichte zur Polarforschung herausgegeben. Sie erscheinen in unregelmäßiger Abfolge.

Die Berichte zur Polar- und Meeresforschung enthalten Darstellungen und Ergebnisse der vom AWI selbst oder mit seiner Unterstützung durchgeführten Forschungsarbeiten in den Polargebieten und in den Meeren.

Die Publikationen umfassen Expeditionsberichte der vom AWI betriebenen Schiffe, Flugzeuge und Stationen, Forschungsergebnisse (inkl. Dissertationen) des Instituts und des Archivs für deutsche Polarforschung, sowie Abstracts und Proceedings von nationalen und internationalen Tagungen und Workshops des AWI.

Die Beiträge geben nicht notwendigerweise die Auffassung des AWI wider.

Herausgeber
Dr. Horst Bornemann

Redaktionelle Bearbeitung und Layout
Susan Amir Sawadkuhi

Alfred-Wegener-Institut
Helmholtz-Zentrum für Polar- und Meeresforschung
Am Handelshafen 12
27570 Bremerhaven
Germany

www.awi.de
www.awi.de/reports

The Reports on Polar and Marine Research are issued by the Alfred Wegener Institute, Helmholtz Centre for Polar and Marine Research (AWI) in Bremerhaven, Germany, succeeding the former Reports on Polar Research. They are published at irregular intervals.

The Reports on Polar and Marine Research contain presentations and results of research activities in polar regions and in the seas either carried out by the AWI or with its support.

Publications comprise expedition reports of the ships, aircrafts, and stations operated by the AWI, research results (incl. dissertations) of the Institute and the Archiv für deutsche Polarforschung, as well as abstracts and proceedings of national and international conferences and workshops of the AWI.

The papers contained in the Reports do not necessarily reflect the opinion of the AWI.

Editor
Dr. Horst Bornemann

Editorial editing and layout
Susan Amir Sawadkuhi

Alfred-Wegener-Institut
Helmholtz-Zentrum für Polar- und Meeresforschung
Am Handelshafen 12
27570 Bremerhaven
Germany

www.awi.de
www.awi.de/en/reports

Titel: Meereis in der Framstrasse (Arktis) während der Polarsternexpedition PS148
(Foto: Jennifer Dannheim, AWI)

Cover: Sea ice in Fram Strait (Arctic) during the Polarstern expedition PS148
(Photo: Jennifer Dannheim, AWI)

The Expedition PS148 of the Research Vessel POLARSTERN to the Arctic Ocean in 2025

Edited by

Jennifer Dannheim
with contributions of the participants

Please cite or link this publication using the identifiers

https://epic.awi.de/id/eprint/60447
https://doi.org/10.57738/BzPM_0803_2025

ISSN 1866-3192

PS148

29 May 2025 – 29 June 2025

Bremerhaven – Tromsø

Chief scientist
Jennifer Dannheim

Coordinator
Ingo Schewe

Contents

1. ÜBERBLICK UND EXPEDITIONSVERLAUF

Jennifer Dannheim DE.AWI

Am Donnerstag, den 29. Mai 2025 verließ *Polarstern* Bremerhaven zur Expedition PS148, die sie in die Framstraße zwischen Grönland und Spitzbergen führte. Die 4-wöchige Expedition wurde genutzt, um Beiträge zu verschiedenen nationalen und internationalen Forschungs- und Infrastrukturprojekten (FRAM, MUSE, HiAOOS, EPOC und Arctic PASSION) sowie dem Forschungsprogramm „Changing Earth – Sustaining our Future" („Erde im Wandel – Unsere Zukunft nachhaltig gestalten") des AWI, zu leisten. Im Rahmen des Topic 6 "Marine and Polar Life: Sustaining Biodiversity, Biotic Interactions and Biogeochemical Functions" (Subtopics 6.1 "Future ecosystem functionality" und 6.3 "The future biological carbon pump") des Forschungsprogramms wurden die mit steigenden Wassertemperaturen und dem Rückgang des Meereises verbundenen Ökosystemverschiebungen im Pelagial und im tiefen Ozean ermittelt und quantifiziert sowie Rückkopplungsprozesse auf ozeanografische Prozesse untersucht. Diese Untersuchungen beinhalteten die Identifizierung räumlicher und zeitlicher Entwicklungen in der Funktion ausgewählter Plankton- und Benthos-Gemeinschaften. In Topic 2 (2.4 „Advanced research methodologies for tomorrow") werden fortgeschrittene Forschungsmethoden, einschließlich neuartiger In-situ- und Fernerkundungsbeobachtungssysteme, entwickelt und angewendet. Die Expedition wird die FRAM-Infrastruktur über die Durchführungsphase (2014–2023) hinaus erhalten und weiterentwickeln, einschließlich des LTER-Observatoriums HAUSGARTEN und des LTO WSC-Observatoriums als Teil des FRAM (Frontiers in Arctic marine Monitoring)-Ozeanbeobachtungssystems.

Die Arbeiten stellten einen weiteren Beitrag zur Sicherstellung der Langzeitbeobachtungen am LTER (Long-Term Ecological Research) Observatorium HAUSGARTEN dar, in denen der Einfluss von natürlichen und durch den Menschen verursachten Umweltveränderungen auf ein arktisches Tiefseeökosystem erfasst und dokumentiert wird. Die Zeitreihenuntersuchungen im HAUSGARTEN wurden an 21 Stationen entlang eines bathymetrischen und longitudinalen Gradienten über die Framstraße durchgeführt, darunter Stationen bis zu 5.500 m (Molloy Deep) und Stationen von der Nähe des Svalbard-Archipels bis zum nordöstlichen Grönlandschelf (Abb. 1.1). Diese Arbeiten wurden in enger Zusammenarbeit der HGF-MPG Brückengruppe für Tiefsee-Ökologie und -Technologie und der Arbeitsgruppe PEBCAO („Phytoplankton Ecology and Biogeochemistry in the Changing Arctic Ocean") des AWI durchgeführt. Desweiteren wurden auf dem Transit zwischen Island und dem Einsatzgebiet HAUSGARTEN wissenschaftliche Arbeiten an vier Stationen als Teil des Projektes AlonGATE (A Long-Term Observatory of the North Atlantic Gateway to the Arctic) durchgeführt, um den Einfluss der Umweltveränderungen auf die benthische Fauna im Zugangsbereich zur Arktis genauer zu untersuchen.

Die Expedition wurde darüber hinaus genutzt, um weitere Installationen im Rahmen der HGF Infrastrukturmaßnahme FRAM vorzunehmen. Das FRAM Ocean Observing System ermöglicht kontinuierliche Untersuchungen von der Meeresoberfläche bis in die Tiefsee und liefert zeitnah Daten zur Erdsystem-Dynamik sowie zu Klima- und Ökosystem-Veränderungen. Daten des Observatoriums werden zu einem besseren Verständnis der Veränderungen in der Ozeanzirkulation, den Wassermassen-Eigenschaften und des Meereisrückgangs sowie deren Auswirkungen auf das arktische, marine Ökosystem beitragen. FRAM führt Sensoren in Observationsplattformen zusammen, die sowohl die Registrierung von Ozeanvariablen, als

auch physiko-chemischer und biologischer Prozesse im Ozean erlauben. Experimentelle und Ereignis-gesteuerte Systeme ergänzen diese Beobachtungsplattformen. Produkte der Infrastruktur umfassen hochaufgelöste Langzeitdaten sowie Basisdaten für Modelle und die Fernerkundung.

Die wissenschaftlichen Arbeiten während der *Polarstern* Expedition PS148 wurden begünstigt durch die guten Wetter- und Eisbedingungen in der Framstraße. Aufgrund der Eisverhältnisse konnten sowohl die östlichen Stationen, aber auch die nördlichsten Stationen nach mehreren Jahren wieder beprobt werden. Dementsprechend konnten nicht nur alle geplanten Arbeiten im Einsatzgebiet mit vertikal eingesetztem, kabel-gebundenem Gerät weitgehend planmäßig durchgeführt werden. Ebenso konnten alle geplanten Verankerungen und Freifallsysteme wie geplant geborgen und wieder ausgesetzt werden. Desweiteren erlaubten die günstigen Wetter- und Eisbedingugnen auch den Einsatz von geschleppten Geräten (Epibenthosschlitten, Kamerasysteme) und den sicheren Einsatz des Autonomen Unterwasserfahrzeugs PAUL (Autonomous Underwater Vehicle, AUV) der Tiefseegruppe des AWI. Leider kam es auf der Expedition zu großen Zeitverzögerungen im wissenschaftlichen Ablauf durch diverse defekte Winden, die nur duch den unermüdlichen Einsatz der Schiffsbesatzung weitestgehend minimiert werden konnte. Trotzdem sind wir mit dem Erreichten insgesamt sehr zufrieden. So konnte u.a. ein sehr komplexes und teures Großgerät der Tiefseegruppe des AWI, ein Meeresboden-Kettenfahrzeug (Benthic Crawler), das auf der Polarstern Expedition PS143/1 im Sommer 2024 ausgebracht wurde, während der PS148 erfolgreich geborgen werden. Die *Polarstern* Expedition PS148 endete am Sonntag, den 29. Juni 2025 in Tromsø, Norwegen (Abb. 1.1).

SUMMARY AND ITINERARY

On Thursday 29 May 2025, *Polarstern* left Bremerhaven for the expedition PS148, which took her to the Fram Strait between Greenland and Svalbard. The four-week expedition was used to contribute to various national and international research and infrastructure projects (FRAM, MUSE, HiAOOS, EPOC and Arctic PASSION) as well as the AWI's research programme ‘Changing Earth - Sustaining our Future’. As part of Topic 6 ‘Marine and Polar Life: Sustaining Biodiversity, Biotic Interactions and Biogeochemical Functions’ (Subtopics 6.1 ‘Future ecosystem functionality’ and 6.3 ‘The future biological carbon pump’) of the research programme, the ecosystem shifts in the pelagic and deep ocean associated with rising water temperatures and the retreat of sea ice were determined and quantified, and feedback processes on oceanographic processes were investigated. These investigations included the identification of spatial and temporal developments in the function of selected plankton and benthic communities. In Topic 2 (2.4 ‘Advanced research methodologies for tomorrow’), advanced research methods, including novel in-situ and remote sensing observation systems, are developed and applied. The expedition will maintain and further develop the FRAM infrastructure beyond the implementation phase (2014–2023), including the LTER observatory HAUSGARTEN and the LTO WSC observatory as part of the FRAM (Frontiers in Arctic marine Monitoring) ocean observing system.

The work represented a further contribution to securing the long-term observations at the HAUSGARTEN LTER (Long-Term Ecological Research) observatory, in which the influence of natural and human-induced environmental changes on an Arctic deep-sea ecosystem is recorded and documented. The time series studies in HAUSGARTEN were carried out at 21

stations along a bathymetric and longitudinal gradient across the Fram Strait, including stations up to 5,500 m (Molloy Deep) and stations from the vicinity of the Svalbard Archipelago to the north-eastern Greenland Shelf (Fig. 1.1). This work was carried out in close co-operation between the HGF-MPG Bridge Group for Deep-Sea Ecology and Technology and the PEBCAO (‘Phytoplankton Ecology and Biogeochemistry in the Changing Arctic Ocean’) working group at the AWI. In addition, scientific work was carried out at four stations during the transit between Iceland and the HAUSGARTEN deployment area as part of the AlonGATE project (A Long-Term Observatory of the North Atlantic Gateway to the Arctic) in order to investigate the influence of environmental changes on the benthic fauna in the access area to the Arctic in more detail.

The expedition was also used to carry out further installations as part of the HGF's FRAM infrastructure programme. The FRAM Ocean Observing System enables continuous investigations from the sea surface to the deep sea and provides timely data on Earth system dynamics as well as climate and ecosystem changes. Data from the observatory will contribute to a better understanding of changes in ocean circulation, water mass properties and sea ice retreat and their impact on the Arctic marine ecosystem. FRAM brings together sensors in observation platforms that allow the recording of ocean variables as well as physico-chemical and biological processes in the ocean. Experimental and event-driven systems complement these observation platforms. Products of the infrastructure include high-resolution long-term data as well as basic data for modelling and remote sensing.

The scientific work during the *Polarstern* expedition PS148 was favoured by the good weather and ice conditions in the Fram Strait. The ice conditions meant that the eastern stations but particularly the northernmost stations could be sampled again after several years. Accordingly, it was not only possible to carry out all planned work in the deployment area with vertically deployed, cable-bound equipment largely according to plan. All planned moorings and free-fall systems were also recovered and deployed as planned. Furthermore, the favourable weather and ice conditions also allowed the use of towed equipment (epibenthic sleds, camera systems) and the safe deployment of the Autonomous Underwater Vehicle (AUV) of the AWI's deep-sea group. Unfortunately, there were major delays in the scientific process during the expedition due to various defective winches, which could only be minimised as far as possible thanks to the tireless efforts of the ship's crew. Nevertheless, we are very satisfied with what we achieved overall. For example, a very complex and expensive piece of large-scale equipment from the AWI's deep-sea group, a benthic crawler, which was deployed on *Polarstern* Expedition PS143/1 in the summer of 2024, was successfully recovered during PS148. *Polarstern* Expedition PS148 ended on Sunday 29 June 2025 in Tromsø, Norway (Fig. 1.1).

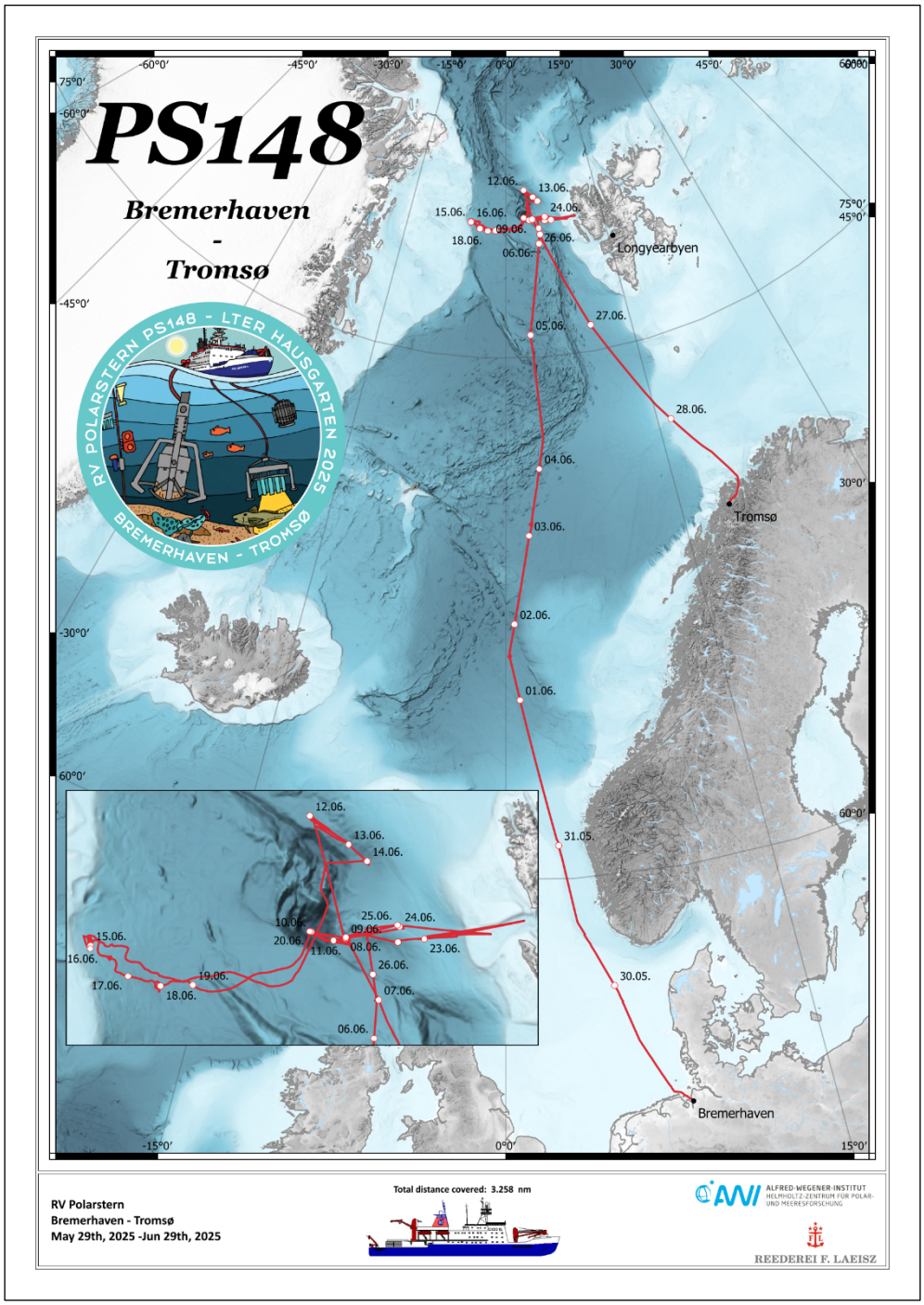

Abb. 1.1: Fahrtverlauf der Expedition PS148 von Bremerhaven nach Tromsø. Siehe https://doi.pangaea.de/10.1594/PANGAEA.984143 für eine Darstellung des Master tracks in Verbindung mit derStationsliste für PS148.

Fig. 1.1: Cruise tack of expedition PS148 from Bremerhaven to Tromsø. See https://doi.pangaea.de/10.1594/PANGAEA.984143 to display the master track in conjunction with the station list for PS148.

WEATHER CONDITIONS DURING PS148

Robert Hausen DE.DWD

Transit (29.05.-08.06.)

The first week of the expedition and thus the period of transit from Bremerhaven to the target area 'Hausgarten' was characterized by unusually calm weather conditions. Although we were hit by the passage of an occluded frontal system with strong winds from the south of Beaufort 6 in average on the 29th of May the limited factor of the relatively short fetch in the German Bight prevented us from higher waves. Afterwards weak lows and short periods of high pressure influence alternated day by day. On Saturday, the 31st of May, we seized the preferable conditions of a high-pressure phase with only few to scattered cumulus clouds with bases at around 1,500 FT above the ground for 2 hours lasting test flights in the northern parts of the North Sea. The only time the conditions were similarly good (sunny and calm) was on Tuesday, the 03rd of June, when we had station work (ALONGate) at close to 70N and 2E. Before that, however, we had to deal with a small, but nasty secondary low developing near the occlusion point and leading to strong winds with Bft 7 in average from the Northeast, later shifting towards Northwest for several hours. In gusts the threshold of Bft 9, which means winds speeds of around 80 km/h, was temporarily exceeded. Luckily, as that strong wind field only covered a small area, significant wave heights remained limited with values close to 3 meters (mainly windsea driven) – the preliminary maximum so far.

The weather along the rest of our route to the 'Hausgarten' was characterized by a large and for the summer season rather intense storm with a center pressure near 970 hPa in the sea area between Iceland and Scotland. Located on its northern flank, humid and cool airmasses were advected with a moderate northeasterly flow with forces of 5 to 6 Bft and a swell of around 2 m. As we approached our final destination, water temperatures dropped below 5°C, generating the first dense fog patches in the course of Thursday, the 05th of June. Additionally, on the edge of a low southeast of Svalbard a backbent occlusion produced the first snowfall of our cruise in the morning hours of Saturday, the 07th of June. The precipitation turned to rain as the winds shifted from northwest to east during the afternoon.

Science part I (09.06.-15.06.)

As soon as the science program started, the weather conditions in the forecast area were mainly influenced by weak low-pressure systems, leading to moderate winds from prevailing southeasterly directions, and a moist boundary layer. Essentially, the advected dewpoints were higher than the predominant water temperatures. That's why we suffered due to longer persisting low stratus clouds with bases of only a few hundred feet above the ground and partly foggy conditions during that time. Repeatedly, the visibility dropped below 100 m after short periods of improvement. In other words: These are the weather conditions which the HAUSGARTEN is notorious for. Luckily, no flight activity was planned in the open water region, it would not have been weather permitting anyway. However, the southeasterly winds led to a crucial advantage: Station N5 near 80N 3E appeared free of ice in the remote sensing images and therefore was moved forward in the schedule. An ice exploration operation with the helicopter was not necessary, which was favorable since the conditions were marginal in terms

of ceiling and visibility. On our return to the ice edge two days later, the weather conditions were much more preferable for flying and finding a suitable flow for ice coring. There were only a few showers in the vicinity, and the cloud ceiling was around 3,000 ft above ground level (AGL). This allowed us to find a suitable ice flow for coring only 15 nautical miles away from the vessel on the evening of Friday, the 13th of June. Also worth mentioning was the incoming swell from the south on Saturday, 14 June, induced by a storm depression near Jan Mayen, which caused slight disturbances to the research activities despite a height of only 2 metres due to the cross-sea character and the longer period of around 9 seconds.

Science part II (16.06.-24.06.)

In the next phase, the most western stations EG-I to EG-IV followed in a partly compact, partly loose sea ice environment. In the meantime, the upper troposphere was characterized by a massive omega pattern, with the ridge's axis spreading from Scandinavia north-westwards up to eastern parts of Greenland. As a consequence, the forecast area remained in an environment of weak pressure gradients without significant synoptic-scale forcings. Besides that, the surface pressure level was rather high, around 1015 hPa, and the weather was produced locally due to mesoscale effects. Hence, we observed the typical variations of the cloud bases above a mixture of ice and open water, combined with occasional snow showers, which reduced the visibility close to fog levels. However, the prevailing conditions, with ceilings around 1,000 FT AGL upwards and visibilities of more than 10 kilometers were surprisingly favorable. Thus, these conditions allowed for short distance flights in the proximity of the ship on four days in a row for a few hours each between the 15th and 18th of June. The only restriction occurred when the helicopter tried to land safely on a flow, but a rather high amount of loose, dry snow coverage in combination with poor contrasts required several landing approaches.

Luckily, the nearly overcast sky during that time prevented us from instant fog surprises. On the contrary, we had a great timing with clearing skies, as we left the ice on Corpus Christi, the 19th of June. However, our good fortune ended immediately when we steamed back to the central part of the HAUSGARTEN, where foggy conditions returned due to water temperature fluctuations of 4°C within only a few nautical miles. Sustainable weather improvement followed on our way towards Svalbard. Water temperatures remained stable above 5°C in the North Atlantic current and dewpoints with slight negative values 'rewarded' us with scattered clouds with high bases of around 2,000 FT. The winds remained largely weak from a mostly north-westerly direction throughout this period.

Return to Tromsø (25.06.-29.06.)

During the last week of our cruise, we experienced slightly unsettled conditions with some passing showers caused by small-scale low-pressure systems from time to time. In general, the weather parameters were still quite comfortable with weak winds, calm sea and good visibility. A last return to the ice edge increased the risk of some fog patches at Station HG-IV in the night of Wednesday, 25th of June, in a smooth westerly flow. However, some benches of fog remained far away to the northwest. Afterwards, a high-pressure system south of the forecast area near Jan Mayen intensified as a consequence of compensative descending and started to move towards the northeast while further strengthening. Hence, the weather situation gained some 'structure' back, as moderate southerly winds set in. In interaction with a complex low, reaching from Iceland via the Norwegian Sea to the Bay of Bothnia, a strong wind field between both systems covered our transect area. Winds picked up, reaching average speeds of around 25 knots (Bft 6), accompanied by maximum significant wave heights close to 3 meters. Overall, the journey ended with conditions similar to those at the beginning. As a final conclusion, the weather conditions during PS148 were unusually favorable and calm, without any big storms or persisting fog like the year before.

2. LTER HAUSGARTEN: IMPACT OF CLIMATE CHANGE ON ARCTIC MARINE ECOSYSTEMS

Christiane Hasemann[1], Jakob Barz[1], Christina Bienhold[1], Stine Bucholz[1], Michael Busack[1], Miriam Claver[3], Jennifer Dannheim[1], Nils Handelmann[1], Ulrich Hoge[1], Katharina Kohlenbach[1], Sascha Lehmenhecker[1], Johannes Markus[2], Normen Lochthofen[1], Janine Ludszuweit[1], Autun Purser[1], Sonja Rückert[2], Ingo Schewe*[1]

not on board: Christopher Krämmer[1], Lilian Boehringer[1], Lucas Arnold[2]

*ingo.schewe@awi.de

[1]DE.AWI

[2]DE.Uni-DUE

[3]DE.UNI-Oldenburg

Grant-No. AWI_PS148_01

Outlines

The establishment of HAUSGARTEN by the Alfred Wegener Institute Helmholtz Centre for Polar and Marine Research (AWI) in 1999 was motivated by the need to study the Arctic marine ecosystem as an interconnected whole — from the dynamics of sea-ice cover and pelagic processes to the functioning of deep-sea communities. The observatory was conceived as a long-term observatory to investigate how physical forcing, biogeochemical fluxes, and ecological interactions are linked across oceanic compartments (Soltwedel et al. 2005; Soltwedel et al. 2016). Within this framework, the benthic realm plays a particularly informative role: its communities are comparatively immobile and long-lived, and thus provide an integrative signal of environmental variability, including shifts in organic carbon flux to the seafloor (Gage and Tyler 1991; Piepenburg 2005).

Over geological timescales, the marine Arctic has been a decisive arena in shaping Earth's climate and biological evolution, exerting profound influence for more than 130 million years. Today, it remains central to the functioning of the global system. Yet, the region is undergoing rapid change: reductions in sea-ice cover and thickness, shifts in water mass temperature and salinity, altered nutrient pathways, and mounting pollution pressures have been widely documented (Bergmann et al. 2022). Arctic life, long adapted to extreme seasonality, now faces an intensity of climatic forcing that threatens the resilience of entire populations and ecosystems. The cumulative weight of these stressors may exceed ecological thresholds, precipitating the collapse of subsystems.

The observatory, situated in the eastern Fram Strait, comprises 21 fixed sampling stations along both a bathymetric transect (250–5,500 m) and a latitudinal transect at the 2,500 m isobath. Since its inception, HAUSGARTEN has supported interdisciplinary investigations spanning the sea-ice domain, pelagic food webs, and benthic processes. Research strategies include repeated sampling, the deployment of moorings, and the operation of both stationary and mobile autonomous platforms such as bottom landers and benthic crawlers. In addition, towed photographic and video systems have been employed to document habitat structures and monitor the distribution of epibenthic megafauna across space and time.

The physical landscape of the Fram Strait adds considerable complexity to benthic ecology. Features such as canyons, ridges, moraines, troughs, banks, and pockmarks create a high degree of habitat heterogeneity. According to the habitat-diversity hypothesis, such structural complexity is expected to enhance biodiversity, abundance, and biomass (Whittaker et al. 2001; Tews et al. 2004). Recent advances in survey techniques—most notably the deployment of side-scan sonar systems (Purser et al. 2019)—have revealed pronounced fine-scale topographic variability at HAUSGARTEN (Schulz et al. 2010; Taylor et al. 2016; Purser 2020). Long-term stations, however, do not yet fully capture these spatial gradients, and current expeditions (e.g. POLARSTERN PS148) are designed to address this shortcoming.

Furthermore, long-term image series have demonstrated an alarming rise in marine debris: between 2004 and 2017, plastic litter increased sevenfold in the region (Parga Martínez et al. 2020). Consequently, a dedicated pollution observatory has been incorporated within HAUSGARTEN, uncovering particularly high levels of microplastics in sediments (Tekman et al. 2020).

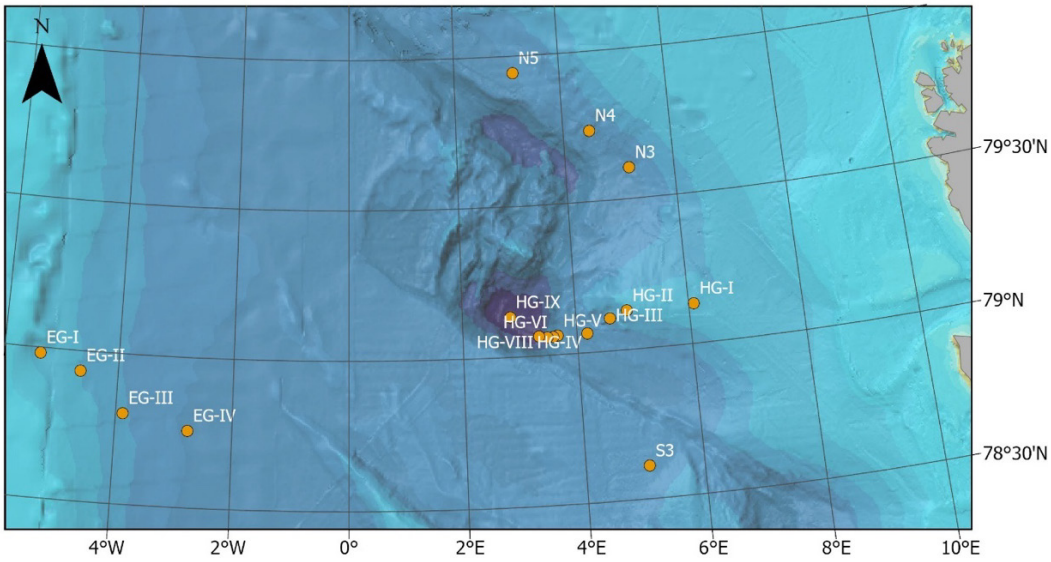

Fig. 2.1: Permanent sampling sites of the LTER (Long-Term Ecological Research) observatory HAUSGARTEN in Fram Strait, Arctic Ocean

Objectives

The central objective of current and future HAUSGARTEN investigations is to elucidate the interactions between Arctic climate change, biodiversity, and ecosystem functioning. Specifically, these studies aim to:

1. **Assess environmental drivers of biodiversity.** By integrating spatial and temporal data across contrasting benthic habitats, research seeks to determine how habitat heterogeneity and organic fluxes govern the structure and resilience of benthic communities.
2. **Quantify the influence of sea-ice dynamics on carbon cycling**. Central to this is the question of how sea-ice cover modulates primary production and the subsequent export of organic matter to the deep sea. Measurements of benthic oxygen fluxes—ranging from annual observations with landers to high-frequency recordings by benthic crawlers—will serve as critical indicators of benthic carbon mineralisation and biological pump efficiency.

3. **Monitor and evaluate anthropogenic impacts.** By incorporating long-term assessments of plastic pollution, including micro- and nanoplastics in sediments and benthic organisms, HAUSGARTEN research will quantify both exposure pathways and biological uptake of pollutants.

Through these combined approaches, HAUSGARTEN aspires to provide an integrated understanding of the ecological consequences of ongoing Arctic transformations, thereby contributing essential knowledge to global assessments of ocean change.

Work at sea

Meiobenthos and biogenic sediment compounds

Virtually undisturbed sediment samples were collected using a multiple corer (MUC; Fig. 2.2). In total, 16 MUC deployments were conducted at 16 HAUSGARTEN stations (Tab. 2.1) to obtain sediments for meiofauna investigations, with a particular focus on nematode communities. The uppermost five centimetres of the recovered sediment cores were sub-sampled to analyse bacterial abundance and biomass, meiofauna densities, as well as nematode diversity patterns and biomass.

Additional subsamples were taken to investigate parameters related to organic matter input to the seafloor, sediment-bound biomass, and benthic activity. Chloroplastic pigments (chlorophyll *a* and its degradation products), which serve as indicators of phytodetritus deposition and represent a key food source for benthic organisms, were analysed fluorometrically due to the high sensitivity of this method. Sediment-bound chloroplastic pigments (chlorophyll a and its degradation products) represent a suitable indicator for the input of phytoplanktonic detritus to the seafloor, representing the major food source for benthic organisms. They can be analysed with high sensitivity by fluorometric methods. To estimate the potential heterotrophic activity of bacteria, we measured cleaving rates of extracellular enzymes using the model-substrate FDA (fluorescein-di-acetate) in incubation experiments. Results will help to describe ecosystem changes in the benthal of the Arctic Ocean. Bacterial activities and chloroplastic pigments were analysed on board. All other sub-samples were stored for later analyses of the meiobenthic fauna and various biochemical bulk parameters at the home lab.

A subset of MUC sediment samples from all HAUSGARTEN stations was preserved at -20°C for further molecular analyses in the home laboratory, i.e. microbial DNA extraction and community analyses. In addition, live deep-sea sediments from the central station HG-IV were stored at 4°C to support an annual student experiment of the International Max Planck Research School MarMic at the Max Planck Institute for Marine Microbiology. As part of the FRAM Molecular Observatory, benthic microbiological sampling links to the annual and year-round sampling in the water column (Chapter 3; PEBCAO), in order to assess pelagic-benthic coupling.

To study the potential diversity of protists associated with the megabenthic organisms, additional samples were taken from the MUC: 1) The upper 2 cm of two cores retrieved by the MUC at each station were sieved through a 125 µm sieve and then fixed in EtOH and Histofix (one sample each). These will be analysed for meio- and macrofauna. Once sorted, collected invertebrates will be dissected to isolate parasitic protists, e.g. gregarine apicomplexans. 2) Small samples of sediment (one duplicate, one triplicate sample) from the middle of each of the two cores were fixed in RNA/DNA Shield for amplicon sequencing to identify any parasitic protists present in the benthos that could not be detected by dissections. 3) The supernatant (1.5 liter) of one core at each station was filtered through a 0.8-µm PES filters (Sylphium) for later DNA extraction and amplicon sequencing to identify potential traces of parasitic protists.

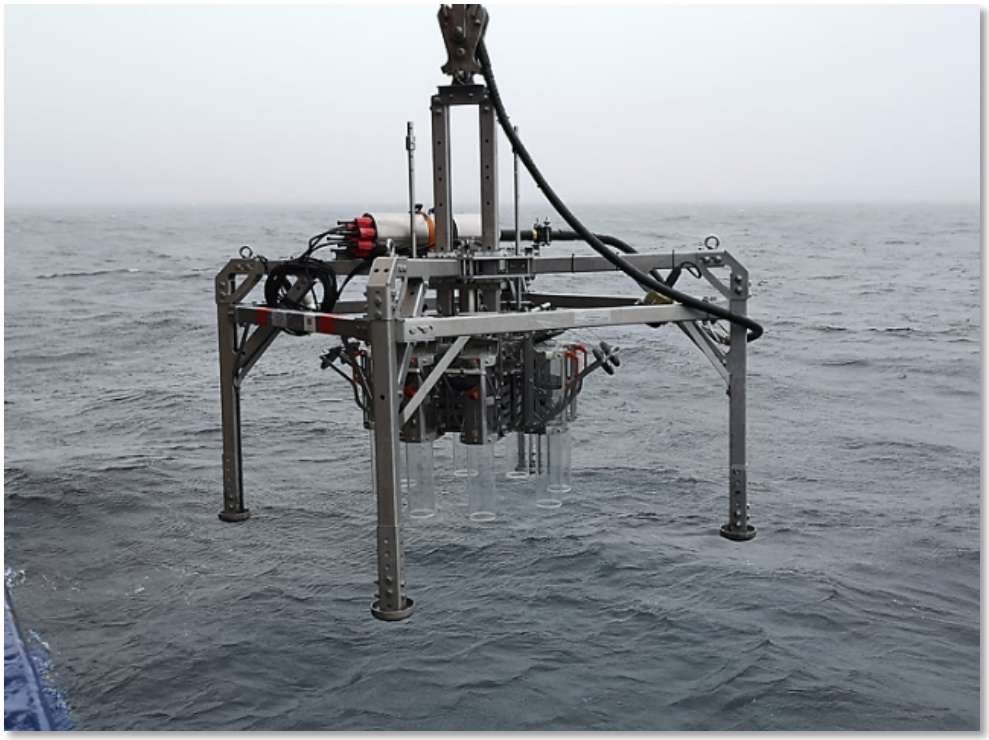

Fig. 2.2: Deployment of Multiple Corer (MUC) during expedition PS148

Tab. 2.1: HAUSGARTEN stations sampled during expedition PS148, including station ID, date, geographic position, and water depth [m]. Sampling was conducted using a multiple corer (MUC) and various types of box corers (BC). BC (MB): box corer samples for macrobenthic organisms, BC (P): for parasite studies, BC (f): failed box corer deployment.

Station	Station ID	Date	Depth [m]	Latitude	Longitude	Gear
HG-I	PS148_35-7	25.06.2025	1239.0	79° 07.983' N	006° 05.416' E	BC (MB)
HG-I	PS148_35-8	26.06.2025	1241.2	79° 08.043' N	006° 05.565' E	MUC
HG-I	PS148_35-9	26.06.2025	1242.9	79° 08.041' N	006° 05.788' E	BC (P)
HG-II	PS148_36-5	26.06.2025	1508.3	79° 07.794' N	004° 54.111' E	BC (MB)
HG-II	PS148_36-6	26.06.2025	1507.5	79° 07.792' N	004° 54.212' E	MUC
HG-II	PS148_36-7	26.06.2025	1510.2	79° 07.787' N	004° 54.136' E	BC (P)
HG-III	PS148_26-1	21.06.2025	1860.9	79° 06.504' N	004° 35.795' E	BC (MB)
HG-III	PS148_26-2	21.06.2025	1861.3	79° 06.506' N	004° 35.855' E	MUC
HG-III	PS148_26-3	22.06.2025	1861.2	79° 06.511' N	004° 35.866' E	BC (P)
HG-IV	PS148_6-15	08.06.2025	2405.9	79° 03.891' N	004° 10.958' E	BC (MB)
HG-IV	PS148_6-16	08.06.2025	2405.0	79° 03.886' N	004° 10.965' E	MUC
HG-IV	PS148_6-17	08.06.2025	2404.4	79° 03.895' N	004° 10.886' E	BC (P)
HG-V	PS148_24-1	20.06.2025	3103.1	79° 03.833' N	003° 39.497' E	BC (MB)
HG-V	PS148_24-2	20.06.2025	3079.2	79° 03.853' N	003° 39.768' E	MUC
HG-VI	PS148_23-5	20.06.2025	3486.9	79° 03.597' N	003° 34.812' E	MUC
HG-VII	PS148_11-5	11.06.2025	4025.0	79° 03.643' N	003° 28.587' E	MUC
HG-VII	PS148_11-6	11.06.2025	4035.0	79° 03.651' N	003° 28.577' E	BC (P)
HG-IX	PS148_9-9	10.06.2025	5544.3	79° 07.990' N	002° 50.661' E	MUC
HG-IX	PS148_9-10	10.06.2025	5545.7	79° 08.004' N	002° 50.540' E	BC (MB)

Station	Station ID	Date	Depth [m]	Latitude	Longitude	Gear
EG-I	PS148_17-9	15.06.2025	1004.3	79° 00.418' N	005° 24.911' W	BC (MB)
EG-I	PS148_17-10	15.06.2025	979.1	79° 00.802' N	005° 27.536' W	MUC
EG-I	PS148_17-12	16.06.2025	995.9	79° 01.522' N	005° 27.065' W	BC (P)
EG-II	PS148_19-8	17.06.2025	1483.7	78° 55.895' N	004° 40.269' W	MUC
EG-III	PS148_20-6	17.06.2025	1936.7	78° 48.182' N	003° 53.333' W	BC (MB)
EG-III	PS148_20-7	17.06.2025	1935.2	78° 48.203' N	003° 53.448' W	MUC
EG-III	PS148_20-8	17.06.2025	1932.3	78° 48.195' N	003° 53.701' W	BC (P)
EG-IV	PS148_21-9	18.06.2025	2563.2	78° 44.816' N	002° 45.327' W	BC (MB)
EG-IV	PS148_21-10	18.06.2025	2558.7	78° 44.717' N	002° 46.938' W	MUC
EG-IV	PS148_21-11	18.06.2025	2563.4	78° 45.063' N	002° 44.015' W	BC (P)
N5	PS148_13-8	12.06.2025	2501.5	79° 56.673' N	003° 07.138' E	BC (MB)
N5	PS148_13-9	12.06.2025	2500.7	79° 56.667' N	003° 07.196' E	MUC
N5	PS148_13-10	12.06.2025	2504.4	79° 56.741' N	003° 07.280' E	BC (P)
N4	PS148_14-11	13.06.2025	2700.3	79° 44.071' N	004° 30.052' E	MUC
N3	PS148_16-6	14.06.2025	2727.7	79° 36.243' N	005° 10.344' E	BC (f)
N3	PS148_16-7	14.06.2025	2725.9	79° 36.198' N	005° 10.527' E	MUC
S3	PS148_5-9	07.06.2025	2278.8	78° 36.619' N	005° 03.935' E	BC (MB)
S3	PS148_5-10	07.06.2025	2278.0	78° 36.582' N	005° 04.023' E	MUC
S3	PS148_5-11	07.06.2025	2277.8	78° 36.620' N	005° 03.989' E	BC (P)

Macrobenthos and parasites

We were able to take a total of 21 box corer samples at 12 sites successfully (11 for macrobenthos and 10 for parasites, Tab. 2.1). The box corer deployment at HAUSGARTEN station N3 failed due to the swell. At HG-VII the box corer did not close properly due to uneven seafloor and thus was partially washed out when setting down on deck. The remainder of this sample was sieved but was only used for the parasite samples.

Macrobenthic samples were obtained with an USNEL box corer (0.25 m²; Fig. 2.3), the preferred sampling gear in deep waters, as it provides reliably deep and relatively undisturbed sediment samples adequate for macrofauna sampling. The samples allow a continuation of the longterm series along depth gradients from the top to deeper adjacent areas and a comparison between samples of ice-free zones and stations covered mainly by ice throughout most of the year.

Box-corer samples were divided into eight equal subsamples. The upper 12 cm of each subsample sediment and the supernatant seawater to catch epibenthic animals from the fluffy layer on top of the sediment, were taken for further sample processing. Quantitative and qualitative samples were sifted over a 500 µm mesh size sieve and sieve residues were preserved in 4% buffered formalin for microbenthic organisms. In the laboratory at AWI, species will be determined to the lowest possible taxonomic level, counted and wet weights per species will be determined. For the parasites four subsamples were preserved with Histofix and four subsamples with 70% EtOH. In the labs at UDE samples will be sorted, macrobenthic species determined to the lowest possible taxonomic level and then dissected to isolate, identify and potentially describe parasites.

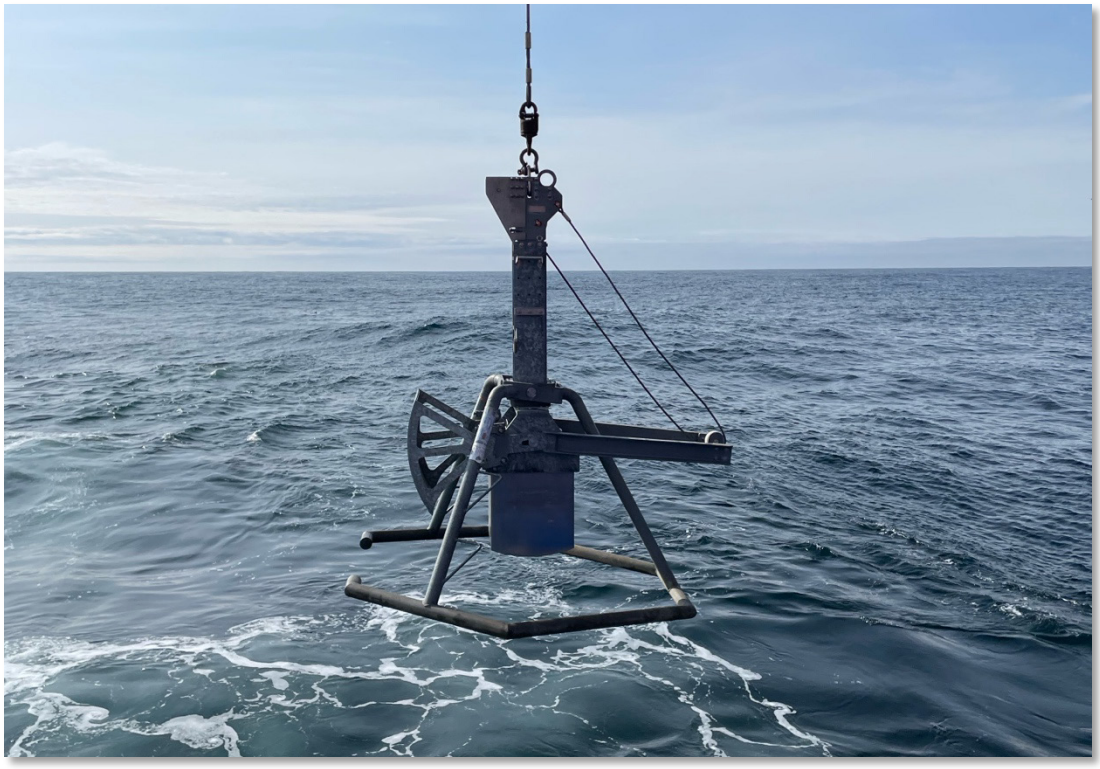

Fig. 2.3: Deployment of USNEL box corer (BC) during expedition PS148

Seafloor imaging – Ocean Floor Observation and Bathymetry System (OFOBS)

During PS148 ten successful deployments of the Ocean Floor Observation and Bathymetry System (OFOBS) were made (Tab. 2.2). During this expedition 2x 12 l water sampling Nisken bottles were additionally mounted on the OFOBS frame, and bottom water was collected from 1 m above the seafloor during the last 15 minutes of each deployment, for vcarious analyses by onship partners. Water samples were retrieved at full depths at OFOBS stations PS148_2-4, PS148_16-1, PS148_21-13, PS148_22-2, PS148_25-1, PS148_32-2, PS148_37-1. Water was filtered on 0.2 µm Sterivex filters and stored at -20°C for later eDNA analyses. With the samples we will be able to complement data from the Molecular Observatory (Chapter 3; PEBCAO), as well as observations of larger organisms at these depths.

In addition, new instrumentation for the recovery of water samples for eDNA analyses was tested on the OFOBS. The Robotic Cartridge Sampling Instrument (RoCSI, McLane) was deployed and tested during OFOBS dives PS148_2-4 and PS148_15-1. Only during the first dive, 5 samples were recovered.

Two of the deployments (PS148_25-3 and PS148_33-1) were to aid in the recovery of the Crawler, which had failed to return to the surface on command. These two dives collected only poor seafloor image data, and during which the OFOBS miniROV was deployed to attempt to connect a recovery rope to the crawler. Technical problems with the fibre LWL cable resulted in the abortion of deployment PS148_5-13 before the OFOBS reached the seafloor.

Tab. 2.2: HAUSGARTEN OFOBS deployments made during expedition PS148, including station ID, date, geographic position of start and end of transects, water depth [m], and number of images (hotkey and timer).

Station ID	Date / time (UTC)	Depth [m]	Latitude	Longitude	Seafloor Image number
PS148_2-4 start	03.06.2025 10:25	3226	69° 48.194' N	001° 56.997' E	11/560
PS148_2-4 end	03.06.2025 13:00	3229	69° 49.571' N	001° 57.99' E	11/560
PS148_5-13	07/06/2025 11:35 – 15:16	NA	78° 36.930' N	001° 57.661' E	Technical problems
PS148_15-1 start	13.06.2025 17:42	2546	79° 59.289' N	003° 04.017' E	51/392
PS148_15-1 end	13.06.2025 21:01	2498	79° 56.337' N	003° 09.288' E	
PS148_16-1 start	14.06.2025 01:55	2729	79° 36.220' N	005° 10.141' E	39/485
PS148_16-1 end	14.06.2025 05:50	2607	79°34.687' N	005° 14.214' E	
PS148_21-13 start	18.06.2025 19:21	1860.9	78° 45.401' N	002° 45.405' E	102/747
PS148_21-13 end	19.06.2025 01:43	2560	78° 42.847' N	002° 46.369' E	
PS148_22-2 start	19.06.2025 21:09	5331	79° 06.291' N	003° 16.316' E	150/710
PS148_22-2 end	20.06.2025 03:15	4494	79° 05.620' N	003° 26.258' E	
PS148_25-1 start	08.06.2025	2405	79° 03.886' N	004° 10.965' E	61/524
PS148_25-1 end	08.06.2025	2404.4	79° 03.895' N	004° 10.886' E	
PS148_25-3 start	21.06.2025 14:14	2437	79° 04.682' N	004° 06.748' E	325 high images – recovery tow
PS148_25-3 end	21.06.2025 17:07	2446	79° 04.644' N	004° 06.182' E	
PS148_32-2 start	24.06.2025 09:06	1240	79° 07.870' N	006° 06.034' E	45/550
PS148_32-2 end	24.06.2025 12:26	1230	79° 07.042' N	006° 10.231' E	
PS148_33-1 start	24.06.2025 19:03	2445	79° 04.642' N	004° 06.231' E	160 high images – recovery tow
PS148_33-1 end	24.06.2025 20:00	2450	79° 04.684' N	004° 05.782' E	
PS148_37-1 start	26.06.2025 14:17	2287	78° 36.971' N	005° 00.211‘ E	88/480
PS148_37-1 end	26.06.2025 17:54	2288	78° 37.096' N	005° 08.011' E	

Seafloor imaging and mapping – Autonomous Underwater Vehicle (AUV)

The Autonomous Underwater Vehicle (AUV) PAUL 3000 was used to visually map a region of the central HAUSGARTEN, the pockmark ridge, and S stations. The AUV operated well during the expedition, though aborted during one dive (PS148_13-12), likely because of extremely strong bottom currents, as indicated by other expedition instruments.

Fig 2.4: PAUL 3000, deployed during the PS148 expedition and preparing to dive

Tab. 2.4: AUV PAUL 3000 deployments made during the PS148 expedition

Station ID	Survey region	Date / dive duration [hrs]	Distance Surveyed [km]	Area acoustically mapped [m^2]	Area imaged (m^2)
PS148_5-12	S3	07.06.2025 03:45	2	638000	9000
PS148_8-1	HG-IV	09.06.2025 10:26	5.3	3025000	28620
PS148_13-12	N5-N4	12.06.2025 04:50	NA	NA	NA
PS148_29-5	SV-IV	23.06.2025 07:04	11	3168000	59400
PS148_32-1	HG-1	24.06.2025 05:15	3.1	2068000	16740

Preliminary (expected) results

Biogenic sediment compounds

Stations EG-I to EG-III, located on the Greenland shelf, are ice-covered for most of the year, which likely limits sedimentation of fresh organic matter and microbial activity. EG-IV, however, is situated within the marginal ice zone (MIZ) and shows slightly elevated values, likely due to increased particle flux during periods of seasonal ice retreat. The HG stations along the bathymetric transect are predominantly ice-free, and here, water depth appears to be a key driver: both CPE and FDA values generally decrease with increasing depth, but CPE concentrations rise again at HG-IX (Molloy Deep), likely due to sediment focusing in this deep, funnel-shaped basin. Along the latitudinal transect (N3 to N5 and S3), pigment concentrations and bacterial activity decrease progressively toward the north. Although N5 is the northernmost station and closest to the ice edge, the ice margin in this particular year was located farther north, leaving N5 largely unaffected. This pattern suggests a decline in fresh organic input and microbial activity with increasing distance from more productive, ice-free southern waters.

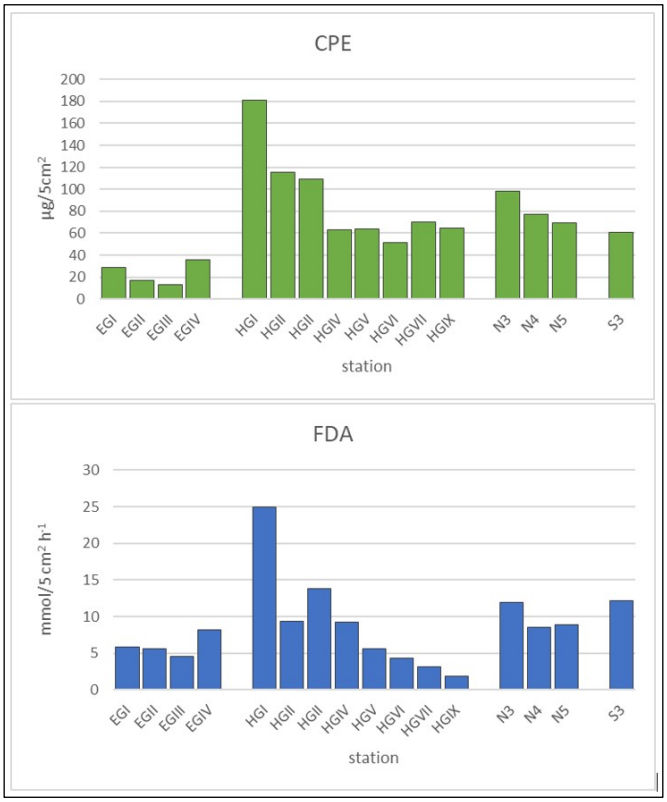

Fig 2.5: Concentrations of sediment-bound pigments (CPE, top) and potential bacterial activity (FDA, bottom)

Seafloor imaging – Ocean Floor Observation and Bathymetry System (OFOBS)

The OFOBS camera and sidescan systems worked well during the PS148 expedition, and the raw images were directly delivered to PANGAEA for archiving on return of ship to shore with associated metadata using the work pipeline currently under development in AWI. Example images from each deployment are given below.

Station PS148_2-4

This was the initial OFOBS deployment in this location, in support of the ALONGate project. There was a considerable heave in ocean conditions, but even so numerous images of this new location were collected. A fine muddy seafloor with occasional small pebble and sessile communities was observed.

Fig. 2.6a: OFOBS image taken during the PS148_2-4 station (SW_RELEASER_2025_06_03 at 12_52_18 IMG_0558.jpg). Red lazer points in the centre of the image have a spacing of 50 cm.

Station PS148_15-1

At this station a typical mix of dropstone and soft seafloor communities was imaged, with conditions allowing high resolution, high detail images of communities to be collected.

Fig. 2.6b: OFOBS image taken during the PS148_15-1 station (SW_RELEASER_2025_06_13 at 19_21_56 IMG_0312.jpg). Red lazer points in the centre of the image have a spacing of 50 cm.

Fig. 2.6c: Detail from an OFOBS image taken during the PS148_15-1 station (SW_RELEASER_2025_06_13 at 19_21_56 IMG_0312.jpg). Red lazer points in the upper left and lower right of the image have a spacing of 50 cm.

Station PS148_16-1

A mix of live and dead sponges and soft bottom communities, with indications of both infauna and surface reworking by mobile fauna was imaged. In the photograph here a cirrate octopus can be seen interacting with the seafloor, likely foraging for infauna.

Fig. 2.6d: OFOBS image taken during the PS148_16-1 station (SW_RELEASER_2025_06_14 at 04_36_15 IMG_0590.jpg). Red lazer points in the centre of the image have a spacing of 50 cm.

Station PS148_21-13

This deployment covered a range of depths and seafloor topographies on the upper flanks of the Molloy Deep. Commonly fauna growth was observed to be clearly influenced by prevalent current conditions, as was surface winnowing and deposition patterns around rocky structures.

Fig. 2.6e: OFOBS image taken during the PS148_21-13 station (SW_RELEASER_2025_06_19 at 00_05_38 IMG_0676.jpg). Red lazer points in the centre of the image have a spacing of 50 cm.

Station PS148_22_2

This deployment covered the central Molloy Deep and lower flanks of the feature. Here, ripples can be clearly seen, much in evidence approaching the flanks.

Fig. 2.6f: OFOBS image taken during the PS148_22-2 station (TIMER_2025_06_20 at 01_41_40 IMG_0605.jpg). Red lazer points in the centre of the image have a spacing of 50 cm.

Station PS148_25-1

During this deployment a far increased quantity of phytodetritus was observed across the seafloor, hydrodynamically trapped within and against microtopographic features.

Fig. 2.6g: OFOBS image taken during the PS148_25-1 station (SW_RELEASER_2025_06_21 at 04_24_42 IMG_0235.jpg). Red lazer points in the centre of the image have a spacing of 50 cm.

Station PS148_25-3 – Crawler recovery dive 1

Harsh surface and deep-water flow conditions prevented a successful attachment of the recovery line during the PS148_25-3 deployment. Despite this, the images collected showed the continued build up on the seafloor of the algal detritus observed during the PS148_25-1 deployment.

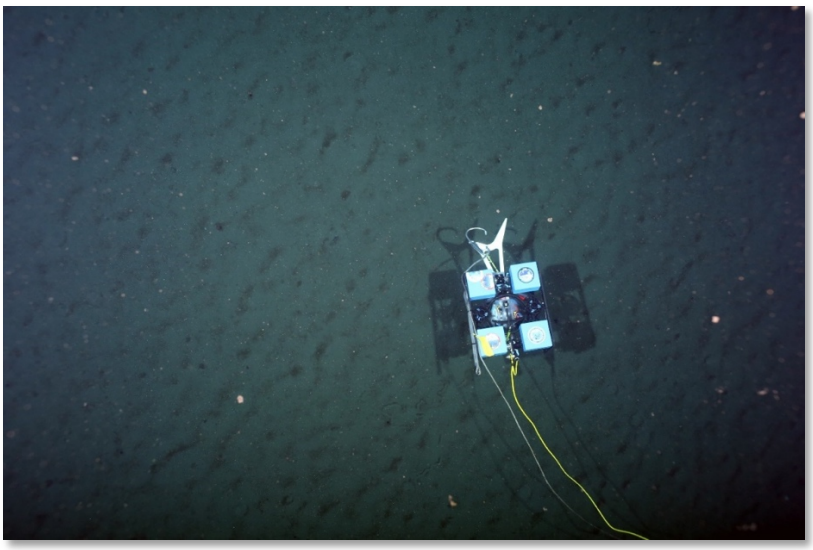

Fig. 2.6h: OFOBS image taken during the PS148_25-3 station (SW_RELEASER_2025_06_21 at 16_11_50 IMG_0196.jpg). Red lazer points in the centre of the image have a spacing of 50 cm.

Station PS148_32-2

Running from the HG-I transect line over the small pockmark features observed in recent HAUSGARTEN expeditions a mixed seafloor ecosystem was observed, with fauna communities correlating with distance from pockmarks. Ray fish were particularly common in close proximity to the pockmarks. Across the survey deployment, thick phytodetritus layers were again observed, as well as 'cleaning' actions by fauna, as in this image.

Fig. 2.6i: OFOBS image taken during the PS148_32-2 station (SW_RELEASER_2025_06_24 at 09_09_13 IMG_0057.jpg). Red lazer points in the centre of the image have a spacing of 50 cm.

Station PS148_33-1 – Crawler recovery dive 2

The recovery rope was successfully and swiftly attached to the Crawler during the PS148_33-1 deployment, and the device successfully winched to the ship. The phytodetritus deposit was still abundant in the vicinity of the Crawler.

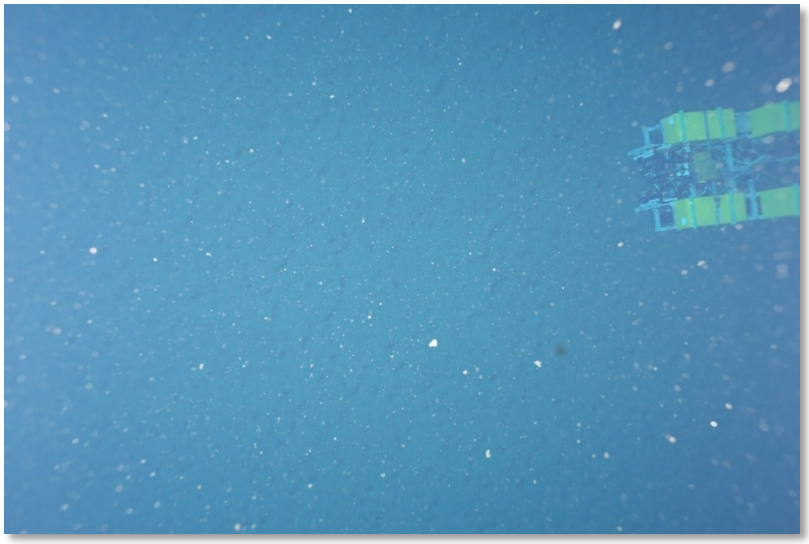

Fig. 2.6j: OFOBS image taken during the PS148_33-1 station (SW_RELEASER_2025_06_24 at 19_11_47 IMG_0087.jpg). Red lazer points in the centre of the image have a spacing of 50 cm.

Station PS148_37-1

During the final OFOBS deployment of the expedition, the seafloor was thickly covered with phytodetritus, with small bioturbidity trails infilled with material, and all infauna burrows also filled with the greenish material.

Fig. 2.6k: OFOBS image taken during the PS148_37-1 station (TIMER_2025_06_26 at 14_33_19 IMG_0144.jpg). Red lazer points in the centre of the image have a spacing of 50 cm.

Seafloor imaging and mapping – Autonomous Underwater Vehicle (AUV)

The AUV acoustic and image data collected during PS148 was of high quality and will be used for future work, particularly for the mapping of the pockmark region to the east of the HAUSGARTEN time series central stations. A large whale skeleton was found in the central HAUSGARTEN area and could be a potential target for revisiting in a decade, to gauge breakdown of the skeleton. The images are currently being archived to PANGAEA and will be available for analysis for fauna composition, particularly in the pockmark region, by the end of 2025.

Data management

Sample processing of the meiofauna and biogenic sediment compounds will be carried out at AWI. Data acquisition from the several types of investigation will require different time spans. The time periods from post processing to data provision will vary from one year maximum for environmental data to several years for meio-organism and macrofauna related datasets.

Obtained data will be deposited at public database (Pangaea) and hence be publicly available to the scientific community. Faunistic data will be publicly available as soon as studies on meiobenthic and macrobenthos classification, quantification and identification will be finished.

Environmental data will be archived, published and disseminated according to international standards by the World Data Center PANGAEA Data Publisher for Earth & Environmental Science (https://www.pangaea.de) within two years after the end of the expedition at the latest. By default, the CC-BY license will be applied.

Molecular data (DNA and RNA data) will be archived, published and disseminated within one of the repositories of the International Nucleotide Sequence Data Collaboration (INSDC, www.insdc.org) comprising of EMBL-EBI/ENA, GenBank and DDBJ).

Any other data will be submitted to an appropriate long-term archive that provides unique and stable identifiers for the datasets and allows open online access to the data.

This expedition was supported by the Helmholtz Research Programme “Changing Earth – Sustaining our Future” Topic 6 “Marine and Polar Life: Sustaining Biodiversity, Biotic Interactions and Biogeochemical Functions” and Topic 2 “Ocean and Cryosphere in Climate”.

In all publications based on this expedition, the **Grant No. AWI_PS148_01** will be quoted and the following publication will be cited:

Alfred-Wegener-Institut Helmholtz-Zentrum für Polar- und Meeresforschung (2017) Polar Research and Supply Vessel POLARSTERN Operated by the Alfred-Wegener-Institute. Journal of large-scale research facilities, 3, A119. http://dx.doi.org/10.17815/jlsrf-3-163.

References

Bergmann M, Collard F, Fabres J, Gabrielsen GW, Provencher, Jennifer F., Rochman C, Van Sebille E, Tekman MB (2022) Plastic pollution in the Arctic. Nature Reviews Earth & Environment 3:323–37. https://doi.org/10.1038/s43017-022-00279-8

Buhl-Mortensen L, Buhl-Mortensen P, Dolan MFJ, Dannheim J, Bellec V, Holte B (2012) Habitat complexity and bottom fauna composition at different scales on the continental shelf and slope of northern Norway. Hydrobiologia 685(1):191–219. https://doi.org/10.1007/s10750-011-0988-6

Buhl-Mortensen L, Vanreusel A, Gooday AJ, Levin LA, Priede IG, Buhl-Mortensen P, Gheerardyn H, King NJ, Raes M (2010) Biological structures as a source of habitat heterogeneity and biodiversity on the deep ocean margins. Marine Ecology - an Evolutionary Perspective 31(1):21–50. https://doi.org/10.1111/j.1439-0485.2010.00359.x

Gage JD, Tyler PA (1991) Deep-sea biology: a natural history of organisms at the deep-sea floor. London: Cambridge University Press. https://doi.org/10.1017/cbo9781139163637

Parga Martínez KB, Tekman MB, Bergmann M (2020) Temporal trends in marine litter at three stations of the HAUSGARTEN observatory in the Arctic deep sea. Frontiers in Marine Science 7. https://doi.org/10.3389/fmars.2020.00321

Piepenburg D (2005) Recent research on Arctic benthos: common notions need to be revised. Polar Biology, 28(10), 733-755. https://doi.org/10.1007/s00300-005-0013-5

Piepenburg D, Brey T, Teschke K, Dannheim J, Kloss MR, Hansen MLS, Kraan C (2024) PANABIO: a point-referenced PAN-Arctic data collection of benthic BIOtas. Earth Syst. Sci. Data 16:1177–1184. https://doi.org/10.5194/essd-16-1177-2024

Purser (2020) Short cruise report – RV Maria S. Merian, MSM95. University of Hamburg.

Purser A, Marcon Y, Dreutter S, Hoge U, Sablotny B, Hehemann L, Lemburg J, Dorschel B, Biebow H, Boetius A (2019) Ocean Floor Observation and Bathymetry System (OFOBS): A New Towed Camera/Sonar System for Deep-Sea Habitat Surveys. IEEE Journal of Oceanic Engineering 44(1):87–99. https://doi.org/10.1109/joe.2018.2794095

Schulz M, Bergmann M, von Juterzenka K, Soltwedel T (2010) Colonisation of hard substrata along a channel system in the deep Greenland Sea. Polar Biology 33(10):1359–1369. https://doi.org/10.1007/s00300-010-0825-9

Soltwedel T, Bauerfeind E, Bergmann M, Budaeva N, Hoste E, Jaeckisch N, von Juterzenka K, Matthiessen J, Mokievsky V, Nöthig E-M, Quéric N-V, Sablotny B, Sauter E, Schewe I, Urban-Malinga B, Wegner J, Wlodarska-Kowalczuk M, Klages M (2005) HAUSGARTEN: Multidisciplinary investigations at a deep-sea, long-term observatory in the Arctic Ocean. Oceanography 18(3): 46–61. https://doi.org/10.5670/oceanog.2005.24

Soltwedel T, Bauerfeind E, Bergmann M, Bracher A, Budaeva N, Busch K, Cherkasheva A, Fahl K, Grzelak K, Hasemann C, Jacob M, Kraft A, Lalande C, Metfies K, Nöthig E-M, Meyer K, Quéric N-V, Schewe I, Wlodarska-Kowalczuk M, Klages M (2016) Natural variability or anthropogenically-induced

variation? Insights from 15 years of multidisciplinary observations at the arctic marine LTER site HAUSGARTEN. Ecological Indicators 65:89–102. https://doi.org/10.1016/j.ecolind.2015.10.001

Soltwedel T, Bauerfeind E, Bergmann M, Budaeva N, Hoste E, Jaeckisch N, von Juterzenka K, Matthiessen J, Mokievsky V, Nöthig E-M, Quéric N-V, Sablotny B, Sauter E, Schewe I, Urban-Malinga B, Wegner J, Wlodarska-Kowalczuk M, Klages M (2016) HAUSGARTEN: Multidisciplinary investigations at the deep-sea observatory in the Arctic Ocean. Deep-Sea Research Part I: Oceanographic Research Papers 108: 1–23. https://doi.org/10.1016/j.dsr.2015.12.015

Taylor J, Krumpen T, Soltwedel T, Gutt J, Bergmann M (2016) Regional- and local-scale variations in benthic megafaunal composition at the Arctic deep-sea observatory HAUSGARTEN. Deep-Sea Research Part I: Oceanographic Research Papers 108:58–72. https://doi.org/10.1016/j.dsr.2015.12.009

Tekman MB, Wekerle C, Lorenz C, Primpke S, Hasemann C, Gerdts G, Bergmann M (2020) Tying up loose ends of microplastic pollution in the Arctic: Distribution from the sea surface, through the water column to deep-sea sediments at the HAUSGARTEN observatory. Environmental Science & Technology 54:4079-4090. https://doi.org/10.1021/acs.est.9b06981.s001

Tews J, Brose U, Grimm V, Tielbörger K, Wichmann MC, Schwager M, Jeltsch F (2004) Animal species diversity driven by habitat heterogeneity/diversity: the importance of keystone structures. Journal of Biogeography 31(1):79-92. https://doi.org/10.1046/j.0305-0270.2003.00994.x

Whittaker RJ, Willis KJ, Field R (2001) Scale and species richness: towards a general, hierarchical theory of species diversity. Journal of Biogeography 28(4):453-470. https://doi.org/10.1046/j.1365-2699.2001.00563.x

3. PLANKTON ECOLOGY AND BIOGEOCHEMISTRY IN A CHANGING ARCTIC OCEAN

Nadine Knüppel[1], Jakob Barz[1], Claudia Brenner[1], Magdalena Dolinkiewicz[1], Barbara Doermbach[1], Katharina Kistrup[2], Tania Klüver[2], Samira Linder[2], Carla Pein[2], Katja Metfies*[1]

not on board: Anja Engel[2], Alexandra Kraberg[1], Morten Iversen[1], Barbara Niehoff[1]

*katja.metfies@awi.de

[1]DE.AWI

[2]DE.GEOMAR

Grant-No. AWI_PS148_02

Outline

The Arctic Ocean has gained increasing attention in recent decades due to the ongoing significant changes in sea-ice cover and increase in sea temperature. Moreover, it is expected that the chemical equilibrium and the elemental cycling in the surface ocean change due to ocean acidification. Over the past two decades, measurements of biogeochemical parameters, microscopy, optical methods, satellite observations, and molecular genetic approaches have provided valuable information on ecosystem variability in response to environmental change. This includes information on biodiversity, biogeography and biomass of the bacterial, microbial and mesozooplankton plankton communities, as well as primary production and bacterial activity on annual basis. These annual measurements are complemented with year-round sampling based on the deployment of sediment traps and automated water samples on long-term moorings within the framework of the FRAM/HAUSGARTEN observatory.

Fram Strait is an ideal location to investigate potential effects of changing environmental conditions, including sea-ice coverage on plankton communities. The long-term observations and process studies have already given us valuable insights into mechanistic linkages between environmental conditions, biodiversity and ecosystem functionality, and into ongoing change in the marine ecosystem of Fram Strait. Our results clearly indicate that chlorophyll a (Chl-a) values increase in summer in the eastern but not in the western Fram Strait (Nöthig et al. 2015 2020). This is in accordance with the increasing contributions of *Phaeocystis pouchetii* and nanoflagellates to the summer phytoplankton community in relation to diatoms, linked to decreasing availability of silicic acid in the water column. Biogeographical studies of PEBCAO based on 18S metabarcoding indicate that a year-round semi-stationary sea-ice edge serves as a strong biogeographical boundary between Atlantic conditions to the southeast and polar conditions to the Northwest of Fram Strait (Metfies et al. 2016). In 2017, the MIZ extended further eastwards and southwards into Fram Strait than in average years, with profound impacts on the ecosystems. Sea ice melt in a sub-mesoscale filament, characterized by a thin surface meltwater layer, led to comprehensive changes in plankton-biodiversity, carbon export and primary production in vicinity of the filament (Fadeev et al. 2021). Moreover, results from an interdisciplinary study in a sub-mesoscale filament suggest that sea-ice melt is enhancing the growth of sea-ice associated phytoplankton, that might be positively linked to zooplankton abundance and biomass (Weiss et al. 2024). In sea-ice impacted regions of Fram Strait

diatoms dominate the diet of zooplankton, while they have less impact in open water areas of Atlantic Water (Kaiser et al. 2025; accepted).

Moreover, the population size of bloom-forming species can also be impacted by mycoplankton (defined here as saprotrophic and parasitic fungi and pseudofungi (oomycetes). These taxonomic groups have not yet been part of our investigations although its ecological impact can be considerable (Buaya et al. 2019). Even in well-studied areas such as the North Sea new species are being described (Buaya et al. 2017), but in polar regions, with few exceptions the diversity and dynamics of the mycoplankton remain to be discovered (Hassett et al. 2019 a,b).

In the past, PEBCAO also contributed to year-round interdisciplinary observations indicating that increased meltwater-stratification during spring/summer of 2017 slowed down the biological carbon pump in AW the central Fram Strait with significant impacts on pelagic and benthic communities in comparison to the warmer year 2018 (von Appen et al. 2021). The data suggest, that sea-ice melt might serve as a barrier for a northward movement of temperate phytoplankton taxa in Fram Strait (Oldenburg et al. 2024). Furthermore, based on our year-round automated water sampling, we characterized the annual succession of microbial communities at a station in West Spitsbergen Current (WSC) and East Greenland Current (EGC). The ice-free West Spitsbergen Current displayed a marked separation into a productive summer (dominated by diatoms and carbohydrate-degrading bacteria) and regenerative winter state (dominated by heterotrophic Syndiniales, radiolarians, chemoautotrophic bacteria, and archaea). In the East Greenland Current, deeper sampling depth, ice cover and polar water masses concurred with weaker seasonality and a stronger heterotrophic signature. Low ice cover and advection of Atlantic Water coincided with diminished abundances of chemoautotrophic bacteria while other taxa such as *Phaeocystis* increased, suggesting that Atlantification alters the microbiome structure and eventually the biological carbon pump (Wietz et al. 2021). PEBCAO was able to show, that a change in microbiome structure might affect the biological carbon pump. For instance, we found, strong correlations between *Phaeocystis* and transparent exopolymer particle concentration (TEP), which are known to play a crucial role in the biological carbon pump (Engel et al. 2017). However, despite the observed shift in phytoplankton community composition, the concentration of dissolved organic carbon (DOC) was relatively stable over the last two decades, but we observed a slight decrease in the particulate organic carbon (POC) during the summer months (Engel et al. 2019). While these results point to inter annual changes in the Fram Strait (von Jackowski et al. 2022) additional data suggest an intra annual (seasonal) succession of prokaryotic microbes, that was related to a succession in the biopolymer pool, indicating seasonally distinct metabolic regimes. Data of our long-term sediment-trap programme suggest that over the period 2009-2016 the abundance of *Micromonas polaris* and *Micromonas commoda*-like cells is positively correlated with lower standing stocks of phosphate and nitrate in the upper water-column at the LTER observatory HAUSGARTEN, and that they are exported to the deep sea, despite of their small size (Bachy et al. 2022).

In summary, our data suggest that already now the ecosystem in Fram Strait is subject to profound changes, likely induced by changing climate conditions, which warrants further, sustained observation.

Objectives

The effects of changes on the polar plankton ecology and biogeochemical processes can only be detected through a combination of dedicated interdisciplinary process studies and long-term observations, as implemented by PEBCAO within the HAUSGARTEN/FRAM observatory for more than a decade. Overall, the overarching objectives of PEBCAO are to improve the mechanistic understanding of biogeochemical and microbiological feedback processes in the changing Arctic Ocean, to document ongoing and long-term changes in the biotic and abiotic

environment and to assess the potential future consequences of these changes. In particular we aim to identify climate-induced changes in the biodiversity of pelagic ecosystems and, concomitantly, in carbon cycling and sequestering and improve our mechanistic understanding of linkages between key environmental parameters and ecosystem functionality in the Arctic Ocean. The objectives are addressed in an interdisciplinary approach. In this context, the current expedition is contributing in specific to the question of how sea ice coverage over different geographical scales affects the composition of plankton and the associated ecological processes.

Primary production is expected to increase in the changing Arctic Ocean, however, it is currently unclear if this will lead to increased export of particulate organic carbon or if organic carbon will remain at the surface, fueling heterotrophic bacteria. Heterotrophic bacteria play a vital role in global biogeochemical cycles. To improve our understanding of bacterial activity, we will determine bacterial abundance, biodiversity and bacterial production. By linking compound dynamics with rate measurements and community structure, we will gain further insights into the flow of carbon through the Arctic food web. To address the effects of global change on microbial biogeochemistry in the Arctic Ocean, we will also continue to monitor concentrations of organic carbon, nitrogen, and phosphorus, as well as specific compounds like amino acids, carbohydrates, and gel particles. To assess cell abundances, we will sample for microscopic counts and flow cytometry that allows us to determine phytoplankton (< 50 µm), bacteria, and viral abundances. Phytoplankton primary production will be determined by radioisotopes (via 3H leucine-incorporation)) and distinguished into particulate primary production (carbon remaining in the cells) and dissolved primary production (organic carbon subsequently released by cells). In addition, active fluorometry will be applied with using a LabSTAF instrument running in underway mode to determine phytoplankton fitness and productivity.

In order to investigate the effects of global change and anthropogenic pollution on the microbial community and biogeochemistry in the Arctic Ocean, we will continue to monitor the concentrations of organic carbon and nitrogen, amino acids, lipids, carbohydrates, and gel particles, and we will assess abundances of phytoplankton, bacteria and viruses.

We expect that the small algae at the base of the food web gain importance in mediating element and matter turnover as well as energy fluxes in Arctic pelagic systems. In order to detect changes, also in this smallest fraction of the plankton, traditional microscopy will be complemented by optical (see below) and molecular methods that are independent of cell-size and morphological features, and we will determine their contribution to Chl-a biomass. Changes in eukaryotic microbial communities are tightly linked to prokaryotic community composition. The assessment of the biodiversity and biogeography of Arctic eukaryotic microbes, including phytoplankton and their linkages to prokaryotic microbial communities, will be based on analyses of eDNA via 16S and 18S meta-barcoding, and quantitative PCR. A suite of automated sampling devices in addition to classical sampling via Niskin bottles attached to a CTD/Rosette Water Sampler will be used to collect samples for eDNA analyses. This includes the automated filtration device AUTOFIM deployed on *Polarstern* for underway filtration, automated Remote Access water Samplers (RAS) and long-term sediment traps deployed on the FRAM moorings for year-round sampling.

Similar to the phytoplankton community, the zooplankton community composition in the Fram Strait may shift due to the increasing inflow of warmer Atlantic water. As primary and secondary consumers, zooplankton play a crucial role in trophic interactions and the biological carbon pump, contributing through the production of sinking fecal pellets and through vertical migrations. Alterations in zooplankton composition will therefore affect trophic dynamics, the flow of organic matter in the water column, and ultimately carbon sequestration and flux. To understand and predict the consequences of future ecosystem changes, we continue to monitor zooplankton community composition, biomass, and vertical distribution. Most of our existing knowledge on species composition and distribution has been derived from traditional

multiple net samplers, which integrate depth intervals of up to several hundred meters. Nowadays, optical systems such as the LOKI (Light frame On-sight Key species Investigations) recorder continuously take pictures of organisms during vertical casts, while simultaneously recording hydrographical parameters such as salinity, temperature, oxygen concentration, and fluorescence. These data allow for precise identification of distribution patterns of key taxa in relation to environmental conditions. In addition, the UVP5 (Underwater Vision Profiler), mounted on the ship's CTD, is used to investigate zooplankton distribution patterns, albeit with less taxonomic resolution than LOKI.

Moreover, we will also include research dedicated to protistan parasites. These are severely understudied in the marine realm although they are likely to affect the population dynamics of phytoplankton (including bloom timing and magnitude) and zooplankton. We will therefore conduct a baseline study of the diversity of different parasite groups and their association with potential hosts. This investigation will also form the basis for future biogeographic studies. The analyses will combine different microscopy techniques (LM, SEM, CFLM) as well as molecular data, the latter facilitating observation of parasitism even at times where easily discernible parasite life-cycle stages are absent. We will also initiate cultures for fungal plankton (in addition to oomycete cultures established on PS143/1). Co-cultures of parasites and their hosts will be used for experiments planned in the upcoming INDIFUN-AI BMBF project in which we wish to investigate the utility of using parasites and saprotrophic fungi as indicators of environmental change.

In summary, during PS148 PEBCAO is addressing the following objectives:

- Monitoring biogeochemical parameters
- Determine autotrophic and heterotrophic microbial activities
- Monitoring plankton species composition and biomass distribution
- Assessing the flux of particulate organic matter to the seafloor
- Investigating selected phyto- and zooplankton (including their parasites)
- Determining the composition of organic matter and gel particles
- Studying host-parasite systems in phyto- and mycoplankton

Work at sea

Measurements and sample collections for a large variety of parameters were accomplished at 18 stations of the 'deep-sea long-term observatory HAUSGARTEN' during PS148, including the frontal zone separating the warm and cold-water masses originating from the West Spitsbergen Current and the East Greenland Current. Measurements and sampling comprised CTD casts, underway sampling with the automated filtration device AUTOFIM, net hauls and LOKI and is summarised in tables.

Biogeochemistry

A diverse set of discrete seawater samples was collected during the cruise consisting of chemical and biological parameters which are associated with organic matter composition and microbial activity, to determine the processes affecting the turnover of organic matter in the Arctic Ocean. In total, 15 stations were sampled, utilizing a CTD/Rosette Water Sampler (Fig. 3.1). The euphotic zone was sampled during a "shallow" cast (surface, Chl a max., below Chl amax., 50 m, and 100 m) at every station. Additionally, samples were taken from a "deep" cast (200, 500, 750, 1,000, and 1,200 m) at 5 selected stations to investigate the connectivity of surface and deep waters via the export of organic matter (Tab. 3.1). Samples were taken for dissolved biogeochemical parameters, such as dissolved organic carbon (DOC/TDN) via

filtration of seawater through 0.45 µm GMF syringe filters into combusted glass ampules, acidification with hydrochloric acid (Suprapur), and storage at 4 °C until HPLC analysis. Dissolved amino acids (DAA) and combined carbohydrates (DCHO) were filtered over 0.45 µm Acrodisc filters into combusted glass vials and stored at -20 °C. Samples for total alkalinity (TA) measurements were filtered through 0.45 µm Acrodisc filters and stored at 4 °C. Dissolved inorganic carbon (DIC) samples were treated with mercury(II)chloride and also stored at 4°C. In addition, we collected seawater samples to determine the concentration (abundance and area) and the carbon content of transparent exopolymer particles (TEP) and Coomassie stainable particles (CSP) using 0.4 µm polycarbonate filters and the dyes Alcian Blue and Coomassie Brilliant Blue for staining, respectively. These filters were stored subsequently at -20 °C until further microscopic and colorimetric analyses in the laboratory. Samples for lipid analysis were filtered over a 0.2 µm hydrophilic durapore filter, flash-frozen in liquid nitrogen, and stored at -80 °C. All samples will be shipped and analyzed in the laboratories at GEOMAR in Kiel, Germany.

Furthermore, multiple methods were applied to determine the phytoplankton and bacterial abundances and growth rates. For bacterial (BA) and picophytoplankton (PA) abundance samples were fixed with GDA 25 % and frozen at -80 °C. Further analysis by flow cytometry will take place at GEOMAR. Phytoplankton primary production (PP) and bacterial biomass production (BBP) rates were determined on board using a radioactive tracer approach with ^{14}C sodium bicarbonate and ^{3}H-leucine, respectively.

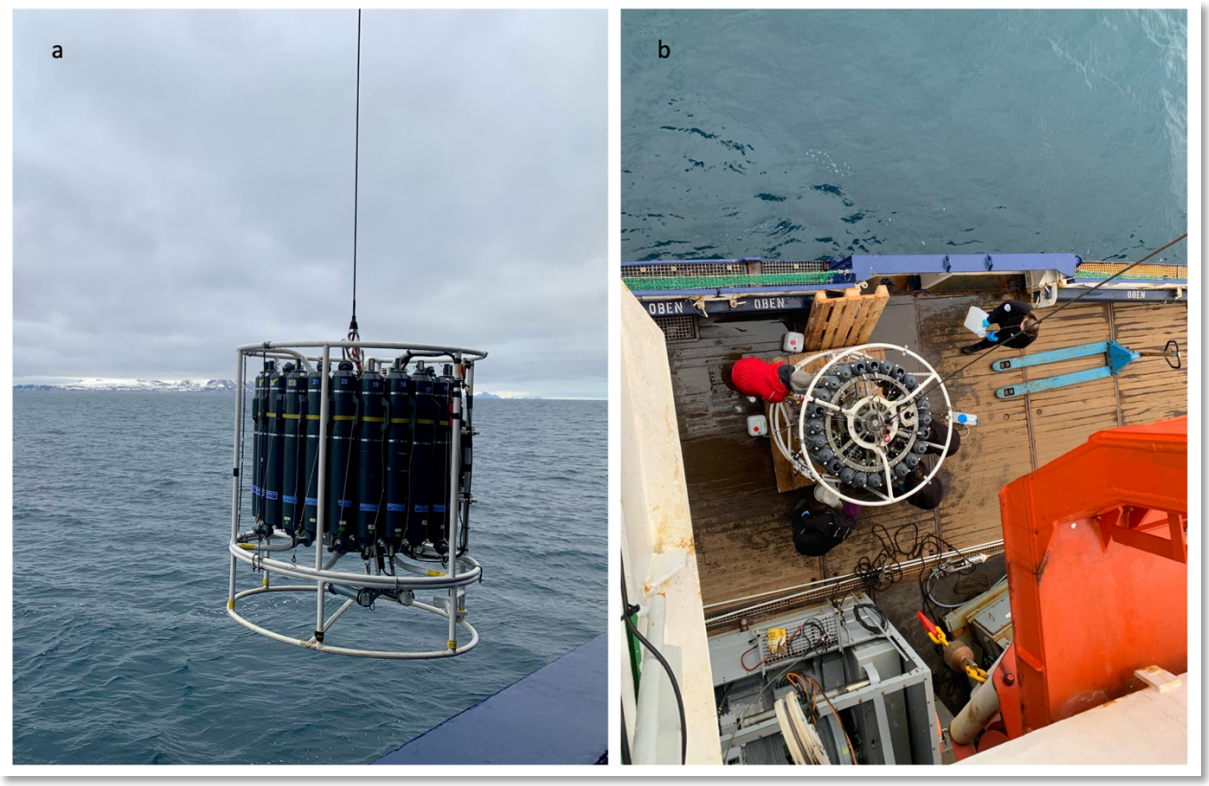

Fig. 3.1: CTD with Rosette
a: deployment of the instrument
b: water sampling rom niskin bottles on deck

In summary, the following parameters were addressed:

- Dissolved organic carbon (DOC)
- Total dissolved nitrogen (TDN)
- Total alkalinity (TA)
- Transparent exopolymer particles (TEP)
- Coomassie-stainable particles (CSP)
- Dissolved combined carbohydrates (dCCHO)
- Hydrolysable amino acids (dHAA)
- Phytoplankton, bacterial and viral abundance
- Lipids

Additionally, a LabSTAF instrument (Chelsea Technologies, UK) was used to determine phytoplankton fitness and productivity, using single turnover active fluometry (STAF) (Fig. 3.2). The system was used in underway mode during the whole station work, automatically taking a new sample every 20 minutes.

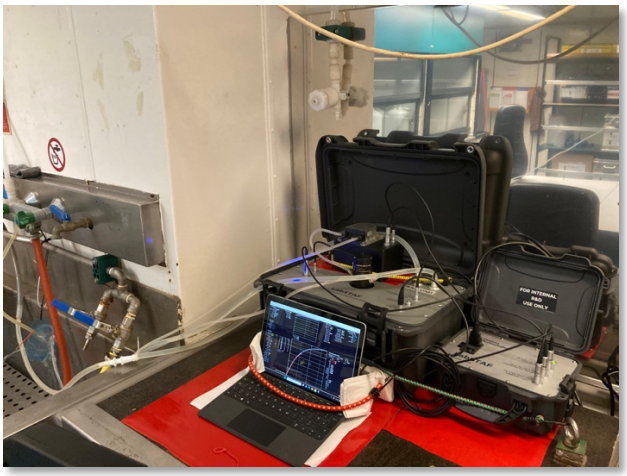

Fig. 3.2: Setup of the LabSTAF instrument on board

Tab. 3.1: Biogeochemical parameters sampled from the CTD/ Rosette Water Sampler. Abbreviations as follows: DOC: dissolved organic carbon; DCHO: dissolved carbohydrates; DAA: dissolved amino acids; DIC: dissolved inorganic carbon; TA: total alkalinity; TEP: transparent exopolymer particles; CSP: Coomassie stainable particle; LIP: lipids; BA/PA: bacterial and picophytoplankton abundance; BBP: bacterial biomass production; PP: phytoplankton primary production

Station-ID	Station	DOC/ DCCHO/ DAA	DIC/ TA	TEP/ CSP	LIP	BA/ PA	BBP	PP
PS148_5-1	S3 shallow	x	x	x	x	x	x	x
PS148_5-3	S3 deep	x	-	x	-	x	-	-
PS148_6-4	HG-IV deep	x	-	x	-	x	-	-
PS148_6-13	HG-IV shallow	x	x	x	x	x	x	x
PS148_9-1	HG-IX shallow	x	x	x	x	x	x	x

Station-ID	Station	DOC/ DCCHO/ DAA	DIC/ TA	TEP/ CSP	LIP	BA/ PA	BBP	PP
PS148_9-6	HG-IX deep	x	-	x	-	x	-	-
PS148_11-1	HG-VII shallow	x	-	x	x	x	x	-
PS148_13-4	N5 shallow	x	x	x	x	x	x	x
PS148_14-2	N4 shallow	x	-	x	x	x	x	-
PS148_14-8	N4 deep	x	-	x	-	x	-	-
PS148_16-2	N3 shallow	x	-	x	x	x	x	-
PS148_17-1	EG-I shallow	x	x	x	x	x	x	x
PS148_19-1	EG-II shallow	x	x	x	x	x	x	x
PS148_21-2	EG-IV shallow	x	x	x	x	x	x	x
PS148_21-14	EG-IV deep	x	-	x	-	x	-	-
PS148_27-1	SV-IV shallow	x	x	x	x	x	x	x
PS148_28-1	SV-I shallow	x	x	x	x	x	x	x
PS148_30-1	SV-III shallow	x	-	x	x	x	x	-
PS148_31-1	SV-II shallow	x	-	x	x	x	x	-
PS148_35-5	HG-I shallow	x	-	x	x	x	x	-

Biogeochemistry: Zooplankton biochemistry

For the INDIFUN-AI BMBF project zooplankton was picked from selected stations using a MultiNet midi (Hydrobios, Germany) or a WP2 Net (Tab. 3.2). The samples were taken to study the biochemistry of zooplankton of different water masses, to analyze the lipidome, amino acids and carbohydrates, in search for as indicators of environmental change. The species *Calanus finmarchicus* and *C. hyperboreus* were chosen as target species. In the project parasites and saprotrophic fungi are analyzed as possible indicators and their impact will be investigated through different trophic levels. As a pilot study, grazing experiments were conducted, to assess whether relevant phytoplankton species, function as mycoplankton parasite hosts are grazed on by C. finmarchicus. CV stages of *C. finmarchicus* were incubated with three different phytoplankton species for 24h on a plankton wheel to assess their grazing rates (Fig. 3.3.)

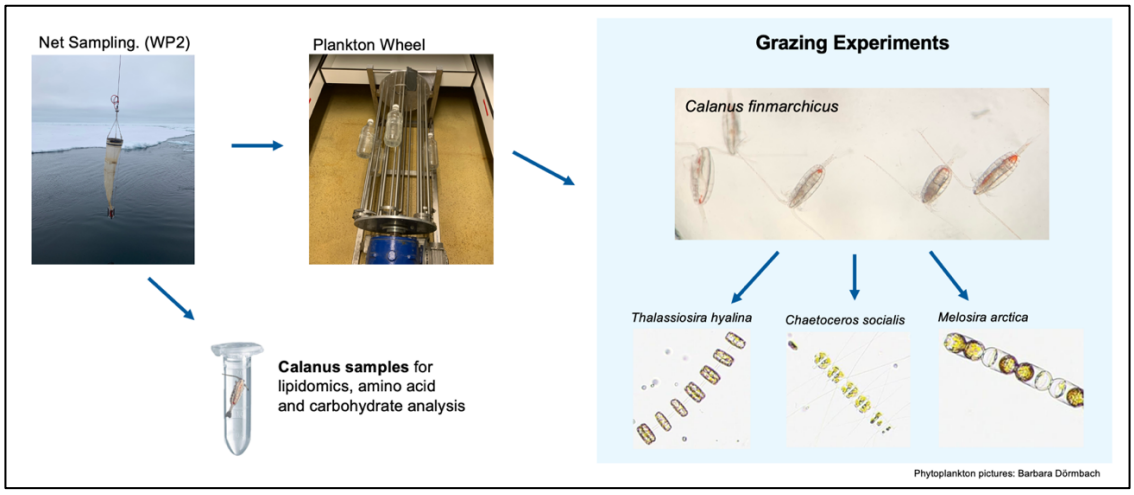

Fig. 3.3: Overview of zooplankton sampling and experimental work

Tab. 3.2: Overview of samples taken from MultiNet midi (Hydrobios, Germany) or WP2 Net for zooplankton (*Calanus* spp.) picking

Station ID	Station	MultiNet	WP2 Net
PS148_5-7	S3	x	
PS148_6-2	HG-IV	x	
PS148_9-4	HG-IX	x	
PS148_13-3	N5	x	
PS148_14-5	N4	x	
PS148_17-8	EG-I		x
PS148_19-7	EG-II		x
PS148_21-5	EG-IV		x
PS148_27-8	SV-IV		x
PS148_28-8	SV-I		x

Phytoplankton and microbial Biodiversity

Seawater samples were taken at 5 - 12 depths by a CTD/Rosette Water Sampler and aliquots were filtered for analyzing biogeochemical parameters such as chlorophyll a, particulate organic carbon (POC), biogenic silica (PbSi), microbial biodiversity and fractionated chlorophyll a biomass (Tab. 3.3). Furthermore, unfiltered water samples were fixed with formol (final concentration 0.5 - 1.0 %) and lugol (final concentration 2 %) for later quantitative assessment of the phytoplankton community and a comparison of the fixation methods. At each station, phytoplankton net hauls were carried out to a depth of ca. 20 m to study the species richness and distribution of life phytoplankton. In the onboard laboratory the net samples were directly analyzed with the PlanktoScope and additionally with inverted microscopy to provide a baseline inventory of the phytoplankton community (Fig. 3.4).

Water samples for analyses of eukaryotic microbial biodiversity and fractionated chlorophyll a measurements were filtered via bottle-top filtration sequentially on filters with pore size of 10 µM, 3 µM and 0.4 µM and for prokaryotic analyses samples were filtered via Sterivex-filtration (pore size 0.22 µM). Subsequent to filtration, samples were directly frozen at -80°C.

Tab. 3.3: Overview of stations sampled for biogeochemical parameters during PS148. POC/PbSI/Chl a: particulate organic carbon, biogenic silica and Chlorophyll a.

StationID	**Station**	POC, PbSi Chl a Shallow **(0-100m)**	POC PbSi Chl a Deep **(below 100m)**	**Hand net 20 µm**	**Plankto Scope**	**Utermöhl counting**	eDNA&Chla fractionated (>10µm; 3-10 µM; 0.4 -3µM for analyses of eukaryotic microbial biodiversity) eDNA **(>0.22 µM for analyses of prokaryotic biodiversity)**
PS148_32	HG-I	X		X	X	X	X
PS148_36	HG-II			X	X	X	

PS148_7	HG-III			X	X	X	
PS148_6	HG-IV			X	X	X	X
PS148_12	HG-V			X	X	X	
PS148_22	HG-VI	X		X	X	X	
PS148_12	HG-VII			X	X	X	
PS148_11	HG-VIII			X	X	X	
PS148_9	HG-IX	X		X	X	X	X
PS148_16	N3	X	X	X	X	X	
PS148_14	N4	X		X	X	X	X
PS148_13	N5	X		X	X	X	X
PS148_17	EG-I	X		X	X	X	X
PS148_19	EG-II	X		X	X	X	X
PS148_20	EG-III	X		X	X	X	X
PS148_21	EG-IV	X		X	X	X	X
PS148_28	SV-I			X	X	X	X
PS148_31	SV-II	X		X	X	X	X
PS148_30	SV-III	X		X	X	X	X
PS148_27	SV-IV	X		X	X	X	X
PS148_5-1	S3	X		X	X	X	X

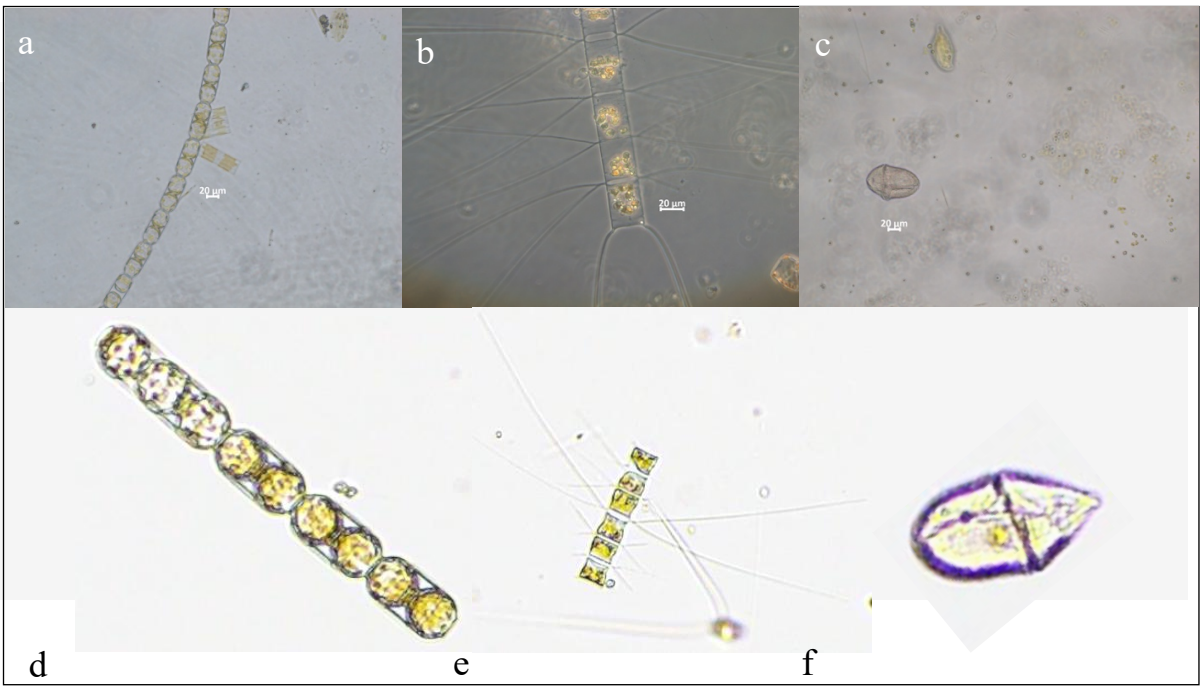

Fig. 3.4: Microscopy images compared to Images provided by the PlanktoScope. a, d) Melosira arctica; b,e) Chaetoceros decipiens; c, f) Gymnodiniaceae sp.

To address spatial variability of microbial plankton communities across different ice-situations, we complemented sampling for molecular analyses using the CTD-rosette with sampling via the underway sampling system AUTOFIM, permanently installed on board *Polarstern* (Tab. 3.4). We used the device to collect samples with a volume of ~ 2 litres during three transects during the transfer from ice-free waters in the WSC to the ice-covered stations in the EGC, during the transfer between the stations in the EGC and during the transfer from the EGC to the stations located on the Svalbard shelf. In total we collected 28 samples with a resolution of ~ 18 nm. All filters for eDNA were frozen at -80°C until further analyses in the laboratory on shore.

Tab. 3.4: List of underway samples collected with the automated filtration device AUTOFIM in vicinity of the MIZ and in ice-covered areas

Transekt	Sample	date	time (UTC)	latitude decimal degrees	longitude decimal degrees	depth [m]	fraction [µm]
Transekt 1	AF1	14/06/2025	15:30	79.60955	4.84107	10	0.4
Transekt 1	AF2	14/06/2025	18:30	79.34157	3.50220	10	0.4
Transekt 1	AF3	14/06/2025	21:30	78.85950	2.30246	10	0.4
Transekt 1	AF4	15/06/2025	00:30	78.82644	0.34181	10	0.4
Transekt 1	AF5	15/06/2025	03:30	78.79154	-2.04987	10	0.4
Transekt 1	AF6	15/06/2025	06:30	78.87546	-3.39061	10	0.4
Transekt 1	AF7	15/06/2025	09:30	79.01454	-4.32218	10	0.4
Transekt 1	AF8	15/06/2025	12:30	78.97872	-5.44838	10	0.4
Transekt 1	AF9	15/06/2025	15:30	79.02022	-5.60696	10	0.4
Transekt 2	AF10	15/06/2025	19:07	79.05930	-5.63816	10	0.4
Transekt 2	AF11	16/06/2025	00:07	79.03559	-5.46750	10	0.4
Transekt 2	AF12	16/06/2025	05:07	78.99942	-5.39868	10	0.4
Transekt 2	AF13	16/06/2025	10:07	79.05222	-5.55300	10	0.4
Transekt 2	AF14	16/06/2025	15:07	79.05897	-5.51130	10	0.4
Transekt 2	AF15	16/06/2025	20:07	78.92001	-4.71936	10	0.4
Transekt 2	AF16	17/06/2025	01:07	78.91082	-4.68164	10	0.4
Transekt 2	AF17	17/06/2025	06:07	78.79960	-3.93611	10	0.4
Transekt 2	AF18	17/06/2025	11:07	78.80436	-3.90244	10	0.4
Transekt 3	AF19	19/06/2025	10:24	78.78210	-2.39609	10	0.4
Transekt 3	AF20	19/06/2025	13:24	78.72880	-0.49957	10	0.4
Transekt 3	AF21	19/06/2025	16:24	78.89639	2.04921	10	0.4
Transekt 3	AF22	19/06/2025	19:24	79.10781	3.22787	10	0.4
Transekt 3	AF23	19/06/2025	22:24	79.10264	3.31474	10	0.4
Transekt 3	AF24	20/06/2025	01:24	79.09699	3.38266	10	0.4
Transekt 3	AF25	20/06/2025	04:24	79.09079	3.46843	10	0.4
Transekt 3	AF26	20/06/2025	07:24	79.14008	2.76158	10	0.4
Transekt 3	AF27	20/06/2025	10:24	79.13791	2.78550	10	0.4
Transekt 3	AF28	20/06/2025	13:24	79.05999	3.59046	10	0.4

Zooplankton

The composition of the mesoplankton community and its distribution in the water column in Fram Strait were studied using three devices. The MultiNet midi (Hydrobios, Germany) was deployed to analyze the large-scale vertical distribution of the zooplankton in the water column

(Fig. 3.5a). It was equipped with five nets with a mesh size of 150 µm and collected samples from five depth intervals (1,500-1,000-500-200-50-0 m) at 13 AWI-HAUSGARTEN stations (Tab. 3.5). The samples were immediately preserved in hexamethylenetetramine-buffered formalin, and their analysis will yield data on abundance and biomass at high taxonomical resolution. In addition, two optical systems were used to determine the distribution patterns of zooplankton taxa in relation to environmental conditions at high vertical resolution: the LOKI (Light frame On-sight Key species Investigations) and the UVP5 (Underwater Vision Profiler). The LOKI was equipped with a plankton net (150µm mesh size) concentrating and leading organisms and particles to a flow-through chamber with a 6 mpixel camera (Fig. 3.5b). LOKI recorded zooplankton with a frame rate of 20 frames per second during 11 vertical casts from 1,000 m depth to the surface. It effectively captured high resolution images of hard-bodied key taxa of up to a maximum size of 1 cm (e.g. the copepod genera *Calanus, Microcalanus,* and *Oncaea*) and simultaneously recorded hydrographic parameters, including salinity, temperature, oxygen concentration, and fluorescence. The UVP5 was mounted on the water rosette with a CTD, and was, thus, operated during every CTD cast (see Tab. 4.2) from the surface to the sea floor which allowed to investigate zooplankton distribution patterns at higher spatial resolution, albeit with lower taxonomic resolution compared to LOKI. It was, however, more effective in detecting large, fragile organisms such as jellyfish that are often destroyed by plankton nets.

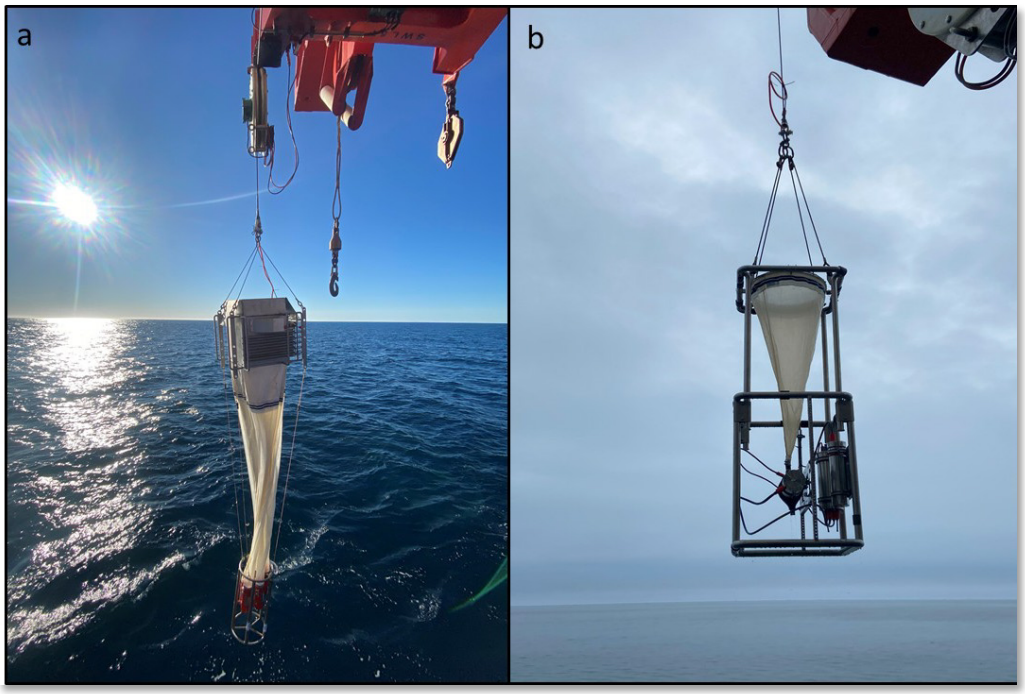

Fig. 3.5: The MultiNet (a) and the LOKI (b) deployment

Tab. 3.5: List of MultiNet midi (Hydrobios, Germany) and LOKI (IsiTec Germany) deployments in Fram Strait during PS148. Presented are the names of the HAUSGARTEN monitoring sites visited yearly, and the respective station numbers with the deployments.

Monitoring site	Station number	MultiNet	LOKI
SV-I	PS148-28	X	X
SV-II	PS148-21	X	X

Monitoring site	Station number	MultiNet	LOKI
S3	PS148-05	X	X
HG-I	PS148-35	X	X
HG-III	PS148-07	X	
HG-IV	PS148-06	X	X
HG-IX	PS148-09	X	X
N4	PS148-14	X	X
N5	PS148-13	X	X
EG-I	PS148-17	X	X
EG-II	PS148-19	X	
EG-III	PS148-20	X	X
EG-IV	PS148-21	X	X

Sea Ice Sampling

At four stations in vicinity of the marginal ice zone (MIZ), sea ice cores were collected for eDNA based characterization of microbial sea ice communities and quantification of chl a-biomass. Ice samples were melted at 4°C aboard *Polarstern* and particles were collected fractionally on filters with pore sizes of 10 µm, 3 µm, and 0.4 µm in analogy to water samples. All samples were preserved, refrigerated or frozen at -20°C or -80°C for storage until analyses in the laboratory (AWI, Bremerhaven).

Exchange of moored autonomous sampling devices for biological and biogeochemical parameters

(AG Iversen with Nadine Knüppel)

The PEBCAO-team accomplished the preparation and post-deployment processing of sediment traps and long-term lander deployed on moorings at the stations F4, EGC-I and HG-IV (Fig. 3.6). Overall, we recovered five sediment-traps, one long-term lander and deployed five sediment-traps and one long-term lander (Tab. 3.6).

Fig. 3.6: Deployment of sediment trap

Tab. 3.6: Overview exchange of long-term installations

Event	Station	Latitude	Longitude	Device ID	Depth [m]	Deployment period
Recoveries of moored sediment traps						
6_7	HG-IV	70°00.000' N	004°19.911' E	Fevi-46 upper	194	31.07.2024-31.05.2025
6_7	HG-IV	70°00.000' N	004°19.911' E	Fevi-46 lower	2333	31.07.2024-31.05.2025
18_3	EG-I	78°59.783' N	005°23.835' W	EGC-10	489	31.07-2024-31.05.2025
27_11	SV-IV F4S	79°00.701' N	007°02.053' E	F4S-8 upper	190	31.07.2024-31.05.2025
27_11	SV-IV F4S	79°00.701' N	007°02.053' E	F4S-8 lower	603	31.07.2024-31.05.2025
Recovery Long-term Lander						
25_2	HG-IV	79°01.777' N	004°13.317' E	Lander 2024	2530	31.07.2024-01.07.2025
Deployment of sediment traps						
8_2	HG-IV	79°00.010' N	004°19.890' E	Fevi-50 upper	199	15.06.2025-10.07.2026
8_2	HG-IV	79°00.010' N	004°19.890' E	Fevi-50 lower	2333	15.06.2025-10.07.2026
18_4	EG-I	79°02.070' N	005°23.489' W	EGC-11	509	17.06.2025-10.07.2026
29_2	SV-IV F4S	79°00.709' N	007°02.046' E	F4S-9 upper	196	01.07.2025-10.07.2026
29_2	SV-IV F4S	79°00.709' N	007°02.046' E	F4S-9 lower	605	01.07.2025-10.07.2026
Deployment of Long-term Lander						
33_2	HI-IV	79°01.913' N	004°13.631' E	Lander2025	2532	01.07.2025-01.07.2026

Preliminary (expected) results

Phytoplankton

The preliminary on-board analysis of the live net samples with the PlanktoScope revealed that the plankton distribution was rather patchy along the east-west transect (Fig. 3.7). *Phaeocystis pouchetii* for instance was very abundant in the central Hausgarten stations but represented only by a small number of cells in the region of Svalbard and the EG stations. *Melosira arctica* was mainly found at EG-III and EG-IV, but completely absent in most other sites. The Svalbard stations were dominated by *Chaetoceros sp.* and *Ciliophora*.

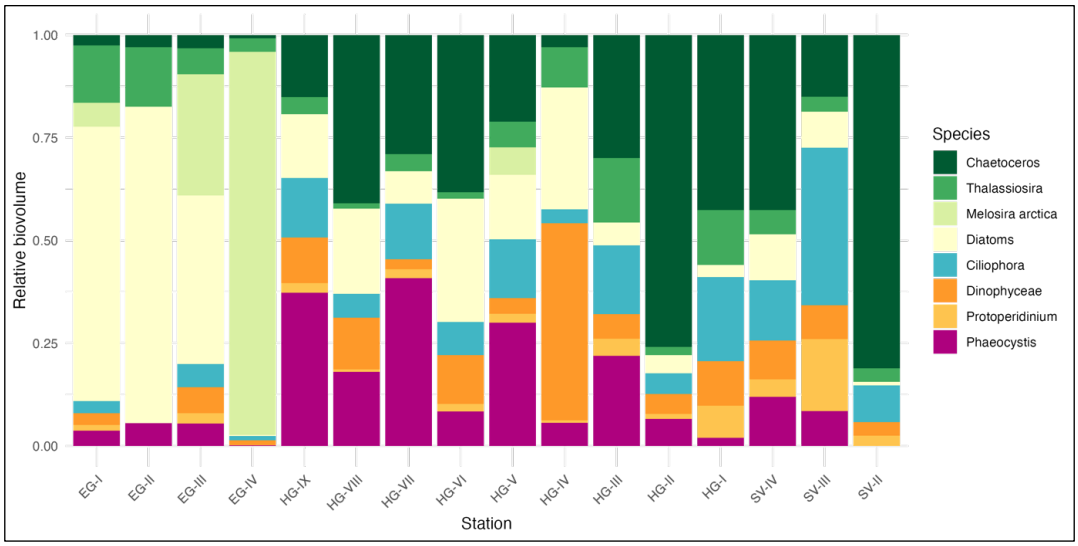

Fig. 3.7: Relative abundance of the preliminary life net phytoplankton PlanktoScope analysis

Particulate Organic Matter along the MIZ

Distribution of particulate organic material (POM) collected underway with the automated filtration device AUTOFIM on two transects along the MIZ varied strongly (Fig. 3.8).

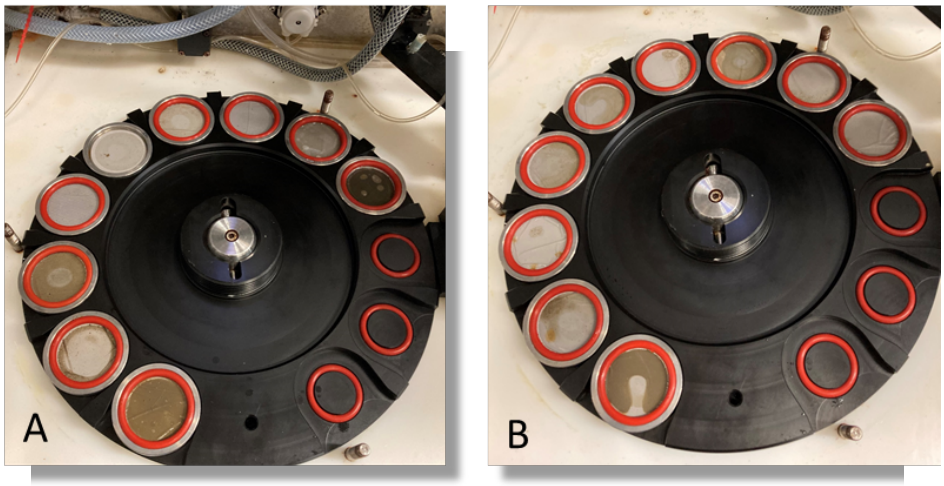

Fig. 3.8: Pictures showing the filters with POM collected on the transfer into the EGC (transect 1: 14.06.-15.06.2025; AF1 – AF9) and out of the EGC into the WSC (transect 2 19.06. -20.06.2025; AF19 – AF28). White filters reflect samples with low amounts of POM, while green filters reflect samples with high amounts of POM.

Sea Ice

Sea ice thickness varied strongly at the different ice-stations, with ~ 2.50 m at station Ice1, 1.50 m at stations Ice2 and Ice4, and 0.5 m at station Ice3. In the sea-ice covered area aggregates of *Melosira arctica* were visible in and under the ice in larger amounts (Fig. 3.9).

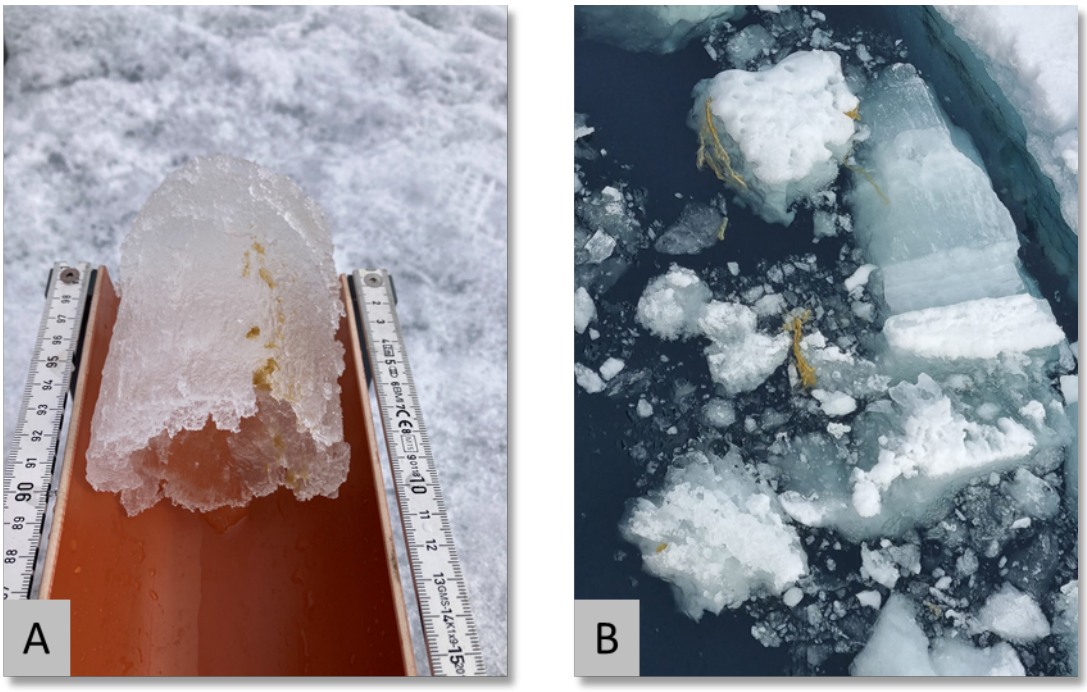

Fig. 3.9: Melosira arctica in a sea ice core (A) and at the interface of water and sea ice(B)

Zooplankton

During the preservation of MultiNet samples, we observed that the zooplankton abundances in the western part of the Fram Strait, influenced by the cold East Greenland Current, were generally lower as compared to those in the eastern part, influenced by the warm, saline West Spitsbergen Current. At all stations, the zooplankton community was dominated by calanoid copepods, i.e. *Calanus* spp.. *Metridia longa* was usually present below 200 m depth as evidenced by visible blue bioluminescence, along with other regularly occurring non-copepod zooplankton taxa such as chaetognaths, ostracods, amphipods, euphausiids, and jellyfish. A preliminary evaluation of LOKI and UVP5 images indicated that the deployments of both imaging systems were successful. The LOKI images revealed patterns that were similar to those observed in the MultiNet samples, but also showed the wide distribution of small cyclopoid copepod families such as Clausocalanidae, Oithonidae and Oncaeidae, as well as larval stages of both holoplanktonic and meroplanktonic organisms (Fig. 3.10). The UVP5 system enabled the observation of gelatinous zooplankton and larger zooplanktonic organisms. Detailed analyses of the MultiNet samples will be carried out later at the AWI laboratories in Bremerhaven using the ZooScan system. The LOKI and UVP5 data will be appropriately formatted and also processed at AWI Bremerhaven.

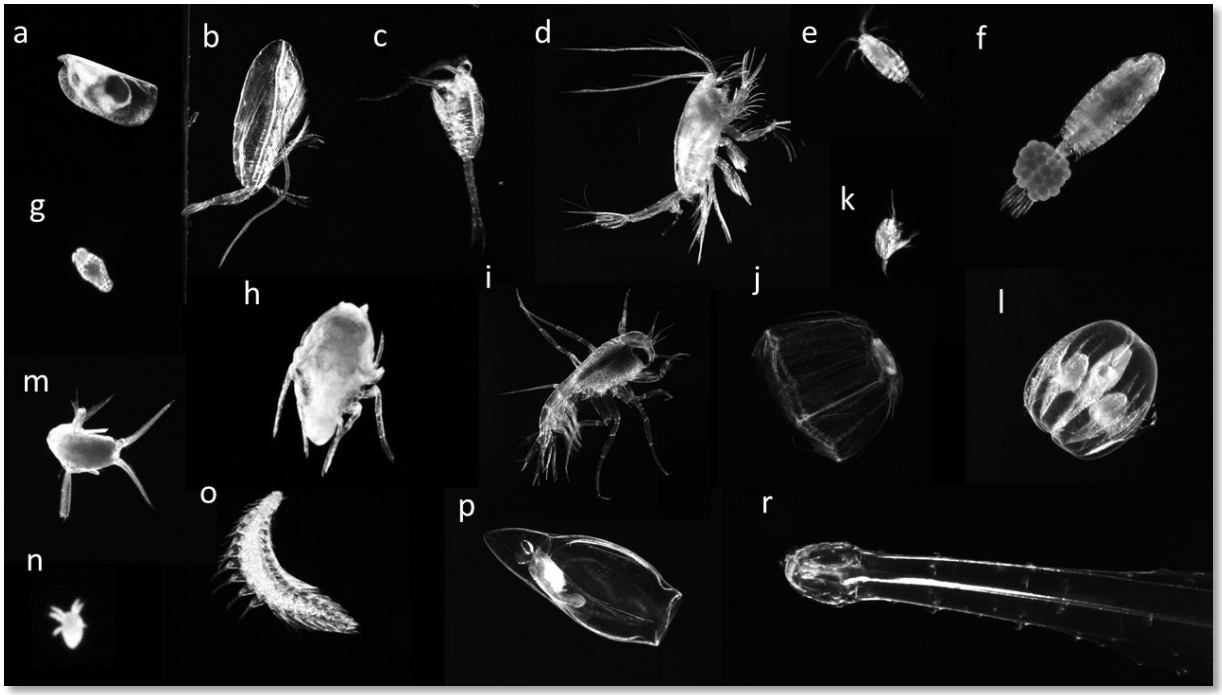

Fig. 3.10: Zooplankton images obtained by the LOKI system: Ostracoda (a), Calanus sp. (b), Metridia longa (c), Paraeuchaeta sp. (d), Acartia sp. (e), Aetideidae individual with eggs sacs (f), larval stage of Mollusca (g), Lanceola sp. (h), Themisto sp. (i), Botrynema sp. (j), Microcalanus sp. (k), Ctenophora (l), Scina sp. (m), nauplii (n), Pelagobia sp. (o), Siphonophorae (p), and Chaetognatha (r).

Data management

During our cruises, we sample a large variety of interrelated parameters. Many of the samples (i.e. Chl, 16S/18S eDNA, phytoplankton and zooplankton biodiversity etc.) will be analysed at AWI or GEOMAR within approximately one year after the cruise. We plan that the full data set will be available at the latest about two years after the cruise. Samples taken for microscopical and molecular analyses, which cannot be analysed within two years after the cruise, will be stored at the AWI for at least ten years and available upon request to other scientists.

Data will be archived, published and disseminated according to international standards by the World Data Center PANGAEA Data Publisher for Earth & Environmental Science (www.pangaea.de) within two years after the end of the expedition at the latest. By default, the CC-BY license will be applied. Molecular data (DNA and RNA data) will be archived, published and disseminated within one of the repositories of the International Nucleotide Sequence Data Collaboration (INSDC, www.insdc.org) comprising of EMBL-EBI/ENA, GenBank and DDBJ). Images from the zooplankton net samples as well as from both *in situ* optical recorders LOKI and UVP will be uploaded to the website EcoTaxa where they will not only be taxonomically analysed but also archived. The resulting tables presenting abundances and, in case of preserved organisms, also biomasses will be archived in PANGAEA. Any other data will be submitted to an appropriate long-term archive that provides unique and stable identifiers for the datasets and allows open online access to the data. Analysis of BOP and SWIPS-Particle-Camera is quite time consuming and will therefore be done in the home laboratories at AWI-Bremerhaven and MARUM.

This expedition was supported by the Helmholtz Research Programme “Changing Earth – Sustaining our Future” Topic 6, Subtopic 6.1.

In all publications based on this expedition, the Grant No. **AWI_PS148_02** will be quoted and the following publication will be cited:

Alfred-Wegener-Institut Helmholtz-Zentrum für Polar- und Meeresforschung (2017) Polar Research and Supply Vessel POLARSTERN Operated by the Alfred-Wegener-Institute. Journal of large-scale research facilities, 3, A119. http://dx.doi.org/10.17815/jlsrf-3-163.

References

Álvares E, Losa S N, Bracher A, Thoms S, Völker C (2022) Phytoplankton light absorption impacted by photoprotective carotenoids in a global ocean spectrally-resolved biogeochemistry model. Journal of Advances in Modeling Earth Systems 14: e2022MS003126. https://doi.org/10.1029/2022MS003126

Artigas F, Créach V, Houliez E, Karlson B, Lizon F, Seppälä J, Wacquet G (2019) Novel methods for automated in situ observations of phytoplankton diversity and productivity: synthesis of exploration, inter comparisons and improvements. WP 3 - D3.2. With assistance of Hedy Aardema, et al. Available online at https://www.jerico-ri.eu/previous-project/jerico-next/deliverables/, checked on 3/11/2024.

Bachy C, Sudek L, Choi CJ, Eckmann CA, Nöthig EM, Metfies K, Worden AZ (2022) Phytoplankton Surveys in the Arctic Fram Strait Demonstrate the Tiny Eukaryotic Alga Micromonas and Other Picoprasinophytes Contribute to Deep Sea Export. Microorganisms, 10(5):961. https://doi.org/10.3390/microorganisms10050961

Bauerfeind E, Nöthig EM, Pauls B, Kraft A, Beszczynska-Möller A (2014) Variability in pteropod sedimentation and corresponding aragonite flux at the Arctic deep-sea long-term observatory HAUSGARTEN in the eastern Fram Strait from 2000 to 2009. Journal of Marine Systems, 132:95–105. https://doi.org/10.1016/j.jmarsys.2013.12.006

Bracher A, Vountas M, Dinter T, Burrows JP, Röttgers R, Peeken I (2009) Quantitative observation of cyanobacteria and diatoms from space using PhytoDOAS on SCIAMACHY data. Biogeosciences 6: 751-764. https://doi.org/10.5194/bg-6-751-2009

Buaya AT, Ploch S, Hanic L, et al. (2017) Phylogeny of Miracula helgolandica gen. et sp. nov. and Olpidiopsis drebesii sp. nov., two basal oomycete parasitoids of marine diatoms, with notes on the taxonomy of Ectrogella-like species. Mycol Progress 16:1041–1050. https://doi.org/10.1007/s11557-017-1345-6

Buaya A, Kraberg A, Thines M (2019) Dual culture of the oomycete Lagenisma coscinodisci Drebes and Coscinodiscus diatoms as a model for plankton/parasite interactions. Helgoland Marine Research 73:2. https://doi.org/10.1186/s10152-019-0523-0

Busch K, Bauerfeind E, Nöthig EM (2015) Pteropod sedimentation patterns in different water depths observed with moored sediment traps over a 4 year period at the LTER station HAUSGARTEN in eastern Fram Strait. Polar Biology, 38:845–859. https://doi.org/10.1007/s00300-015-1644-9

Cornils A, Thomisch K, Hase J, Hildebrandt N, Auel H, Niehoff B (2022) Testing the usefulness of optical data for zooplankton long-term monitoring: Taxonomic composition, abundance, biomass, and size spectra from ZooScan image analysis. Limnology and Oceanography: Methods 20(7):428–450. https://doi.org/10.1002/lom3.10495

Engel A, Piontek J, Metfies K, Endres S, Peeken I, Gäbler-Schwarz S, Nöthig EM (2017) Inter-annual variability of transparent exopolymer particles in the Arctic Ocean reveals high sensitivity to ecosystem changes. Scientific Reports, 7:4129. https://doi.org/10.1038/s41598-017-04106-9

Engel A, Bracher A, Dinter T, Endres S, Grosse J, Metfies K, Peeken I, Piontek J, Salter I, Nöthig E-M (2019) Inter-Annual Variability of Organic Carbon Concentration in the Eastern Fram Strait During Summer (2009–2017). Frontiers in Marine Science, 6:187. https://doi.org/10.3389/fmars.2019.00187

Fadeev E, Rogge A, Ramondenc S, Nöthig EM, Wekerle C, Bienhold C, Salter I, Waite A, Hehemann L, Boetius A, Iversen M (2021) Sea ice presence is linked to higher carbon export and vertical microbial connectivity in the Eurasian Arctic Ocean, Communications Biology, 4:1255. https://doi.org/10.1038/s42003-021-02776-w

Hassett BT, Bo rrego EJ, Vonnahme TR, et al (2019a) Arctic marine fungi: biomass, functional genes, and putative ecological roles. ISME J 13:1484–1496. https://doi.org/10.1038/s41396-019-0368-1

Hassett BT, Thines M, Buaya A, et al. (2019b) A glimpse into the biogeography, seasonality, and ecological functions of arctic marine Oomycota. IMA Fungus 10:6. https://doi.org/10.1186/s43008-019-0006-6

Hátún H, Azetsu-Scott K, Somavilla R, et al. (2017) The subpolar gyre regulates silicate concentrations in the North Atlantic. Scientific Reports, 7:14576. https://doi.org/10.1038/s41598-017-14837-4

Heinrichs ME, Piedade GJ, Popa O, Sommers P, Tubl G, Weissenbach J, Rhalff J (2024). Breaking the Ice: A Review of Phages in Polar Ecosystems. Methods in Molecular Biology, 2738:31–71. https://doi.org/10.1007/978-1-0716-3549-03/TABLES/1

Hirata, T, Hardman-Mountford NJ, Brewin RJW, Aiken J, Barlow R, Suzuki K et al. (2011): Synoptic relationships between surface Chlorophyll-a and diagnostic pigments specific to phytoplankton functional types. Biogeosciences 8:311–327. https://doi.org/10.5194/bg-8-311-2011

Houliez E, Lizon F, Thyssen M, Artigas LF, Schmitt FG (2012): Spectral fluorometric characterization of Haptophyte dynamics using the FluoroProbe: an application in the eastern English Channel for monitoring Phaeocystis globosa. Journal of Plankton Research 34:136–151. https://doi.org/10.1093/plankt/fbr091

von Jackowski A, Becker KW, Wietz M, Bienhold C, Zäncker B, Nöthig EM, Engel A (2022) Variations of microbial communities and substrate regimes in the eastern Fram Strait between summer and fall" Environmental Microbiology 24:4124–4136. https://doi.org/10.1111/1462-2920.16036

John SG, Mendez CB, Deng L et al. (2011). A simple and efficient method for concentration of ocean viruses by chemical flocculation. Environmental Microbiology Reports, 3:195–202. https://doi.org/10.1111/J.1758-2229.2010.00208.X

Lalande C, Nöthig E-M, Fortier L (2019) Algal Export in the Arctic Ocean in Times of Global Warming Geophysical Research Letters. https://doi.org//10.1029/2019GL083167

Kraft A, Nöthig EM, Bauerfeind E, Wildish DJ, Pohle GW, Bathmann UV, Beszczynska-Möller A, Klages M. (2013) First evidence of reproductive success in a southern invader indicates possible community shifts among Arctic zooplankton. Marine Ecological Progress Series, 493:291–296. https://doi.org/10.3354/meps10507

Krause JW, Schulz IK, Rowe KA, et al. (2019) Silicic acid limitation drives bloom termination and potential carbon sequestration in an Arctic bloom. Scientific Reports, 9:8149. https://doi.org/10.1038/s41598- 019-44587-4

Kaiser P, Hagen W, Schukat A, Metfies K, Biederbick J, Dorschner S, Auel H (2024) Phytoplankton diversity and zooplankton diets across Fram Strait: Spatial patterns with implications for the future Arctic Ocean, Progress in Oceanography, submitted

Metfies K, von Appen WJ, Kilias E, Nicolaus A, Nöthig EM (2016) Biogeography and photosynthetic biomass of Arctic marine pico-eukaryotes during summer of the record sea ice minimum 2012. PLoS ONE 11. https://doi.org/10.1371/journal.pone.0148512

Nöthig E-M, Bracher A, Engel A, Metfies K, Niehoff B, Peeken I, et al. (2015) Summertime plankton ecology in Fram Strait - a compilation of long- and short-term observations. Polar Research, 34:23349. https://doi.org/10.3402/polar.v34.23349

Nöthig EM, Ramondenc S, Haas A, Hehemann L, Walter A, Bracher A, Lalande C, Metfies K, Peeken I, Bauerfeind E, Boetius A (2020) Summertime Chlorophyll a and Particulate Organic Carbon Standing Stocks in Surface Waters of the Fram Strait. Frontiers of Marine Systems 7. https://doi.org/10.3389/fmars.2020.00350

Oelker J, Losa S N, Richter A, Bracher A (2022) TROPOMI-retrieved underwater light attenuation in three spectral regions in the ultraviolet to blue. Frontiers in Marine Science 9: 787992. https://doi.org/10.3389/fmars.2022.787992

Oldenburg E, Popa O, Wietz M, von Appen WJ, Torres-Valdes S, Bienhold C, Ebenhöh O, Metfies K (2024) Sea-ice melt determines seasonal phytoplankton dynamics and delimits the habitat of temperate Atlantic taxa as the Arctic Ocean atlantifies, ISME communications, ycae027. https://doi.org/10.1101/2023.05.04.539293

Suttle CA (2007). Marine viruses—major players in the global ecosystem. Nature Reviews Microbiology, 5:801–812. https://doi.org/10.1038/nrmicro1750

Schoemann V, Becquevort S, Stefels J, Rousseau V, Lancelot, C (2005): Phaeocystis blooms in the global ocean and their controlling mechanisms: a review. Journal of Sea Research 53: 43–66. https://doi.org/10.1016/j.seares.2004.01.008

Soltwedel T, Bornemann H (2023): The Expedition PS136 of the Research Vessel POLARSTERN to the Fram Strait in 2023. In Berichte zur Polar- und Meeresforschung = Reports on polar and marine research 780. https://doi.org/10.57738/BzPM_0780_2023

Taylor BB, Torrecilla E, Bernhardt A, Taylor MH, Peeken I, Röttgers R, Piera J, Bracher A (2011) Bio-optical provinces in the eastern Atlantic Ocean. Biogeosciences 8: 3609-3629. https://doi.org/10.5194/bg-8-3609-2011

Thyssen M, Alvain S, Lefèbvre A, Dessailly D, Rijkeboer M, Guiselin N. et al. (2015): High-resolution analysis of a North Sea phytoplankton community structure based on in situ flow cytometry observations and potential implication for remote sensing. Biogeosciences 12: 4051–4066. https://doi.org/10.5194/bg-12-4051-2015

von Appen WJ, Waite AM, Bergmann M, Bienhold C, Boebel O, Bracher A, Cisewski B, Hagemann J, Hoppema M, Iversen MH, Konrad C, Krumpen T, Lochthofen N, Metfies K, Niehoff B, Nöthig EM, Purser A, Salter I, Schaber M, Scholz D, Soltwedel T, Torres-Valdes S, Wekerle C, Wenzhöfer F, Wietz M, Boetius A (2021) Sea-ice derived meltwater stratification slows the biological carbon pump: results from continuous observation, Nature Communications, 12:7309. https://doi.org/10.1038/s41467-021-26943-z

von Jackowski A, Becker KW, Wietz M, Bienhold C, Zäncker B, Nöthig EM, Engel A (2022) Variations of microbial communities and substrate regimes in the eastern Fram Strait between summer and fall" Environmental Microbiology, 24:4124–4136. https://doi.org/10.1111/1462-2920.16036

Weiss J, von Appen WJ, Niehoff B, Hildebrand N, Graeve M, Neuhaus S, Bracher A, Nöthig EM, Metfies K (2024) Unprecedented insights into extents of biological responses to physical forcing in an Arctic sub-mesoscale filament by combining high-resolution measurement approaches, Scientific Reports, accepted

Wietz M, Bienhold C, Metfies K, Torres-Valdes S, von Appen WJ, Salter I, Boetius A (2021) The polar night shift: seasonal dynamics an drivers of Arctic Ocean microbiomes revealed by autonomous sampling", ISME Communications 1:76. https://doi.org/10.1038/s43705-021-00074-4

Xi H, Losa SN, Mangin A, Garnesson P, Bretagnon M, Demaria J, Soppa MA, d'Andon OHF, Bracher A (2021) Global chlorophyll a concentrations of phytoplankton functional types with detailed uncertainty assessment using multi-sensor ocean color and sea surface temperature satellite products. Journal of Geophysical Research - Oceans 126: e2020JC017127. https://doi.org/10.1029/2020JC017127

4. PHYSICAL OCEANOGRAPHY AND PHYTOOPTICS

Rebecca McPherson*[1], Luise Becker[1,3], Moritz Zeising[1], Ina Schmidt[1], Jan Bretinger[1,2]

Not on board: Wilken-Jon von Appen[1], Astrid Bracher[1,3], Sonja Wiegmann[1], Hongyan Xi[1]

* rebecca.mcpherson@awi.de

[1]DE.AWI

[2]DE.UNI-DUE

[3]DE.UNI-Bremen

Grant-No. AWI_PS148_04

Objectives

The physical conditions that lead to enhanced primary and export production in the Arctic Ocean remain poorly understood. As ocean temperatures continue to rise—particularly in the Arctic, where warming is amplified—and sea ice retreats further each year, understanding how these physical changes affect polar marine ecosystems becomes increasingly critical.

The recirculation of Atlantic Water (AW) through Fram Strait regulates how much warm, nutrient-rich AW enters the Arctic Ocean via the northward-flowing West Spitsbergen Current (WSC). This inflow determines oceanic heat transport and influences the extent of the partially ice-free halocline north of Svalbard. It also affects light and nutrient availability, shaping habitat distribution, Arctic biogeography, and their future evolution. A monitoring programme for AW inflow via the WSC was initiated in 1997. Cruise PS148 contributed to the maintenance of this long-standing time series, which captures key physical, biogeochemical, and biological changes in the Arctic Ocean.

Intermittent sea-ice cover and surface meltwater influence the vertical structure of both physical and biochemical properties in the water column. They also limit direct observations to the ice-free summer months. Long-term monitoring is essential to detect the effects of environmental change on polar marine biodiversity. The *Frontiers in Arctic Marine Monitoring* (FRAM) Helmholtz infrastructure initiative enhances our ability to track the temporal evolution of the coupled physical–chemical–biological system from the ocean surface to the seafloor.

The HAUSGARTEN observatory includes CTD water sampling stations across contrasting regimes: the Atlantic-influenced West Spitsbergen Current (east Fram Strait), the Arctic-influenced East Greenland Current (west Fram Strait), and transitional zones in the central and northern parts of the strait (Fig. 4.1). The FRAM observatory further supports this effort through year-round moored observations, collecting sensor data and physical samples across representative sites of those different water masses. These observations span the entire water column, with a particular focus on the upper euphotic zone. Maintaining these interdisciplinary time series allows for the evaluation of multi-decadal and interannual variability, as well as shorter-term processes on seasonal to mesoscale timescales. The moorings – equipped with a diverse array of physical and biogeochemical sensors (see details below) – enable direct comparisons between environmental drivers and ecosystem responses in Fram Strait.

Within the framework of FRAM and its continuation, two primary multidisciplinary time series sites were targeted (Fig. 4.1):

- F4 (also referred to as HG-IV): Located at ~1,200 m water depth within the inflowing AW boundary current of the WSC.
- EG-I: Located at ~1,000 m depth within the outflowing Polar Water boundary current of the East Greenland Current (EGC).

These contrasting sites—situated within distinct water masses representing endpoints of Arctic environmental conditions—serve as critical reference points for understanding current trends and projecting future changes in the Arctic Ocean.

During PS148, the Phytooptics team focused on the continuation of the high-resolution time series data on phytoplankton, particulate and chromophoric dissolved organic matter (CDOM) abundance and composition in conjunction with the PEBCAO team on board. Optical measurements directly give information on inherent and apparent optical properties (IOPs, and AOPs, respectively) and were acquired continuously. The aim was to determine the phytoplankton overall (Total) and group specific Chlorophyll *a* (Chla) concentration as well as the concentration of other pigments, and also the absorption by other particles and coloured dissolved organic matter. This large data set will be combined with ocean colour satellite data to upscale the station-based information on linkages between the various trophic layers and biogeochemical cycling. Furthermore, these data will be used for validating several ocean colour satellite products (e.g., Oelker et al. 2022; Xi et al. 2021; Bracher et al. 2009).

The group's specific objectives for PS148 were to

- collect a highly spatially and temporally resolved data set on phytoplankton (total and composition) and its degradation products at the surface and for the full euphotic zone using continuous optical observations during the cruise and from ocean colour remote sensing calibrated with discrete water sample measurements,
- develop and validate (global and regional) algorithms and associated radiative transfer models in accordance to the previous objective by using discrete water samples for pigment analysis and absorption measurement,
- obtain a big data set for ground-truthing ocean colour satellite data, specifically from the PACE, Sentinel-3 (A and B) OLCI and the Sentinel-5-Precursor TROPOMI sensors,
- obtain a spectral characterisation of the underwater light field and its interplay with optical constituents, such as phytoplankton and CDOM abundance and composition.

Work at sea

The cruise covered a number of working areas over the duration of PS148 (Fig. 4.1).

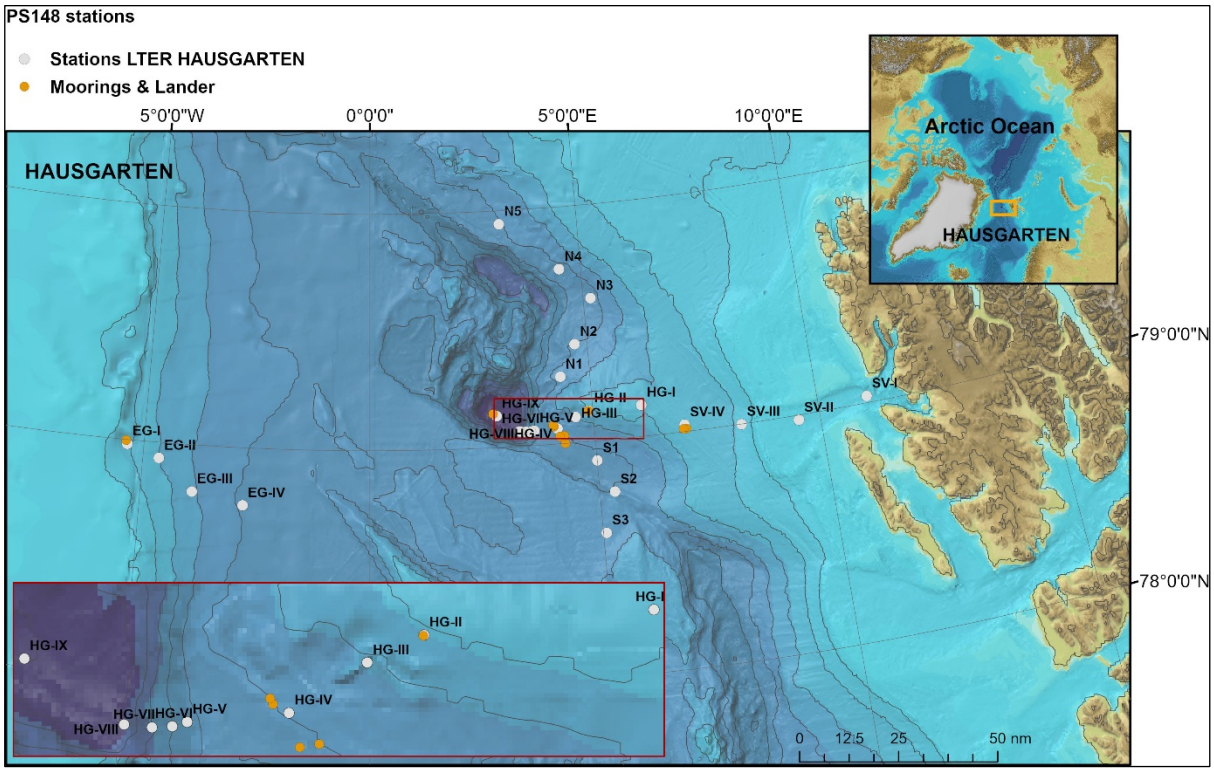

Fig. 4.1: Map of Arctic Ocean and HAUSGARTEN area marked (yellow box); zoomed in HAUSGARTEN region with the CTD stations (grey), and mooring sites (orange) from PS148. Each site is labelled.

Moorings

Recoveries

During expedition PS148, a total of four moorings were successfully recovered: three from the central HAUSGARTEN area, and one from the East Greeland continental shelf (Fig. 4.1, Tab. 4.1). All had been deployed in summer 2023 during PS143_2 and had sampled continuously for one year. A total of 58 instruments (hydrographic and biogeochemical) were recovered without major complications or losses. Conditions at the central HAUSGARTEN sites were ideal, with no sea ice and calm seas, facilitating smooth recovery operations.

At HG-IV-FEVI48, some line entanglement occurred near the bottom of the mooring, likely due to the low wind conditions keeping the ship and floats relatively stationary, allowing slack line to rise upwards. This delayed recovery slightly but caused no instrument damage.

The mooring F4-W5 was partially recovered using a Zodiac. The winch and profiler, released separately, were retrieved by the Zodiac, while the lower section, including the BioOptical Platform, was recovered via the ship's side as is normal procedure. The winch system on F4-W5 appeared not to have functioned as programmed. Preliminary observations suggest the corrosion links securing the profiler did not release in the time-frame estimated. As a result, the winch attempted to initiate a profile, tightening repeatedly without spooling the cable. This likely led to the cable embedding into the drum. However, the exact cause remains uncertain and requires further investigation.

In contrast, the EGC site was heavily ice-covered, with both first-year, relatively thin, sea ice and multi-year sea ice thicker than 2m. Fortunately, a large lead had opened over the mooring position, allowing recovery, though the process had to be expedited as the lead began to close.

Unusually, both ocean currents and sea ice were flowing northward during the mooring operations at the site – opposite to the typical southwards flow of the EGC boundary current. Northerly winds also prevailed, contrary to expectations. The VMADCP data also confirmed that the northward/north-northwestward flow persisted for over 24 hours. These conditions were taken into account by the Bridge when positioning the ship to recover the EGC-10 mooring.

All hydrographic instruments and the ADCPs were downloaded onboard (except one) had sampled successfully throughout the deployment. The ADCP on F4-S-8 was found to have flooded, and no data were recovered. The timing of the flooding remains unknown. Battery life and instrument programming were otherwise without issue.

Deployments

A total of four moorings were redeployed during PS148 (Tab. 4.1). Minor adjustments were made to sensor placements – especially within the upper 50m - to improve resolution of the near-surface physical and biological structure of the upper water column.

At the EGC site, a large ice floe covered the intended deployment position of HG-EGC-11, so the mooring was deployed approximately 1 nautical mile away, following the 1,000m isobath of the continental shelf and where a lead had opened in the heavy sea-ice cover.

The BioOptical Platform (BOP) originally planned for redeployment on F4-W-6 was instead deployed at the Molloy Deep site (Frank Wenzhöfer). Due to insufficient turnaround time for the BOP recovered from F4-W-5 (the deployment followed the recovery by one day, while ~2 days were needed for refurbishment), no BOP was installed on F4-W-6. Minor modifications to buoyancy and mooring line configuration were made to ensure the winch maintained its target depth. The F4-W-6 deployment proceeded smoothly.

Calm sea conditions prevailed during all deployments. Aside from heavy ice cover at the EGC site, little to no sea ice was present at the remaining stations.

Tab. 4.1: Summary of all the mooring stations for both deployments and recoveries during PS148

Name	Longitude		Latitude		Depth	Top	Deployment time UTC					Deployment station	Recovery time UTC					Recovery station
	Degrees	Minutes	Degrees	Minutes	Meters	Meters	Year	Month	Day	Hour	Minute		Year	Month	Day	Hour	Minute	
Recoveries																		
F4-S-8	7	2.05 E	79	0.70 N	1222	19	2024	7	17	16	50	PS143_2_010_01	2025	6	22	17	6	PS148_027_11
F4-W-5	6	58.02 E	79	0.71 N	1213	134	2024	7	20	14	20	PS143_2_021_01	2025	6	22	15	48	PS148_027_10
HG-IV-FEVI-48	4	19.91 E	79	0.00 N	2531	34	2024	7	29	19	40	PS143_2_059_02	2025	6	8	7	41	PS148_006_07
HG-EGC-10	5	23.83 W	78	59.78 N	979	49	2024	7	28	8	16	PS143_2_057_01	2025	6	16	4	59	PS148_018_03
LT-Lander-2024	4	13.40 E	79	1.86 N	2526	2524	2024	7	29	20	33	PS143_2_059_03	2025	6	21	7	22	PS148_025_02
Deployments																		
F4-S-9	7	2.08 E	79	0.70 N	1240	15	2025	6	23	13	38	PS148_029_02						
F4-W-6	6	58.05 E	79	0.70 N	1223	131	2025	6	23	15	21	PS148_029_03						
HG-IV-FEVI-50	4	19.90 E	78	59.99 N	2535	43	2025	6	9	11	11	PS148_008_02						
HG-EGC-11	5	27.95 W	79	3.02 N	1040	55	2025	6	16	14	20	PS148_018_04						
LT-Lander-2025	4	13.64 E	79	1.89 N	2532	2530	2025	6	24	22	49	PS148_033_02						

CTD

A total of 37 CTD casts were conducted during PS148 using a 24-bottle rosette system (12 L Niskin bottles) provided by the Physical Oceanography group at DE.AWI (“OZE rosette”). Metadata for all CTD stations are listed in Tab. 4.2.

Sensor Configuration

The standard sensor configuration ("conf1") of the CTD system throughout the cruise consisted of two temperature sensors, two conductivity cells, a pressure sensor, two oxygen sensors, two fluorescence sensors, a transmissometer and a photosynthetically active radiation (PAR) sensor.

A SUNA nitrate sensor was installed on the rosette and included on all casts shallower than 2000 m, in accordance with its depth rating. For casts deeper than 200 m, an Underwater Vision Profiler (UVP) was also run. The UVP was powered by an external battery and activated automatically when the rosette descended below 20 m; it deactivated when the ascent exceeded 30 m.

Sampling Procedure

When the UVP was running, casts began with a short descent to ~22 m where the CTD waited to initiate the pumps, followed by a return to the surface. The downcast proceeded at 0.5 m/s for the first 100 m, then increased to 1 m/s. Near the bottom, the speed was reduced again: to 0.5 m/s approximately 150 m above the seafloor, and 0.2 - 0.3 m/s within 100 m. Casts targeted a maximum depth ~50 m above bottom. Water samples were taken on the upcast, with Niskin bottles triggered after a 60-second pause at each target depth to allow sensor stabilization and ensure accurate sampling.

Technical Issues

Several operational issues were encountered during the cruise.

Computer Failures:

- After cast PS148_07_01, the CTD computer froze, the screen turned black and required a restart.
- During PS148_014_02, the system blacked out momentarily, then shut down during the upcast after the first bottle had been triggered. A new file was initiated upon restart, resulting in two files for the station:
    - *PS148_014_02* (downcast + first bottle)
    - *PS148_014_02_2* (upcast + bottles 2–24)

  Both files were complete and not corrupted.

No further computer issues occurred after this cast.

Niskin Bottle Closures:
Some bottles failed to close, with varying bottle numbers affected between casts. The release mechanisms were rinsed and tested after each failure, which generally resolved the issue.

- Bottle 24 consistently failed to close for the first three casts and was swapped with bottle 23 on 10.06.2025, prior to cast PS148_010_02**.** This switch resolved the issue and was maintained for the remainder of the cruise.
- During PS148_021_02**,** the bottom O-ring on bottle 4 slipped and meant water was leaking from the bottom of the Niskin. The bottle was replaced for cast PS148_021_14**,** the O-ring repaired, and bottle 4 was reinstalled for subsequent casts with no further issues.

Winch Operations:

The principal winch used was EL31, which functioned for most of the cruise. Key exceptions include:

- PS148_009_06:
  The CTD was lowered to 5,500 m (Molloy Deep), but a coil error during the upcast forced repeated lowering and heaving by up to 100 m to continue the cast. This resulted in major delays and the full cast lasted almost 7 hours until the CTD was back on deck. This procedure was repeated in subsequent casts with similar issues.
- PS148_023_01:
  A major technical issue of EL31 occurred during the downcast, and the cast was aborted at 150 m. No bottles were closed, but hydrographic data was saved.
- PS148_027_01 to PS148_028_03:
  The winch was temporarily replaced with AWI004 (EL30). However, due to the winch's weight limitations, only 17 bottles could be triggered per cast to ensure the total weight was less than 1 tonne (the empty CTD weighed 780 kg). Multiple casts at the same station were performed to collect sufficient water. Bottles were triggered in a way that balanced weight evenly across the rosette.
- From PS148_029_04 onward:
  EL31 was back in operation. Minor lowering/heaving was still required during upcasts, but no significant issues occurred.

Tab. 4.2: Meta-data of all CTD stations from PS148. The station names refer to the file numbers and header information of the CTD files

Station	Name	Date (DD.MM.YY)	Time (UTC)	Latitude	Longitude	Water depth (m)	CTD depth (m)
PS148_001_01	AG1	01/06/25	20:19	66°22.362'N	00°15.785'E	3091	3070
PS148_002_02	AG5	03/06/25	03:12	69°49.179'N	01°57.085'E	3219	3180
PS148_004_01	AG7	05/06/25	10:32	75°40.417'N	02°55.780'E	3083	3051
PS148_005_01	S3	06/06/25	13:39	78°36.536'N	05°03.725'E	2280	99
PS148_005_03	S3	06/06/25	15:01	78°36.577'N	05°03.984'E	2280	1750
PS148_006_04	HG-IV	07/06/25	23:51	79°03.960'N	04°10.800'E	2408	2356
PS148_006_13	HG-IV	08/06/25	16:25	79°03.895'N	04°10.946'E	2407	1750
PS148_007_01	HG-III	09/06/25	00:26	79°06.527'N	04°35.746'E	1855	1750
PS148_009_01	HG-IX	09/06/25	19:00	79°08.014'N	02°50.449'E	5543	1750
PS148_009_06	HG-IX	10/06/25	01:35	79°08.004'N	02°50.386'E	5540	5500
PS148_010_02	HG-VIII	10/06/25	21:55	79°03.862'N	03°20.003'E	5072	1750
PS148_011_01	HG-VII	11/06/25	01:05	79°03.587'N	03°28.620'E	4028	1750
PS148_012_01	HG-V	11/06/25	10:38	79°03.823'N	03°39.155'E	3110	1750
PS148_013_04	N5	12/06/25	02:03	79°56.676'N	03°07.164'E	2500	1750
PS148_014_02	N4	13/06/25	00:10	79°44.182'N	04°29.528'E	2661	1750
PS148_014_08	N4	13/06/25	07:54	79°44.144'N	04°29.795'E	2685	2656
PS148_016_02	N3	14/06/25	07:05	79°36.246'N	05°10.316'E	2725	1750
PS148_017_01	EG-I	15/06/25	12:33	78°58.782'N	05°27.162'W	927	898
PS148_018_01	EG-II	16/06/25	03:15	79°02.170'N	05°29.330'W	984	100
PS148_018_05	EG-II	16/06/25	15:20	79°03.778'N	05°31.800'W	999	100
PS148_019_01	EG-II	16/06/25	18:13	78°55.678'N	04°40.712'W	1472	1423

Station	Name	Date (DD.MM.YY)	Time (UTC)	Latitude	Longitude	Water depth (m)	CTD depth (m)
PS148_020_01	EG-III	17/06/25	06:37	78°48.240'N	03°54.533'W	1920	1750
PS148_021_02	EG-IV	17/06/25	22:55	78°45.420'N	02°46.876'W	2552	1750
PS148_021_14	EG-IV	19/06/25	03:44	78°45.406'N	02°46.146'W	2559	2518
PS148_023_01	HG-VI	20/06/25	13:20	79°03.613'N	03°35.317'E	3453	150
PS148_027_01	SV-IV	22/06/25	05:07	79°00.695'N	06°01.957'E	1710	100
PS148_027_04	SV-IV	22/06/25	06:04	79°00.712'N	06°02.034'E	1710	1676
PS148_027_09	F4	22/06/25	14:12	79°00.917'N	06°59.608'E	1236	100
PS148_028_01	SV-I	22/06/25	23:44	79°01.728'N	10°48.947'E	320	100
PS148_028_03	SV-I	23/06/25	00:54	79°01.854'N	10°48.881'E	330	276
PS148_029_04	F4	23/06/25	15:44	79°00.785'N	06°56.332'E	1217	100
PS148_029_04	SV-IV	23/06/25	18:46	79°01.090'N	07°00.356'E	1245	1205
PS148_030_01	SV-III	23/06/25	21:38	79°00.046'N	08°14.837'E	872	833
PS148_031_01	SV-II	24/06/25	01:26	78°58.693'N	09°30.197'E	213	177
PS148_034_01	HG-VI	24/06/25	23:56	79°03.682'N	03°34.678'E	3504	1751
PS148_035_05	HG-I	25/06/25	16:40	79°08.015'N	06°05.731'E	1240	1200
PS148_036_01	HG-II	26/06/25	03:23	79°07.819'N	04°54.166'E	1508	1461

Salinometer (OPS)

To obtain high-precision salinity measurements from CTD water samples, an Optimare Precision Salinometer (OPS, SN006) was used. These measurements can be used for potential recalibration of the CTD's conductivity sensors.

A total of 28 samples were collected, from depths with minimal salinity and temperature gradients—typically well-mixed layers. Of these, 26 samples were successfully measured.

Sampling was conducted using glass bottles with rubber caps. Each bottle was rinsed three times with sample water before being filled and sealed with a rubber stopper and an additional aluminum cap.

Prior to measurement:

- Samples were heated in a water bath to 30 °C for at least one hour the day before analysis.
- A surgical needle was used to release internal pressure.
- Bottles were then left to equilibrate at room temperature for at least 15 hours.

The salinometer was initially rinsed multiple times using expired standard seawater, followed by calibration with fresh standard seawater. Once standardization was successful, the sample measurements were performed. Two samples could not be measured due to initial issues with salinometer operation. These were likely caused by rinsing with high-salinity water which prevented proper standardization and invalid measurements for the two water samples. The issue was resolved by thoroughly cleaning the system and rinsing it—using both open and closed loops—with expired standard seawater before reattempting standardization.

The results of the salinity measurements are summarized in Tab. 4.3.

Tab. 4.3: Results of the salinometer measurements and comparison with salinity measurements from CTD bottle files

Station	Date (DD.MM.YY)	Niskin Bottle	Press [dbar]	Sal00	Sal01	OPS	OPS - Sal00	OPS - Sal01
PS148_004_01	05/06/25	3	2031	34.9146	34.9192	34.9165	0.0019	-0.0027
PS148_004_01	05/06/25	3	2031	34.9146	34.9192	34.9163	0.0017	-0.0029
PS148_004_01	05/06/25	6	1217	34.9093	34.9138			
PS148_004_01	05/06/25	6	1217	34.9093	34.9138			
PS148_005_03	06/06/25	1	1777	34.9132	34.9175	34.9155	0.0023	-0.0020
PS148_005_03	06/06/25	1	1777	34.9132	34.9175	34.9154	0.0022	-0.0021
PS148_005_03	06/06/25	4	1217	34.9108	34.9152	34.9130	0.0022	-0.0022
PS148_005_03	06/06/25	4	1217	34.9108	34.9152	34.9137	0.0029	-0.0015
PS148_006_04	07/06/25	2	2031	34.9168	34.9208	34.9184	0.0016	-0.0024
PS148_006_04	07/06/25	2	2031	34.9168	34.9208	34.9183	0.0015	-0.0025
PS148_006_04	07/06/25	7	1014	34.9078	34.9117	34.9102	0.0024	-0.0015
PS148_006_04	07/06/25	7	1014	34.9078	34.9117	34.9098	0.002	-0.0019
PS148_007_01	09/06/25	1	1777	34.9148	34.9189	34.9171	0.0023	-0.0018
PS148_007_01	09/06/25	1	1777	34.9148	34.9189	34.9173	0.0025	-0.0016
PS148_007_01	09/06/25	3	1217	34.9108	34.9149	34.9136	0.0028	-0.0013
PS148_007_01	09/06/25	3	1217	34.9108	34.9149	34.9134	0.0026	-0.0015
PS148_009_06	10/06/25	7	2542	34.9236	34.9268	34.9233	-0.0003	-0.0035
PS148_009_06	10/06/25	7	2542	34.9236	34.9268	34.9223	-0.0013	-0.0045
PS148_009_06	10/06/25	10	1216	34.9118	34.9152	34.9127	0.0009	-0.0025
PS148_009_06	10/06/25	10	1216	34.9118	34.9152	34.9126	0.0008	-0.0026
PS148_011_01	11/06/25	1	1777	34.917	34.9207	34.9187	0.0017	-0.0020
PS148_011_01	11/06/25	1	1777	34.917	34.9207	34.9184	0.0014	-0.0023
PS148_011_01	11/06/25	3	1217	34.9116	34.9154	34.9133	0.0017	-0.0021
PS148_011_01	11/06/25	3	1217	34.9116	34.9154	34.9133	0.0017	-0.0021
PS148_021_14	19/06/25	5	2031	34.9149	34.9183	34.9160	0.0011	-0.0023
PS148_021_14	19/06/25	5	2031	34.9149	34.9183	34.9162	0.0013	-0.0021
PS148_021_14	19/06/25	8	1522	34.9124	34.9156	34.9137	0.0013	-0.0019
PS148_021_14	19/06/25	8	1522	34.9124	34.9156	34.9137	0.0013	-0.0019
						mean	0.0016	-0.0022
						std	0.0009	0.0007

Underway measurements

During PS148, standard oceanographic underway measurements by means of a thermosalinograph (TSG) with a double sensor configuration, as well as a vessel-mounted ADCP (VMADCP), were continuously recorded.

Optical Measurements

Active and passive bio-optical measurements for the survey of the underwater light field, specific light attenuation, as well as particle and phytoplankton composition and distribution were performed continuously both on the surface water and also in the profile during CTD stations:

a. Continuous measurements of inherent optical properties (IOPs) with a hyperspectral spectrophotometer: For the continuous underway surface sampling, an in-situ–spectrophotometer (AC-S; Seabird) was operated in flow-through mode to obtain total and particulate matter attenuation and absorption of surface water (Fig. 4.2). The instrument was mounted to a seawater supply taking surface ocean water. A flow-control with a time-programmed filter was mounted to the AC-S to allow alternating measurements of the total and the CDOM inherent optical properties of the sea water. Flow-control and debubbler-system ensured water flow through the instrument with no air bubbles. The AC-S was operated on the seawater supply at the Nasslabor-1, with seawater pumped at Kastenkiel via Spargel with the membrane pump through the Teflon tubing in order to deliver living phytoplankton cells continuously throughout the cruise, also within the regions of sea ice cover.
b. Optical profiler: a second AC-S instrument was mounted on a steel frame together with a depth sensor and a set of hyperspectral (300 to 900 nm, ~10 nm spectral resolution) radiometers (Ramses sensors from TRIOS) and operated during CTD stations (Fig. 4.2). The frame was lowered down to maximum depth of 150 m with a continuous speed of 0.1 m/s or, during daylight, with additionally stops at 5, 10, 15, 20, 25, 30, 35, and 40 m to allow a better collection of radiometric data (further discussed below). The Apparent Optical Properties of water (AOPs) (surface reflectance and light attenuation through the water column) were estimated based on downwelling and upwelling irradiance measurements in the surface water profile (down to the 0.1% light depth) from the radiometers calibrated for the incident sunlight with measurements of a radiometer on deck. The AC-S measured the inherent optical properties (IOPs: total attenuation, scattering and absorption) in the water profile.
c. Discrete measurements of IOPs (absorption) at water samples were performed 1) on samples from the underway surface sampling (from the AC-S flow-through system connected to the ship's seawater pump) at an interval of 3 hours, and 2) for samples from the CTD station water sampling at 6 depths within the top 100 m. Water samples for CDOM absorption analysis are filtered through 0.2 µm filters and analysed onboard with a 2.5-m path length liquid waveguide capillary cell system (LWCC, WPI) following Lefering et al. (2017). Particulate and phytoplankton absorption coefficients were determined with the quantitative filter techniques using sample filtered onto glass-fibre filters (QFT-ICAM) and measuring them in a portable QFT integrating cavity setup following Röttgers et al. (2016).
d. Samples for the determination of phytoplankton pigment concentrations and composition were taken at a 3-hourly interval from the underway-sampling system, and from 5 depths (max. 150 m) at CTD-stations. These water samples were filtered on board immediately after sampling and the filters were thermally shocked in liquid nitrogen. Samples were stored at -80°C until ship will return to Bremerhaven in autumn 2025. Then, the samples will be analysed within the next three months by High Performance Liquid Chromatography Technique (HPLC) at AWI following Taylor et al. (2011) and adapted to our new instrumentation as described in Álvarez et al. (2022).

Fig. 4.2: Left: Continuous measurements of the extinction and absorption of light in Arctic surface waters using a AC-S (Seabird) mounted to Polarstern's surface seawater pump system. From those measurements directly, the absorption and scattering of particles and CDOM is determined for the whole spectrum in the visible resolved with about 3 nm resolution. This data then can be decomposed various specific algorithms to determine the particle size distribution and the various phytoplankton pigment composition. Right: Underwater light field measurements with TRIOS RAMSES radiometers detecting the hyperspectral up- and downwelling radiation and the AC-S (Seabird, including pressure sensor, data logger and battery) measuring extinction and absorption.

e. At a few stations when the sea was calm, we tested a high spectral resolution self-configurated hand-held above-water radiometer system (Ocean Optics Sensor System, OOSS), operated from the backend of the ship (Fig. 4.3). The OOSS has been developed by the group of Dr. Peter Gege (DLR-Oberpfaffenhofen) and re-built by AWI Phytooptics Group based on a cooperation contract with DLR. The instrument is configured on a gimbal with three spectrometers (Ocean Optics STS-VIS, 350-810 nm, 1.5 nm spectral resolution), 7A-DA Direct-attach Collimating Lens for the upwelling and sky radiance measurements, CC_attach Cosine Corrector for the sunlight irradiance measurements (all from Ocean Optics, USA: https://www.oceaninsight.com), a motor enabling the coordinated alternation of the spectrometers into the different observation geometries, and a laser guaranteeing the correct position of the spectrometers at measurement. The spectrometers' measurements were steered via a python-based software using a raspberry computer sending data via Wi-Fi to the steering computer. Calibration of the system was done at the beginning of each station measuring the dark signal using a shutter and measurement against a reflection.

Fig. 4.3: Ocean Optics Sensor System (OOSS) operated from the backend of the ship. The instrument is configured on a gimbal with three spectrometers (Ocean Optics STS-VIS, 350-810 nm, 1.5 nm spectral resolution), 7A-DA Direct-attach Collimating Lens for the upwelling and sky radiance measurements CC_attach Cosine Corrector for the sunlight irradiance measurements (all from Ocean Optics, USA: https://www.oceaninsight.com), a motor enabling the coordinated alternation of the spectrometers into the different observation geometers, and a laser guaranteeing the correct position of the spectrometers at measurement.

Preliminary (expected) results

Moorings

The mooring work conducted during PS148 are part of a long-term observation campaign, mainly focused with measuring the changes and variability of the hydrography, biology and biogeochemistry in West Spitsbergen Current (WSC) from seasonal to decadal timescales. The WSC carries warm, saline water from the North Atlantic into Fram Strait. Approximately half of the warm Atlantic Water (AW) that flows northwards in the WSC is recirculated westwards across Fram Strait towards East Greenland; the rest continues northwards and enters the central Arctic Ocean. The AW in the WSC is the major source of oceanic heat and salt for the Arctic Ocean and changes in the properties of the AW inflow strongly influence both ocean and sea ice conditions there.

The mooring F4-S-8 is stationed in the offshore branch of the WSC which follows the continental shelf of Svalbard. Records in the near-surface, at 22 m, show a pronounced seasonal cycle of the warm, saline AW (Fig. 4.4). Towards the end of the summer months, temperatures peak between August and September 2024 up to almost 10°C and reach maximum salinities. Temperatures decrease towards 2°C over the winter months, with a highly variable salinitiy signal from September to November that tends towards freshening. Temperatures reach a minimum of ~3°C in January and salinities remain relatively high and stable through to May 2025. AW temperatures begin to increase again from June 2025, as salinities become more variable. The strength of the inflow can be inferred from the changing

depth of the instrument, with vertical mooring motion ('knockdowns') due to strong horizontal currents. The largest knockdowns occurred during the winter months, with the largest down to over 200m in early February 2025, indicating a stronger flow than during summer where knockdowns were generally much weaker (about 50m).

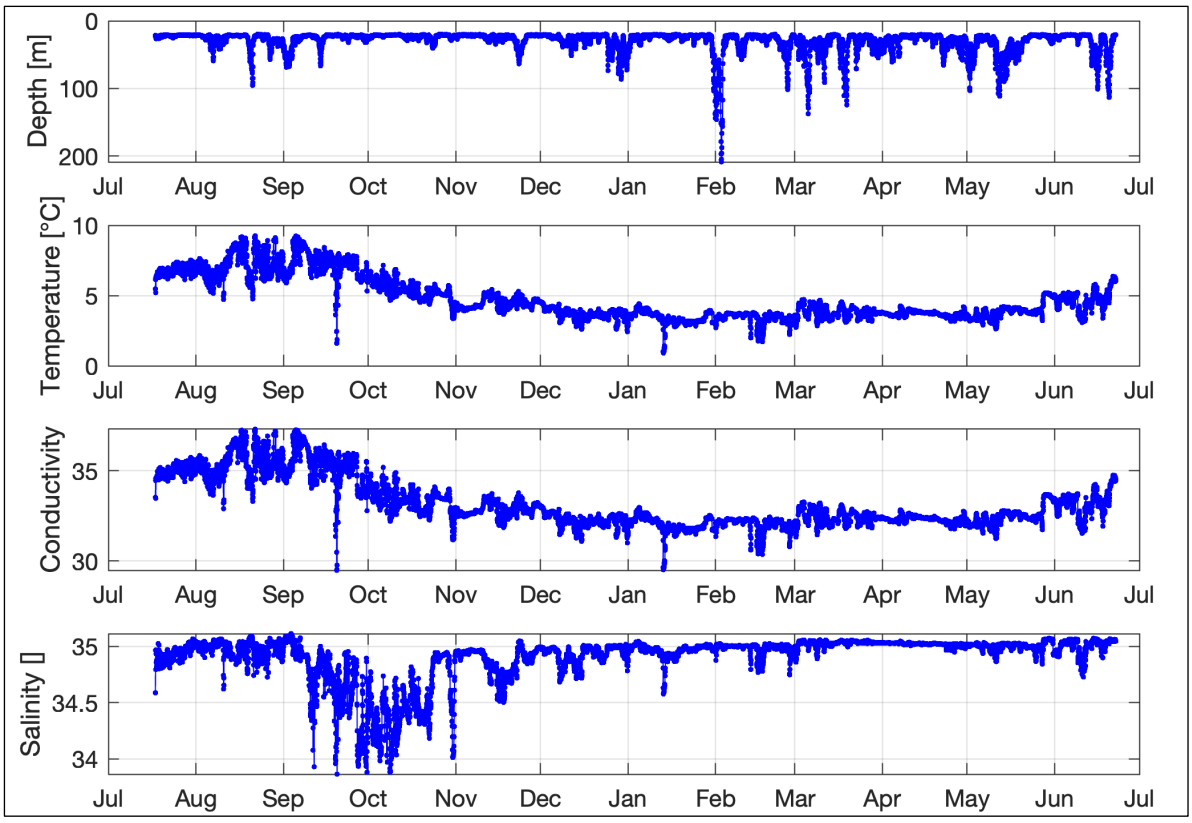

Fig. 4.4: Timeseries at 22m depth at mooring F4-S-8 over the deployment period, showing (top to bottom) depth (m), temperature (°C), conductivity, and salinity.

CTD

During PS148, the CTD stations formed a lateral transect across the Fram Strait at approximately 79°N, covering the WSC in eastern Fram Strait and the EGC in western Fram Strait, ranging from 05°31.800'W to 10°48.947'E (the AG, S and N stations excluded). In eastern Fram Strait, the CTD transect captured to West Spitzbergen Current (WSC) which transports warm and saline Atlantic Water (AW) to the north, flowing along the continental shelf of Svalbard (Fig. 4.5 A, B). The WSC can be identified here with maximum temperatures of over 6°C found close to Svalbard in the upper 200 m, and temperatures decreases with depth. Further to the west in central Fram Strait between 4 – 6°E, a layer of cold and fresher water (< 0°C, < 34.5) about ~50m thick separates the warm AW from the surface, though this is not constant across the transect as AW once again reaches the surface at 3°E. Note that the results between 3°W and 3°E have to be interpreted with caution, since in this area no CTD casts were performed and therefore the data was interpolated. Close to the Greenland continental shelf, west of 3°W, a cold and fresh surface layer (< 0°C) reaches down to 150 m. Below, warm water of Atlantic-origin sits on the shelf break. Below 1,000 m, a cold (< 0°C) and saline layer persists aross the Strait.

The fluorescence, which acts as an indicator for chlorophyll, showed a variable distribution across the width of Fram Strait. Maximum values greater than 18 mg/m^3 were observed in the central Hausgarten region, reaching depths of up to 100 m (Fig. 4.5, C). Weaker values (< 3 mg/m^3) were observed in the WSC to the east and concentrated in the upper 50 m. Closer to Greenland, the chlorophyll concentrations were lower at 2 - 4 mg/m^3, but peaks were observed as deep as 150 m.

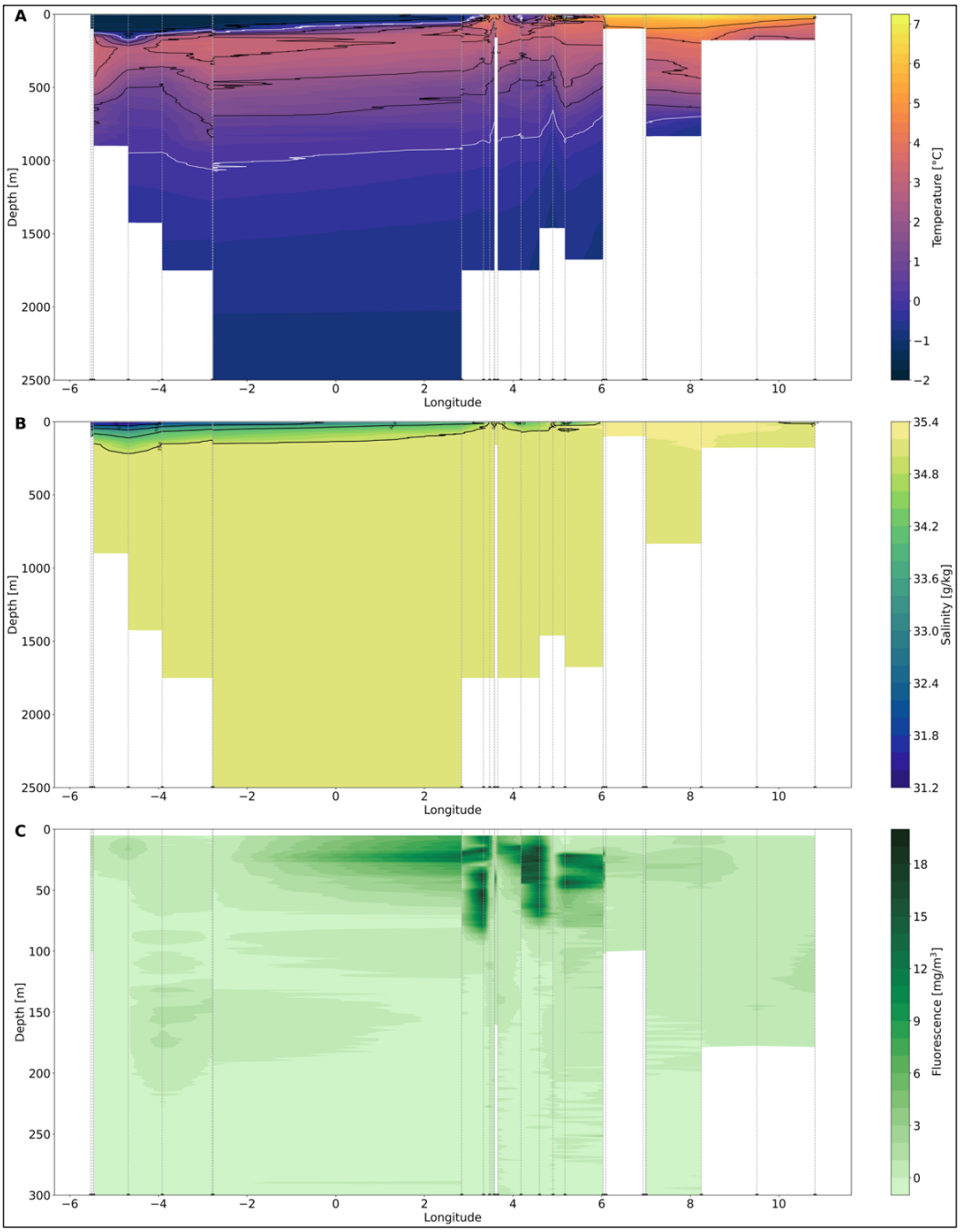

Fig. 4.5: Preliminary results from the CTD data on a transect from west to east of the hydrographic data. (A) conservative temperature, (B) absolute Salinity and (C) Fluorescence as an indicator for Chlorophyll. Selected isotherms and isohalines are the black lines in (A) and (B), and the 0°C isotherm is the white line in (A). Note that (C) is zoomed into the upper 300 m.

Optical Measurements

The continuously measured optical data are used via using inverse modelling, semi-analytical and principal-component-based methods to determine the spectrally resolved underwater light attenuation and the concentration of optical constituents, such as a Chla concentration of the whole phytoplankton community and the major phytoplankton groups and CDOM absorption (Bracher et al. 2020, Bracher et al. submitted). These data are also used together with the data set determined on the discrete water samples regarding pigment concentration and derived phytoplankton group Chla concentration from the HPLC data and the absorption properties, for validating satellite ocean colour retrievals following formerly established procedures for FRAM or other *Polarstern* cruises (e.g., Cherkasheva et al. 2014; Liu et al. 2018; Soppa et al. 2014; Losa et al. 2017; Xi et al. 2023; Bracher et al. 2025; Xi et al. 2025). We expect this new data set for our long-term measurements to elucidate further changes in the Fram Strait pelagic environment due to global change and/or other environmental shifts.

So far, we have obtained the following measurements/data:

- Underway flowthrough measurements:
    - 30 days (May 29 to June 17, June 19 to 28, 2025) of total and particulate absorption/attenuation measurements of surface water from AC-S. Part of the post-processing completed on bord, processing to particulate absorption and preliminary Chla concentration, while phytoplankton groups and absorption of CDOM will be retrieved back at AWI.
- Discrete samples (underway samples see Tab. 4.4, station samples see Tab. 4.5):
    - HPLC pigments: 121 samples from CTDs, 113 samples from Underway. Filters send back to AWI and analysed in home laboratory.
    - CDOM absorption: 121 samples from CTDs, 113 samples from Underway. Measurements were completed and data will be analysed back at AWI.
    - Particulate, non-algal and phytoplankton absorption: 121 samples from CTDs, 113 samples from underway. All measurements completed on bord and data processing finalized on board.
- Station work from light profiler mostly until 100 m (seven stations until 150 m, details see Tab. 4.6):
    - 18 valid RAMSES underwater hyperspectral radiance and irradiance profiles. All data have been processed to final AOPs (remote sensing reflectance, diffuse attenuation) on bord.
    - 18 valid AC-S profiles for the total absorption. Processing to total absorption, Chla and phytoplankton groups Chla will be done back at AWI.
- OOSS stations
    - 14 measurements of upwelling and sky radiance measurements, which will be analysed when back at AWI after the cruise.

On board we finished all measurements, except for the phytoplankton pigment data for which the filters will be analysed in the home laboratory. From the completed measurements already on bord we analysed the RAMSES station and the QFT particulate, phytoplankton and non-algal absorption data. Further, we pre-processed part of the AC-S flowthrough data to particulate and the LWCC data to CDOM absorption data.

Tab. 4.4: Positions of underway discrete water samples used for measurements of absorption by phytoplankton, all particles and non-algal particles (PABS) and by CDOM and collected for analysis by High Pressure Liquid Chromatography (HPLC) to determine phytoplankton pigments

Sample ID	Date	Time	Latitude	Longitude
UW2	29/05/25	21:00:00	54.491453	7.2
UW3	30/05/25	00:00:00	54.947475	6.8
UW4	30/05/25	03:00:00	55.44757	6.4
UW5	30/05/25	05:58:00	55.954625	6.1
UW6	30/05/25	09:43:00	56.58574	5.8
UW7	30/05/25	11:59:00	56.94861	5.5
UW8	30/05/25	15:01:00	57.431789	5.1
UW9	30/05/25	18:00:00	57.910807	4.7
UW10	30/05/25	20:59:00	58.385309	4.2
UW11	31/05/25	00:00:00	58.86716	3.8
UW12	31/05/25	03:00:00	59.386116	3.6
UW13	31/05/25	06:00:00	59.90867	3.4
UW14	31/05/25	08:59:00	60.438068	3.3
UW15	31/05/25	12:00:00	60.948448	3.1
UW16	31/05/25	15:00:00	61.469177	2.8
UW17	31/05/25	18:00:00	61.983847	2.5
UW18	31/05/25	21:00:00	62.504283	2.3
UW19	01/06/25	00:00:00	63.023435	2
UW20	01/06/25	03:00:13	63.549774	1.8
UW21	01/06/25	06:00:00	64.071199	1.5
UW22	01/06/25	09:00:03	64.579144	1.2
UW23	01/06/25	12:00:16	65.098159	1
UW24	01/06/25	15:00:00	65.615569	0.7
UW25	01/06/25	18:04:38	66.149004	0.4
UW26	01/06/25	21:00:20	66.372751	0.3
UW27	02/06/25	00:00:20	66.331805	0.2
UW28	02/06/25	00:03:00	66.326905	0.2
UW29	02/06/25	00:06:00	66.322092	0.2
UW30	02/06/25	09:00:00	66.741649	0.4
UW31	02/06/25	12:00:00	67.269406	0.7
UW32	02/06/25	15:00:00	67.791386	0.9
UW33	02/06/25	18:00:09	68.318065	1.2
UW34	02/06/25	21:00:00	68.840019	1.4
UW35	03/06/25	00:00:00	69.35849	1.7
UW36	03/06/25	03:00:00	69.794143	2
UW37	03/06/25	15:03:05	69.827426	2
UW38	03/06/25	21:00:00	70.194283	2.2
UW39	04/06/25	00:00:10	70.156639	2.2
UW40	04/06/25	05:09:40	70.560783	2.4
UW41	04/06/25	06:00:00	70.706749	2.5
UW42	04/06/25	09:00:00	71.209846	2.8

Sample ID	Date	Time	Latitude	Longitude
UW43	04/06/25	12:00:00	71.743331	3.1
UW44	04/06/25	15:00:00	72.260114	3.4
UW45	04/06/25	18:00:00	72.786724	3.6
UW46	04/06/25	21:00:00	73.319994	3.5
UW47	05/06/25	00:00:00	73.850771	3.4
UW48	05/06/25	03:00:00	74.377987	3.3
UW49	05/06/25	06:00:00	74.907029	3.2
UW50	05/06/25	09:00:04	75.432688	3
UW51	05/06/25	18:00:00	75.71559	2.9
UW52	06/06/25	00:00:00	76.247953	3.3
UW53	06/06/25	03:00:00	76.775442	3.7
UW54	06/06/25	06:16:50	77.34829	4.1
UW55	06/06/25	09:00:00	77.822256	4.4
UW56	06/06/25	12:00:00	78.348476	4.9
UW58	07/06/25	03:00:00	78.609566	5.1
UW59	07/06/25	15:00:00	78.616215	5.1
UW60	07/06/25	18:03:15	79.008619	4.3
UW61	07/06/25	21:00:10	79.06536	4.2
UW62	08/06/25	06:00:00	79.064665	4.2
UW63	08/06/25	09:00:00	79.01327	4.3
UW64	08/06/25	12:00:00	79.078227	4.1
UW65	09/06/25	00:00:25	79.086925	4.4
UW66	09/06/25	12:00:00	79.071529	4.1
UW67	09/06/25	17:52:00	79.103753	3.5
UW68	10/06/25	08:16:30	79.133758	2.8
UW69	10/06/25	21:12:00	79.064165	3.3
UW70	11/06/25	18:00:00	79.328141	3.8
UW71	11/06/25	21:00:00	79.853774	3.2
UW72	12/06/25	21:01:15	79.851613	3.8
UW73	13/06/25	07:00:00	79.736005	4.5
UW74	13/06/25	18:00:00	79.923506	3.1
UW75	14/06/25	00:00:00	79.659383	4.9
UW76	14/06/25	18:00:00	79.423536	3.3
UW77	14/06/25	21:00:00	78.938627	2.5
UW78	15/06/25	03:00:00	78.794446	-1.8
UW79	15/06/25	06:00:00	78.85602	-3.2
UW80	15/06/25	09:05:36	79.014964	-4.2
UW81	17/06/25	05:12:35	78.826558	-4.3
UW82	19/06/25	03:00:00	78.704648	-2.8
UW83	19/06/25	09:03:07	78.753932	-2.8
UW84	19/06/25	12:00:00	78.764259	-1.6
UW85	19/06/25	15:00:00	78.848777	0.8
UW86	19/06/25	18:03:00	79.139581	2.8

Sample ID	Date	Time	Latitude	Longitude
UW87	19/06/25	23:58:10	79.101197	3.4
UW88	20/06/25	06:03:00	79.139453	2.8
UW89	20/06/25	22:00:00	79.063486	3.7
UW90	21/06/25	01:20:00	79.054172	3.9
UW91	21/06/25	12:02:25	79.078757	4.1
UW92	22/06/25	18:00:00	79.010841	7
UW93	22/06/25	21:00:00	79.019125	8.5
UW94	23/06/25	06:04:45	79.030321	9.4
UW95	23/06/25	09:00:45	79.029133	7.2
UW96	23/06/25	12:03:15	79.011852	7
UW97	24/06/25	05:05:30	79.062732	7.7
UW98	24/06/25	09:11:00	79.130813	6.1
UW99	24/06/25	12:00:00	79.119493	6.2
UW100	24/06/25	15:00:15	79.106297	6.2
UW101	24/06/25	18:00:00	79.075761	4.1
UW102	25/06/25	09:00:00	79.074752	4.1
UW103	25/06/25	12:00:00	79.132187	6.1
UW104	26/06/25	09:06:00	79.130636	4.9
UW105	26/06/25	12:00:00	78.80226	5
UW106	26/06/25	15:00:00	78.616865	5
UW107	26/06/25	21:00:00	78.195267	5.9
UW108	27/06/25	00:00:00	77.70548	6.8
UW109	27/06/25	03:02:00	77.223316	7.7
UW110	27/06/25	06:00:00	76.742077	8.6
UW111	27/06/25	09:04:45	76.24714	9.4
UW112	27/06/25	12:00:00	75.769606	10.2
UW113	27/06/25	15:00:00	75.296938	11.1

Tab. 4.5: List of date, time, sample depth of Phytooptics discrete water samples at CTD Stations including the Hausgarten long-term observation name (LTO-Name) with measurements of absorption by phytoplankton, all particles and non-algal particles (PABS) and by CDOM (CDOM) and collected for analysis by High Pressure Liquid Chromatography (HPLC) to determine phytoplankton pigments

Sample ID	Station	LTO-Name	Date	Time at 100 m	Sampled Depth (m)	Lat at 100m	Lon at 100m
CTD1	PS148_1-1	AG1	01/06/25	22:46:20	17,25,40,50,100	66.37234	0.26482
CTD2	PS148_2-2	AG5	03/06/25	05:32:35	10,21,29,50,100	69.80256	1.94782
CTD3	PS148_4-1	AG7	05/06/25	13:03:03	11,18,32,50,100	75.67786	2.9428
CTD4	PS148_5-1	S3	06/06/25	13:48:15	10,32,50,73,99	78.60848	5.06028
CTD5	PS148_6-13	HG-IV	08/06/25	17:36:29	9,25,61,75,100	79.06548	4.1809
CTD6	PS148_7-1	HG-III	09/06/25	02:03:12	10,27.5,50,75,100	79.10804	4.59906
CTD7	PS148_9-1	HG-IX	09/06/25	20:28:47	10,19,50,75,100	79.1336	2.84346
CTD8	PS148_10-2	HG-VIII	10/06/25	23:30:02	10,25,35,50,100	79.06404	3.34328
CTD9	PS148_11-1	HG-VII	11/06/25	03:03:25	10,25,50,60,100	79.05998	3.47726
CTD10	PS148_12-1	HG-V	11/06/25	12:22:22	9,18,27,50,100	79.06392	3.65367

Sample ID	Station	LTO-Name	Date	Time at 100 m	Sampled Depth (m)	Lat at 100m	Lon at 100m
CTD11	PS148_13-4	N5	12/06/25	04:24:07	10,17,24,50,100	79.94346	3.12072
CTD12	PS148_14-2	N4	13/06/25	02:21:45	10,18,50,75,100	79.7359	4.49304
CTD13	PS148_16-2	N3	14/06/25	08:41:06	10,20,40,50,100	79.60426	5.17126
CTD14	PS148_17-1	EG-I	15/06/25	13:23:56	10,20,30,50,100	78.99026	-5.50054
CTD15	PS148_19-1	EG-II	16/06/25	19:40:28	10,25,35,50,100	78.92184	-4.70431
CTD16	PS148_20-1	EG-III	17/06/25	08:15:50	10,39,50,70,100,149	78.80844	-3.95532
CTD17	PS148_21-2	EG IV	18/06/25	00:30:24	10,50,60,100,149	78.75038	-2.81206
CTD18	PS148 27-1	SV-IV	22/06/25	05:15:40	10,20,35,49,100	79.01166	6.03476
CTD19	PS148 28-1	SV-I	23/06/25	23:53:35	10,35,45,50,100	79.02842	10.81534
CTD20	PS148 30-1	SV-III	24/06/25	22:39:34	10,30,45,50,100	79.00042	8.24547

Tab. 4.6: Station positions and max. depth of profiling for hyperspectral upwelling and downwelling radiation in the water with the RAMSES radiometers and for hyperspectral total absorption and attenuation with the AC-S spectrophotometer

RAMSES station	LTO-Name	Date	Time at start profile	Latitude	Longitude	Max depth (m)
	AG1	01/06/25	no cast			
PS148_2-5	AG5	03/06/25	failed	69.827367	1.973516	70
	AG7	05/06/25	no cast			
PS148_5-5	S3	06/06/25	failed	78.608546	5.065936	100
PS148_6-11	HG-IV	08/06/25	failed	79.066334	4.17747	70
PS148_7-4	HG-III	09/06/25	05:03:00	79.107888	4.602047	5
PS148_7-4	HG-III	09/06/25	05:12:35	79.107783	4.602002	20
PS148_7-4	HG-III	09/06/25	05:26:50	79.107893	4.600369	30
PS148_7-4	HG-III	09/06/25	05:42:00	79.107886	4.600834	50
PS148_7-4	HG-III	09/06/25	05:57:00	79.10803	4.600047	70
PS148_9-8	HG-IX	09/06/25	08:13:50	79.133612	2.839401	68
PS148_10-1	HG-VIII	10/06/25	21:08:50	79.064171	3.33538	100
PS148_11-4	HG-VII	11/06/25	03:28:00	79.060658	3.471802	100
PS148_12-4	HG-V	11/06/25	12:48:40	79.063528	3.653026	100
PS148_13-7	N5	12/06/25	04:54:15	79.944778	3.121214	100
PS148_14-7	N4	13/06/25	07:00:44	79.736006	4.497511	100
PS148_16-5	N3	14/06/25	failed	79.603871	5.171261	100
PS148_17-4	EG-I	15/06/25	failed	78.995855	-5.531924	80
PS148_19-4	EG-II	16/06/25	failed	78.931559	-4.636112	20
PS148_19-4	EG-II	16/06/25	20:39:42	78.931559	-4.636112	70
PS148_20-3	EG-III	17/06/25	08:40:32	78.809118	-3.967496	70
PS148_21-8	EG IV	18/06/25	05:24:24	78.745416	-2.740308	150
PS148_27-5	SV-IV	22/06/25	08:07:02	79.011808	6.034174	150
PS148_28-5	SV-I	23/06/25	01:46:02	79.030594	10.813194	150

RAMSES station	LTO-Name	Date	Time at start profile	Latitude	Longitude	Max depth (m)
PS148_30-4	SV-III	24/06/25	23:05:17	78.999982	8.242266	150
PS148_31-4	SV-II	24/06/25	02:19:33	78.979234	9.501194	100
PS148_34-3	HG-VI	25/06/25	02:14:26	79.059719	3.571352	150
PS148_35-6	HG-I	25/06/25	18:09:45	79.133357	6.094886	150
PS148_36-4	HG-II	26/06/25	05:17:04	79.131094	4.892916	150

The continuous flowthrough measurements of both the total and non-particulate absorption and attenuation measurements of surface water by the AC-S instrument resulted in approximately 25k particulate absorption spectra. The Chla concentration have already been retrieved from these samples using the absorption line height (aLH) method (Roesler and Barnard 2013) and applying coefficients as determined in the previous HAUSGARTEN spring cruises (Chla proxy = 27.6 * (aLH^0.73); PS136; Bracher et al. 2025). The preliminary results are presented in Fig. 4.6. The dataset will be quality-controlled based on HPLC pigment concentrations back at AWI and further processed to retrieve phytoplankton groups. So far, highest Chla concentration were found in the northern Atlantic and central Hausgarten stations, which aligns with the distribution of Chla concentrations from the CTD profiles (Fig. 4.5).

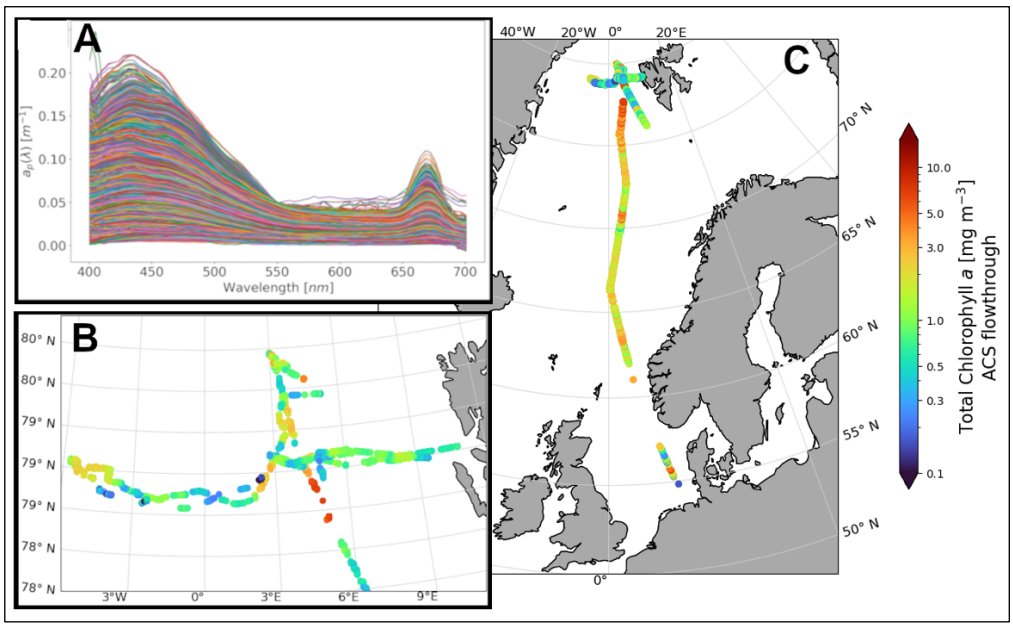

Fig. 4.6: Approximately 25k particulate absorption spectra measured with the AC-S flowthrough technique (A), preliminary estimates of Chla concentration in the Fram Strait (B), and along the PS148 cruise track (C). The Chla concentration is estimated from the absorption line height at 676 nm derived from the particulate absorption spectra following Roesler and Barnard (2013) and using coefficients from Bracher et al. (2025) for PS136.

From the measurements of the QFT-ICAM we calculated the total particulate, phytoplankton and non-algal absorption and the aLH. From the latter, we obtained a proxy for the Chla concentrations using the coefficients from Liu et al. (2018) determined for the Fram Strait in early summer PS99-2 (Chla proxy = 57.5 * (aLH^0.91)). Fig. 4.7 shows the results of derived Chla conc. for the underway measurements sampled for the entire PS148 transect combined

with the CTD sampling at 10 m depth. As for the continuous measurements by the AC-S system, the maximum Chla concentrations were measured in the Atlantic waters on the way north to Fram Strait at the beginning of the cruise, at the central Hausgarten stations, and in the underway samples to the northern stations (5 to 7.3 mg m^{-3}). Around the East Greenland Current (EGC) and at the eastern side of the transect back to Tromsø, Chla concentrations were quite low.

The Chla concentrations were also determined from the water samples from the CTD casts, shown in Fig. 4.8. At 15 stations, the Chla concentration was highest in the surface sample (~ 10m), while nine stations (EG-III, N3, N4, HG-II, HG-III, HG-VI, S3, SV-I and SV-IV) showed a subsurface Chla maximum between 20 to 40 m depth, already indicating nutrient deficiency at the surface water. Interestingly, very deep Chla maxima (140 to 150 m depth) were found at the stations EG-III (1.6 mg m^{-3}) and EG-IV (0.7 mg m^{-3}), as well as SV-II (0.6 mg m^{-3}). Compared to former spring expeditions PS126 and PS136, Chla is similarly high in Fram Strait but even higher along the northward journey.

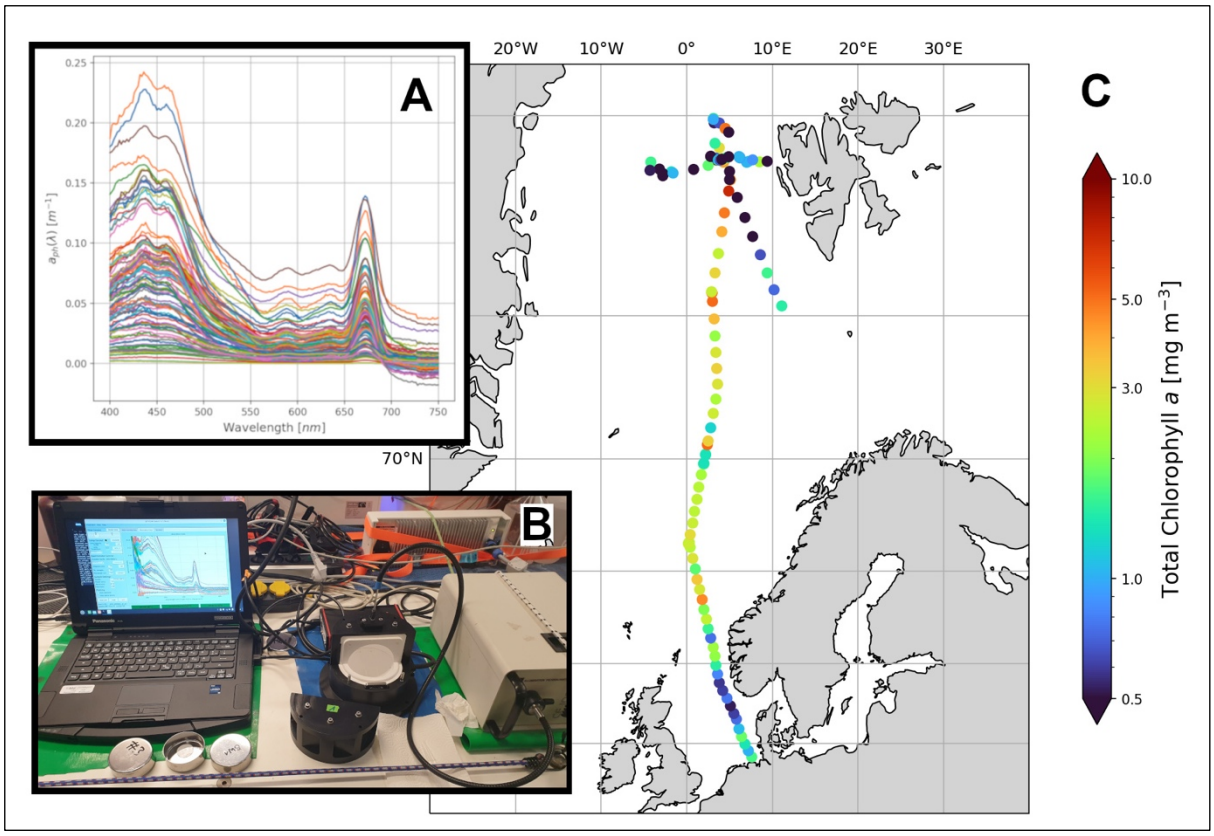

Fig. 4.7: Particulate absorption spectra measured with the QFT-ICAM technique (A), a photograph of the set-up of QFT-ICAM system (B), and retrieved Chla concentration along the PS148 cruise track (underway) combined with the CTD sampling at 10 m depth estimated from particulate absorption, used to determine the absorption line height at 676 nm following Roesler and Barnard (2013 and using coefficients from Liu et al. (2018) for PS99-2.

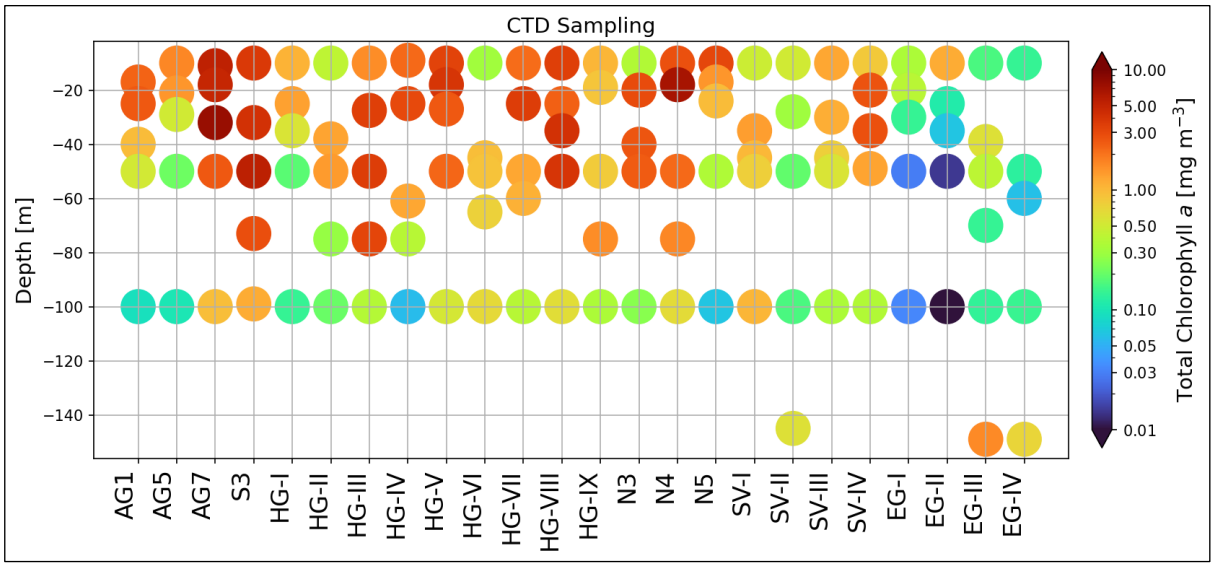

Fig. 4.8: Chla concentration at the PS148 ALONGate and Hausgarten stations estimated from particulate absorption, measured with the QFT-ICAM technique (Röttgers et al. 2016), used to determine the absorption line height at 676 nm following Roesler and Barnard (2013) using coefficients from Liu et al. (2018).

Finally, preliminary results from the discrete water sample CDOM measurements with the LWCC technique show diverse CDOM absorption spectra at 440 nm (Fig. 4.9). The final data set in consideration of the temperature and salinity measurements taken at the CTD stations and from the thermo-salinograph will enable the clear identification of the different water masses (Polar, mixed and Atlantic-origin waters).

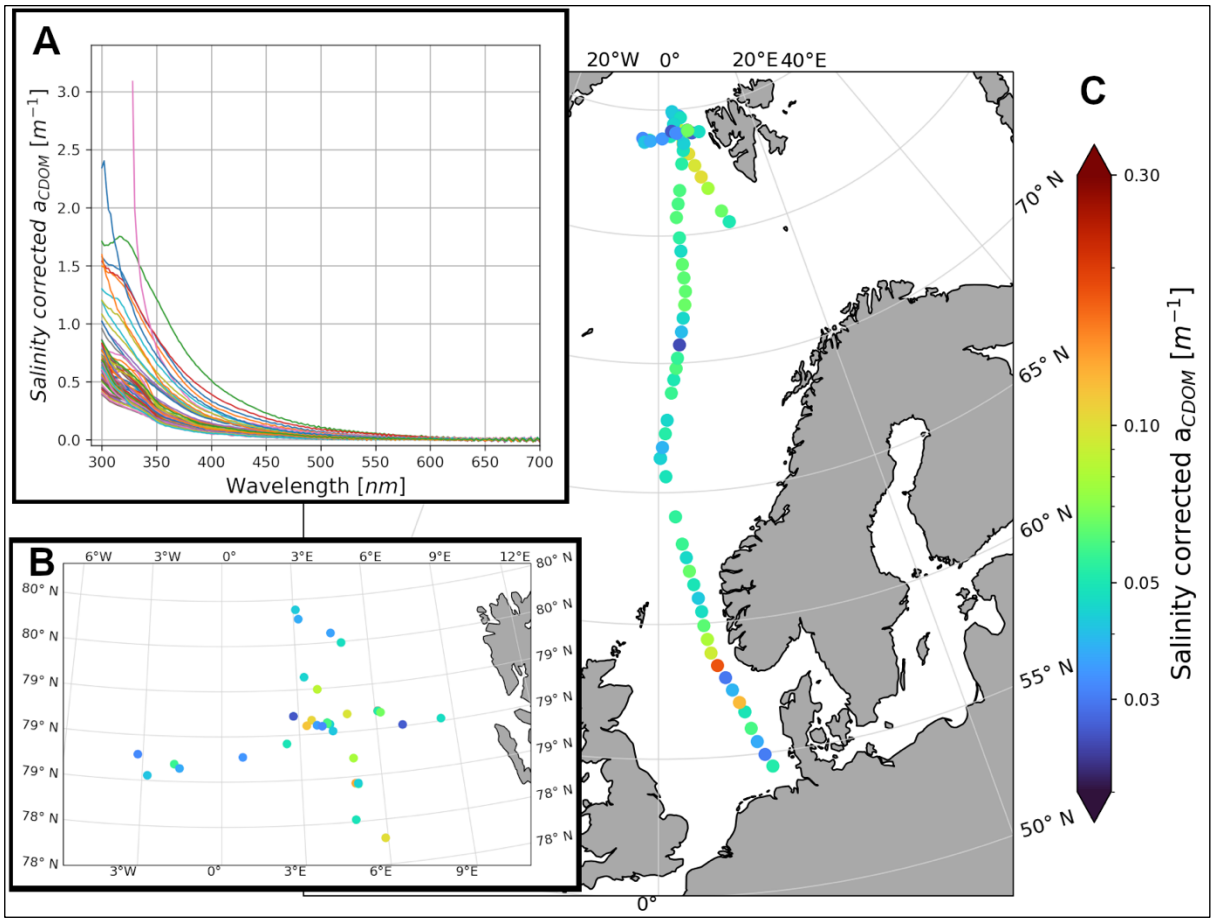

Fig. 4.9: Preliminary underway CDOM absorption spectra (A), line height at 440 nm for Hausgarten stations (B) and along the PS148 cruise track (C). CDOM absorption is measured with the LWCC technique and corrected for salinity and null-point following Levering et al. (2017) adapted in Alvarez et al. (2022)

Data management

Environmental data will be archived, published and disseminated according to international standards by the World Data Center PANGAEA Data Publisher for Earth & Environmental Science (https://www.pangaea.de) within two years after the end of the expedition at the latest. By default, the CC-BY license will be applied.

Any other data will be submitted to an appropriate long-term archive that provides unique and stable identifiers for the datasets and allows open online access to the data.

This expedition was supported by the Helmholtz Research Programme “Changing Earth – Sustaining our Future” Topic 2, Subtopic 1 and Topic 6, Subtopic 3.

In all publications based on this expedition, the **Grant No. AWI_PS148_04** will be quoted and the following publication will be cited:

Alfred-Wegener-Institut Helmholtz-Zentrum für Polar- und Meeresforschung (2017) Polar Research and Supply Vessel POLARSTERN Operated by the Alfred-Wegener-Institute. Journal of large-scale research facilities, 3, A119. http://dx.doi.org/10.17815/jlsrf-3-163.

References

Álvarez E, Losa S, Bracher A, Thoms S, Völker C (2022) Phytoplankton Light Absorption Impacted by Photoprotective Carotenoids in a Global Ocean Spectrally-resolved Biogeochemistry Model. J. Advances in Modeling Earth Systems. https://doi.org/10.1029/2022MS003126

Bracher A, Vountas M, Dinter T, Burrows JP, Röttgers R, Peeken I (2009) Quantitative observation of cyanobacteria and diatoms from space using PhytoDOAS on SCIAMACHY data. Biogeosciences 6:751–764. https://doi.org/10.5194/bg-6-751-2009

Bracher A, Xi H, Dinter T, Mangin A, Strass VH, von Appen W-J, Wiegmann S (2020) High resolution water column phytoplankton composition across the Atlantic Ocean from ship-towed vertical undulating radiometry. Frontiers in Marine Science 7:235. https://doi.org/10.3389/fmars.2020.00235

Bracher A, Banks AC, Xi H, Dessailly D, Gossn J, Lebreton C, Röttgers R, Kwiatkowska E, Chaikalis S, Mehdipour E, Pitta E, Soppa MA, Wevers J, Zeri C (2025) Assessment of OLCI absorption coefficients for non-water components across all optical water classes. Frontiers in Remote Sensing, section Multi- and Hyper-Spectral Imaging. https://doi.org/10.3389/frsen.2025.1545664

Bracher A, Xi H, von Appen W-J, Mehdipour E, Metfies K, McPherson R, Zeising M, Nöthig E-M, (submitted 14 May 2025) Resolving the interannual variability of phytoplankton community composition in Fram Strait using ship-based high-frequency spectrophotometric measurements from 2015 to 2024. Deep-Sea Research Part II - the Topical Studies in Oceanography “25th years of Long-Term Ecological Research at the HAUSGARTEN Observatory“.

Cherkasheva A, Bracher A, Melsheimer C, Köberle C, Gerdes R, Nöthig E-M, Bauerfeind E, Boetius A (2014) Influence of the physical environment on phytoplankton blooms: a case study in the Fram Strait. Journal of Marine Systems 132:196–207. https://doi.org/10.1016/j.jmarsys.2013.11.008

Dinter T, Rozanov V, Burrows JP, Bracher A (2015) Retrieval of light availability in ocean waters utilizing signatures of vibrational Raman scattering in hyper-spectral satellite measurements. Ocean Science 11:373–389.

Lefering I, Röttgers R, Utschig, McKee D (2017) Uncertainty budgets for liquid waveguide CDOM absorption measurements. Applied Optics 56(22):6357. https://doi.org/10.1364/AO.56.006357

Liu Y, Roettgers R, Ramírez-Pérez M, Dinter T, Steinmetz F, Noethig EM, Hellmann S, Wiegmann S, Bracher A (2018) Underway spectrophotometry in the Fram Strait (European Arctic Ocean): a highly resolved chlorophyll a data source for complementing satellite ocean color. Optics Express 26(14):A678-A698.

Losa S, Soppa MA, Dinter T, Wolanin A, Brewin RJW, Bricaud A, Oelker J, Peeken I, Gentili B, Rozanov VV, Bracher A (2017) Synergistic exploitation of hyper- and multispectral precursor Sentinel measurements to determine Phytoplankton Functional Types at best spatial and temporal resolution (SynSenPFT). Frontiers in Marine Science 4:203.

Oelker J. Richter A. Dinter T. Rozanov VV, Burrows JP, Bracher A (2019) Global diffuse attenuation coefficient derived from vibrational Raman scattering detected in hyperspectral backscattered satellite spectra. Optics Express 27(12) A829–A855. https://doi.org/10.1364/OE.27.00A829

Oelker J, Losa SN, Richter A, Bracher A (2022) TROPOMI-retrieved underwater light attenuation in three spectral regions in the ultraviolet to blue. Frontiers in Marine Science 9. 787992. https://doi.org/10.3389/fmars.2022.787992

Röttgers R, Doxaran D, Dupouy C (2016) Quantitative filter technique measurements of spectral light absorption by aquatic particles using a portable integrating cavity absorption meter (QFT-ICAM). Opt. Express 24(2):A1–A20.

Roesler S, Barnard AH (2013) Optical proxy for phytoplankton biomass in the absence of photophysiology: Rethinking the absorption line height, Methods in Oceanography 7:79–94.

Sadeghi A, Dinter T, Vountas M, Taylor B, Peeken I, Altenburg Soppa M, Bracher A (2012) Improvements to the PhytoDOAS method for identification of coccolithophores using hyper-spectral satellite data. Ocean Sciences 8:1055–1070.

Soppa MA, Hirata T, Silva B, Dinter T, Peeken I, Wiegmann S, Bracher A (2014) Global retrieval of diatoms abundance based on phytoplankton pigments and satellite. Remote Sensing 6:10089–10106.

Taylor BB, Torrecilla E, Bernhardt A, Taylor MH, Peeken I, Röttgers R, Piera J, Bracher A (2011) Bio-optical provinces in the eastern Atlantic Ocean. Biogeosciences 8:3609–3629. https://doi.org/10.5194/bg-8-3609-2011

Xi H, Losa SN, Mangin A, Soppa MA, Garnesson P, Demaria J, Liu Y, d'Andon OHF, Bracher A (2020) Global retrieval of phytoplankton functional types based on empirical orthogonal functions using CMEMS GlobColour merged products and further extension to OLCI data. Remote Sensing of Environment 240:111704. https://doi.org/10.1016/j.rse.2020.111704

Xi H, Losa SN. Mangin A, Garnesson P, Bretagnon M, Demaria J, Soppa MA, d'Andon OHF, Bracher A (2021) Global chlorophyll a concentrations of phytoplankton functional types with detailed uncertainty assessment using multi-sensor ocean color and sea surface temperature satellite products. Journal Geoph. Res.-Oceans 126:e2020JC017127. https://doi.org/10.1029/2020JC017127

Xi H, Bretagnon M, Losa SN, Brotas V, Gomes M, Peeken I, Alvarado LMA, Mangin A, Bracher A (2023) Two-decade satellite monitoring of surface phytoplankton functional types in the Atlantic Ocean. State of the Planet 1-osr7:5. https://doi.org/10.5194/sp-1-osr7-5-2023

Xi H, Bretagnon M, Mehdipour E, Demaria J, Mangin A, Bracher A (2024) Consistent long-term observations of surface phytoplankton functional types from space. 9th Copernicus Ocean State Report. State Planet Discuss. [preprint]. https://doi.org/10.5194/sp-2024-15, accepted 14 Jun 2025.

5. PELAGIC BIOGEOCHEMISTRY: NUTRIENTS

Daniel Scholz[1], Mathias Westphal[2], Rebecca Gorniak[1]

not on board: Sinhué Torres-Valdés[1]*

*sinhue.torres-valdes@awi.de

[1]DE.AWI

[2]DE.HSBHV

Grant-No. AWI_PS148_03

Objectives

Our overarching goals are two-fold: 1) to understand and quantify nutrient variability in inflowing and outflowing waters to/from the Arctic Ocean within the context of the Arctic Ocean nutrient budget and its implications for its biogeochemical system (i.e., relevance for primary production, ecosystems, interaction between physical, chemical and biological processes); 2) to contribute to the wider goals of the FRAM/HAUSGARTEN community regarding long term observations of the Arctic System through a multidisciplinary approach. Therefore, our aim during PS148 is to continue our time series observations of selected biogeochemical variables, dissolved nutrients and dissolved oxygen. Our work involves the collection of seawater samples for analyses onboard and/or later, and via the deployment of remote access samplers (RAS) and sensors for moored, year-long observations and sensor-based profiles. As of 2024, sensor (in particular pH and pCO_2) and RAS biogeochemical data from deployments in the West Spitsbergen Current also represent the AWI contribution and commitment to the ICOS (Integrated Carbon Observation System) program. Nutrient and sensor data collected feed into an INSPIRES PhD project, started February 2025, related to the first overarching goal above.

Work at sea

5.1 Nutrients

For PS148 a 7-channel Seal Analytical AA-500 autoanalyser was set up in the wet lab for the analysis of micro-molar concentrations of 1) dissolved inorganic nutrients; nitrate plus nitrite (NO_3^-+NO_2^-) - hereafter referred to as nitrate -, nitrite (NO_2^-), silicate ($Si(OH)_4$), phosphate (PO_4^{3-}), and ammonium (NH_4^+) and 2) total nutrients, total phosphorus (TP) and total nitrogen (TN). Installation of the AA-500 involved the fitting of new cadmium columns for TN and nitrate. The nutrient analyser was controlled by the Seal Analytical Software AACE version 8.04, which allows for automated and simultaneous analysis of up to 7 channels. Following analyser set up, analytical reagents (stock and working solutions), standards (stock solutions and calibrants) and lab-made quality control solutions were prepared. ‘Stocks’ are concentrated solutions from which ‘working’ reagents/standards are prepared as required by solution stability or usage. We started with a new set of pump tubing installed in the analyser. Analyses have been carried out following current Seal Analytical Methods, which are based on standard and widely used colorimetric techniques for the analysis of nutrients in water and seawater.

The methods used during PS148 are listed below:

1. Total dissolved nitrogen in seawater No. G-218-98 revision 14 (MT23).
2. Nitrate and nitrite in water and seawater No. A-044-19 revision 5 (MT519A).
3. Nitrite in water and seawater No. A-003-18 revision 3 (MT518).
4. Total dissolved phosphorus in seawater No. G-439-16 revision 2 (MT33).
5. Phosphate in water and seawater No. A-004-18 revision 4 (MT518).
6. Silicate in water and seawater No. A-006-19 revision 3 (MT519).
7. Ammonium in water and seawater No. G-327-05 revision 8.

Best practices procedures for the analyses of nutrients in seawater following GO-SHIP recommendations, as described in Hydes et al. (2010) and Becker et al. (2020) were adopted.

After seven test runs, we decided to stop operating the analyser due to complications with the ammonium channel. Therefore, all nutrient samples collected during the current expedition were frozen at -20°C and will be analysed at a later point. 40 mL of seawater were collected directly into 50 mL sterile Falcon tubes. Tubes were rinsed three times with seawater before the sample was drawn. Two duplicate samples were randomly collected from each CTD cast. Samples included sea water from ALONGate casts, OFOBS, lander, remote access samplers from previous expeditions and recovered in the current expedition, samples from deep CTDs as well as from shallow CTD casts, where our SUNA Nitrate sensor was deployed in order to obtain high vertical resolution nitrate profiles. Samples collected from shallow casts will be used to calibrate the SUNA Nitrate sensor. All hydrographic stations occupied with the regular CTD were sampled.

5.2 Dissolved oxygen

Samples were also collected for the analysis of dissolved oxygen from CTD-Rosette casts from selected depths. We aimed to have as best vertical resolution as possible. Dissolved oxygen was measured as an important biogeochemical variable linked to nutrient cycling and also in order to calibrate the CTD-O_2 sensors and to have reference values for the CTD-O_2 sensors attached to moorings. Samples for dissolved oxygen were the first drawn from the Niskin bottles. Samples were collected using a tygon tube attached to the spigot of the Niskin bottles and placed directly into volume-calibrated borosilicate glass bottles with narrow necks. Care was taken to avoid bubbles inside the sampling tube and the sampling bottles. Water was left to spill over approximately three or more times the volume of the sampling bottle before the sample was drawn. A hand-held thermometer was used to measure the temperature of the seawater at the time of sample collection (i.e., fixing temperature) using a relatively fast-response temperature probe. Samples were immediately fixed by dispensing 1 mL of manganese chloride, followed by 1 mL of alkaline iodide, and then mixed thoroughly. When sampling was completed, the precipitate of the sample was let to settle to about a third of the volume (~1.5 hours). Then, samples were mixed thoroughly for a second time and the precipitate let to settle for a minimum of one hour more or until analysis. Analysis was carried out using a Metrohm Ti-Touch titration unit set up with the amperometric end point detection. Before analysis, 1 mL of 5 M sulphuric acid was added to a sample for titration. We followed the method and best practices procedures as described by Langdon (2010). All hydrographic stations were sampled. Samples were collected at the same vertical resolution as for nutrients, including two random duplicates per CTD cast.

One of the first steps in the lab was preparing 1 L of thiosulphate solution (titrant) (50 g/L), as it takes one to two days to stabilise. Thiosulphate calibrations were carried out using 1.667 mM OSIL Scientific certified Iodate Standards. Calibrations are done by first measuring 5 blanks (involving 2 x 1 mL additions of iodate standard, each titrated one at a time) and then 5

standards (each with 10 mL of iodate standard). The first calibration was carried out 3 days after the thiosulphate solution was prepared. There on, calibrations were carried out approximately every 3 days, with a total of 7 calibrations carried out for the first thiosulfate solution and 5 for the second thiosulfate solution (Tab. 5.1). Every time a calibration was done, calculation sheets were updated with the blank and standard titration volumes. Thus, the concentrations of dissolved oxygen for a given number of CTD casts were calculated with the most recent calibration results. Provided calibrations are consistent with each other and show no trend which may suggest degradation of reagents, results from calibrations represent analytical 'noise', that is, the combination of human, reagents and titration unit error associated with each analysis.

We present the results from each calibration in Table 5.1 and Figure 5.1. Toward the end of the expedition, calculation sheets were updated as appropriate, with the blank-mean and standard-mean of the first Thiosulphate solution, and blank-mean and standard-mean of the second Thiosulphate solution. Thereby, dissolved oxygen concentrations were standardized. A comparison of profiles/data calculated from individual calibrations and from the cruise mean is presented in Figure 5.2. CTD profiles from station PS148_001-01 to PS148_001-01 were analysed with the first thiosulfate solution. Stations PS148_017-01 to PS148_037-01 were analysed with the second thiosulfate solution.

After recalculations, data from the Winkler measurements were plotted against dissolved oxygen profiles recorded by two CTD-O_2 sensors in order to compare results and find outliers, which will be excluded within the sensor calibration (Fig. 5.3).

As mentioned above, on every cast, a minimum of two randomly selected Niskin bottles were sampled in duplicate to evaluate precision. A total of 446 samples were taken, of which 61 (13.7%) were duplicates. The absolute difference between all duplicate samples taken during the expedition is shown in Figure 5.4. Absolute differences greater than 1µmol/L were considered outliers. The mean difference and standard deviation of all duplicates taken (n = 61) is 2.33 ± 6.30 µmol/L, while without outliers (n = 40) values are 0.44 ± 0.25 µmol/L.

Tab. 5.1: Thiosulfate solution calibrations (titrations) done for the determination of dissolved oxygen. Blank (Blk), Standard (STD), STD minus Blk (STD - Blk) titration volume (mL), and calculated thiosulfate molarity

	Calibration	Date	Blank (mL)	Standard (mL)	STD - Blk	Thiosulfate Molarity
Thiosulfate Batch 1	1	01/06/2025	0.0023	0.4951	0.4928	0.2030
	2	01/06/2025	0.0041	0.4959	0.4918	0.2034
	3	02/06/2025	0.0025	0.4989	0.4964	0.2015
	4	03/06/2025	0.0035	0.4986	0.4951	0.2020
	5	05/06/2025	0.0013	0.4955	0.4942	0.2024
	6	10/06/2025	0.0023	0.4960	0.4937	0.2026
	7	13/06/2025	0.0036	0.4945	0.4909	0.2038
	Average		**0.0028**	**0.4964**	**0.4936**	**0.2027**
	Standard deviation		**0.0010**	**0.0017**	**0.0019**	**0.0008**
Thiosulfate Batch 2	8	14/06/2025	0.0020	0.4936	0.4916	0.2035
	9	15/06/2025	0.0008	0.4945	0.4938	0.2026
	10	18/06/2025	0.0016	0.4956	0.4940	0.2025
	11	21/06/2025	0.0024	0.4945	0.4921	0.2033
	12	24/06/2025	0.0024	0.4948	0.4924	0.2031
	Average		**0.0018**	**0.4946**	**0.4928**	**0.2030**
	Standard deviation		**0.0007**	**0.0007**	**0.0011**	**0.0004**

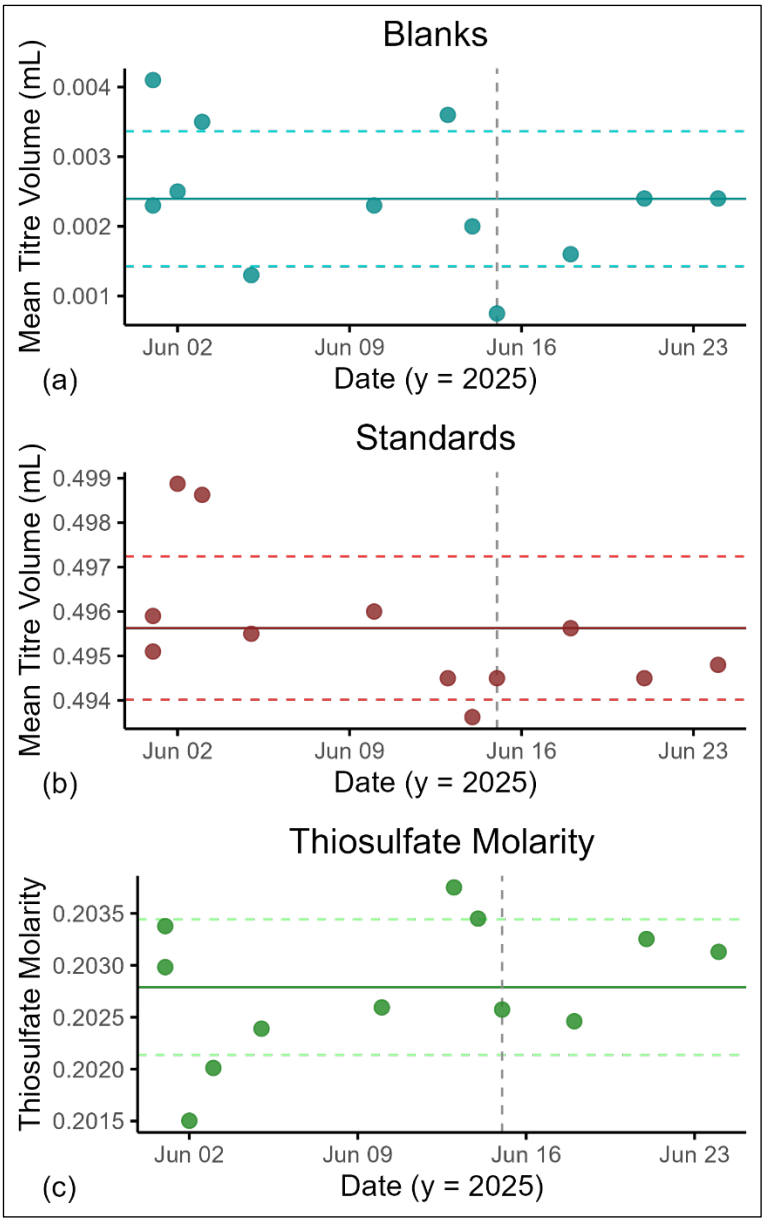

Fig. 5.1: Results from thiosulfate calibration carried out during PS148 for the determination of dissolved oxygen in seawater. Solid and dashed horizontal lines show the mean and respective standard deviations, as indicated in the two bottom rows of Table 5.2.1. Vertical dashed line indicates swap from the first to second thiosulfate titre solution.

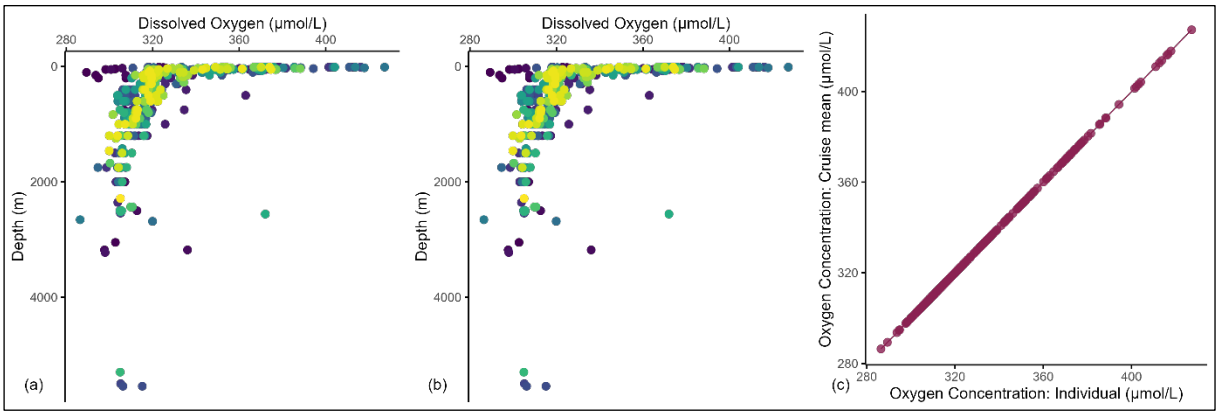

Fig. 5.2: (a) Dissolved oxygen profiles (data from all casts) as calculated with the respective calibration results (b) dissolved oxygen profiles (data from all casts) as calculated from the cruise-mean blank and standard titration volumes for the two thiosulfate batches. Colours represent individual casts. (c) Dissolved oxygen concentration measured with respective calibration results plotted against cruise mean. The black dotted line shows the 1:1 relation.

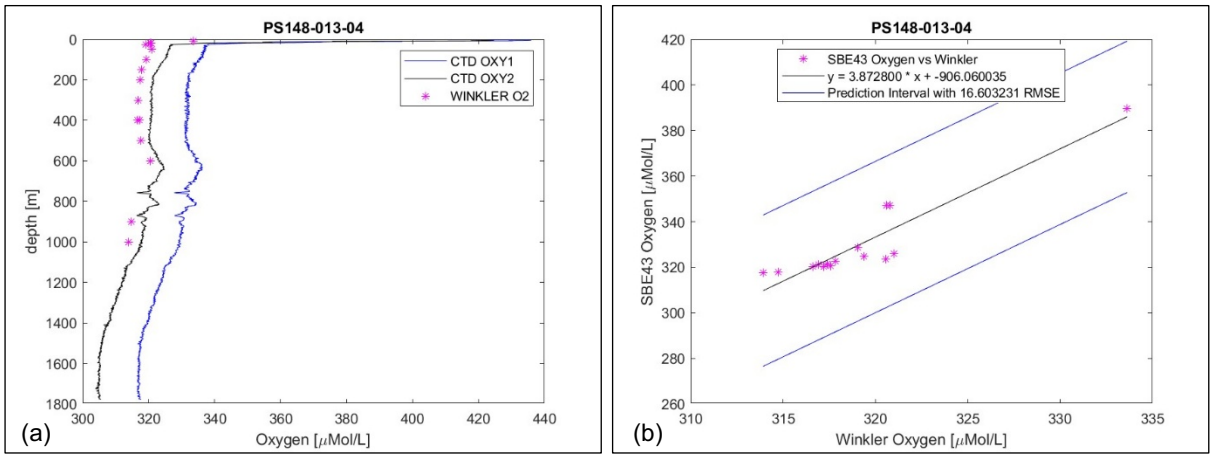

Fig. 5.3: (a) Measurements of dissolved oxygen according to Winkler (pink asterisks) and with two CTD-O_2 sensors mounted on the CTD rosette sampler (black and blue line) exemplified by PS148-013-04 (b) Fit between dissolved oxygen measurements according to Winkler and CTD-O_2 sensor records exemplified by PS148-013-04.

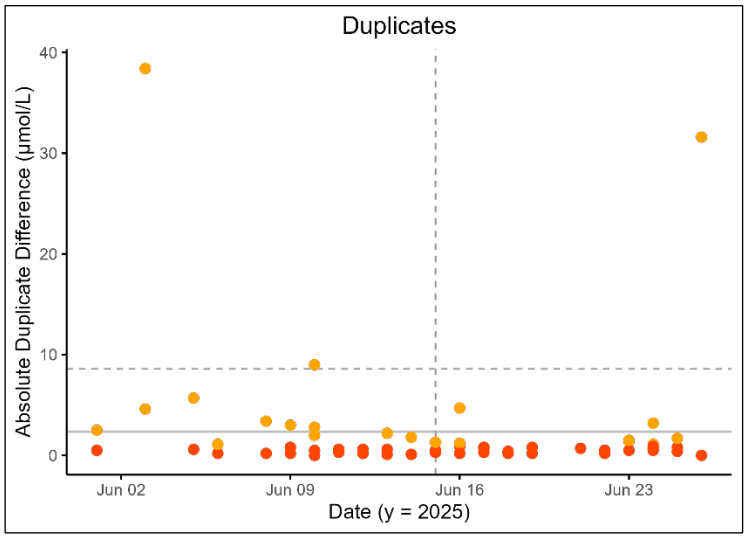

Fig. 5.4: Absolute difference between duplicate samples taken during PS148. Yellow dots show outliers, here considered as difference between duplicates >1 µmol L^{-1}. Orange dots show the absolute difference of duplicates without outliers (<1 µmol/L). Solid and dashed grey lines showed the mean difference of all duplicates taken (n = 61; 2.33 ± 6.30 µmol L^{-1}). Vertical dashed line indicates change from first to second thiosulfate solution.

5.3 Sensors and remote access samplers

In order to monitor biogeochemical activities within the inflowing Atlantic waters and the outflowing Arctic waters in Fram Strait, two biogeochemical sensor packages, deployed during PS143/2, were recovered and two new setups were deployed at the F4-S-9 and EGC10 site in the West Spitzbergen current and the East Greenland Current, respectively.

Tab. 5.2: This table summarizes the sensors, samplers, measured parameters and sampling intervals of the deployed sensor packages

sensor	parameter	interval
Seabird Suna	NO_3	4h
Wetlabs EcoTriplet	CDOM, chla, backscatter	2h
Wetlabs EcoPar	PAR	1h
Seabird SBE37ODO	CTD, O_2	1h
Sunburst Sami pH	pH	4h
Sunburst Sami CO_2	CO_2	4h
McLane remote access sampler (RAS)	500 ml seawater	8d

Preliminary data analysis and processing show reasonable results for all sensors except the pH sensor in the F4-S-8 mooring which was flooded and the CO_2 sensor in the EGC10 mooring which stopped recording data about two months into the deployment due to power issues. Both RAS sampled the programmed amount of water samples which were subsampled for nutrients, stored for post-cruise analysis and are further needed for sensor data correction.

Fig. 5.5: Biogeochemical sensor package: SeaBird Suna (NO_3), Wetlabs Ecopar (PAR), Wetlabs EcoTriplet (CDOM, chla, backscatter), SeaBird SBE37ODO (CTD + O_2), Sunburst Sami pH (pH), Sunburst Sami CO_2 (CO_2), McLane remate access sampler (48 water samples)

Besides moored deployments that generated time series data, 30 high resolution NO_3 profiles were recorded at stations shallower than 2000 m by deploying a Suna sensor along with the ship's CTD system. The sensor was setup to record full spectral data internally, measuring at 1 Hz. Temperature and salinity data needed to apply data processing algorithms described in Sakamoto et al. 2009 are provided by the ship's CTD. Synchronizing the Suna and CTD time stamp regularly is essential to match both datasets precisely.

Preliminary (expected) results

Data from dissolved oxygen measurements onboard will be processed for further quality control after the expedition. It is envisaged that this will take no longer than six months after the end of the expedition. This data set will also be made available to the physical oceanography team for the calibration of the CTD-O_2 sensors.

Samples collected for dissolved nutrient observations require longer times for processing. Since analyses onboard were not possible, later analyses may take place within 12 months after the expedition, plus another 6 months for data processing and quality control.

Sensor data takes much longer for processing as first there is the need to process data from discrete samples. However, raw sensor data will be submitted to PANGAEA as soon as it is possible as we have been doing in conjunction with colleagues from the sections Physical Oceanography of Polar Seas, Polar Biological Oceanography and Deep-Sea Ecology and Technology.

DIC and TA samples will be analysed within 6-8 months of sample collection. Once analyses are done data will be processed and quality controlled, and made available as part of the AWI ICOS contribution, likely within 6 months of analyses.

In Figure 5.6 we show a high-resolution nitrate profile on the left-hand side, already processed following Sakamoto et al. (2009), yielding a precision of ±0.3 µMol. Once available, further

offset correction will be applied utilizing the auto-analyser's inorganic nutrient data. The blue line in the plot on the right-hand side shows oxygen data recorded by a SBE43 sensor during the same cast. Comparison with Winkler oxygen data (pink asterisk) confirms that the sensor data lays within the manufacturer's calibration range. The oxygen data can also be helpful to validate features in the nitrate data e.g. the decrease in nitrate between 150 m and 200 m.

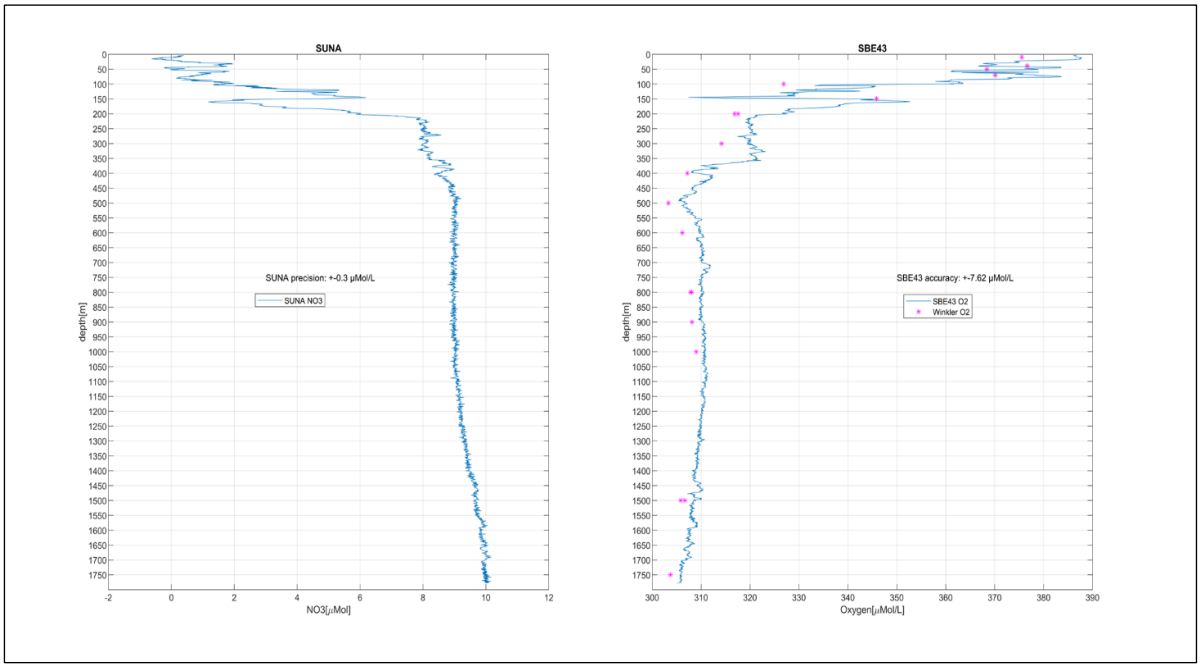

Fig. 5.6: Nitrate and oxygen profiling at station PS148-21-01

left plot: Suna NO_3 sensor data (blue line); processed with CTD's temperature and salinity data following Sakamoto et al. 2009

right plot: SBE43 oxygen sensor data (blue line) compared against Winkler oxygen measurements (pink asterisk)

In Figure 5.7 we show preliminary results from sensors deployed in mooring F4-S-8 (West Spitsbergen Current, 24 m), deployed in 2024 and recovered in 2025 during PS143/2. Data show the annual cycle of all deployed sensors except for pH. Low nitrate concentrations are observed in Aug-Sep 2024, presumably following or during a late summer phytoplankton bloom (consistent with declining dissolved oxygen concentrations). Some spikes in nitrate concentration are visible, which are consistent with pressure increases, likely due to the mooring being knocked down by ocean currents and thus measuring deeper waters with higher nitrate levels. As temperature decreases towards the winter months, nitrate replenishes due to convection. Some spikes of low salinity and temperature, with higher oxygen, suggest fresh water flowing by. Increases in pressure during winter months do not result in changes in nitrate concentration as the water column is well mixed.

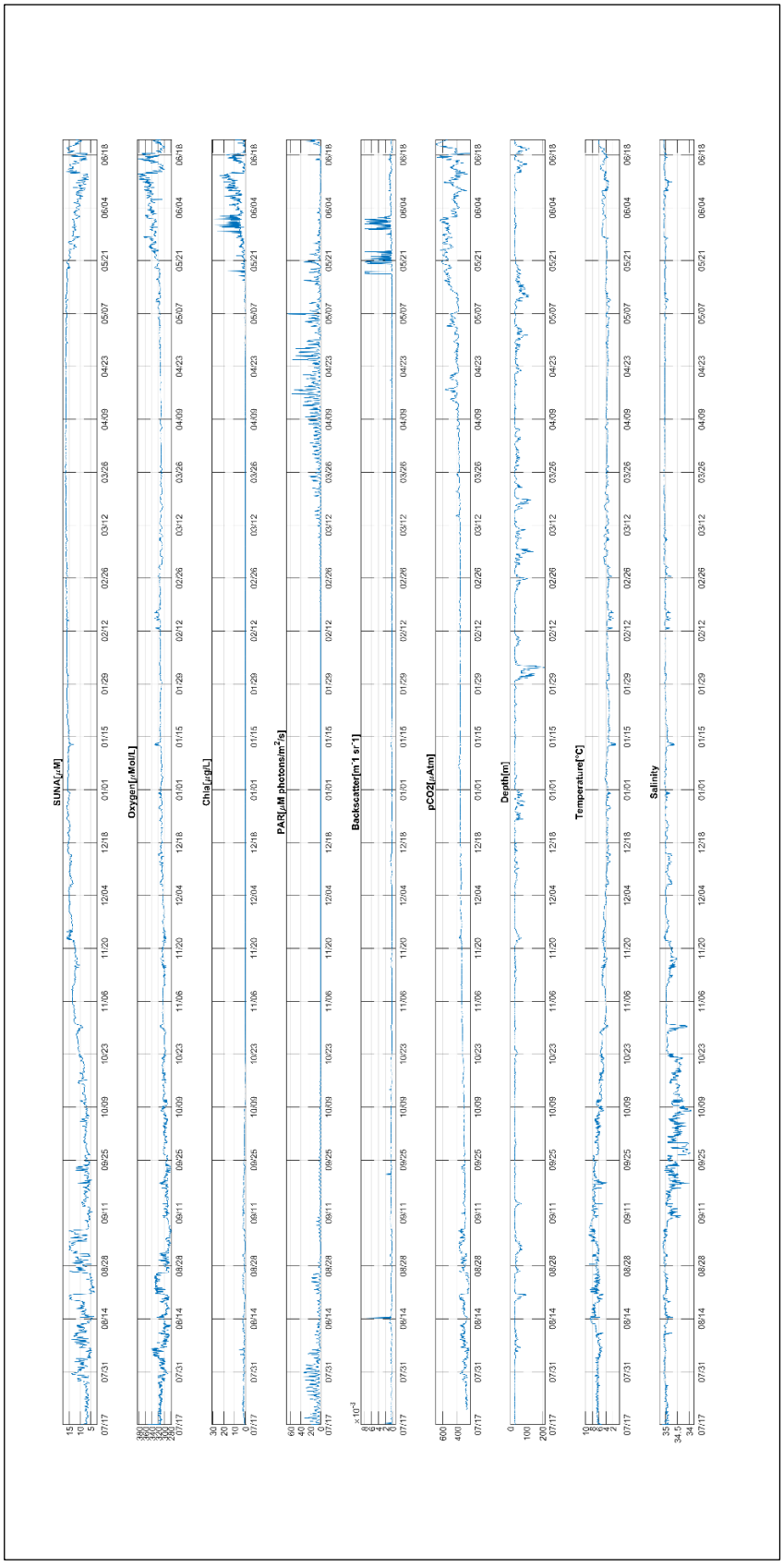

Fig. 5.7: Available time series sensor data of the F4-S-8 mooring deployed during PS143/2

Data management

Dissolved nutrients, dissolved oxygen and DIC/TA data will be archived, published and disseminated according to international standards by the World Data Center PANGAEA Data Publisher for Earth & Environmental Science (https://www.pangaea.de), as soon as data is available and fully quality controlled. A 2-year moratorium will be requested in order to analyse the data for scientific purposes and publishing of results. By default, the CC-BY license will be applied.

Any other data will be submitted to an appropriate long-term archive that provides unique and stable identifiers for the datasets and allows open online access to the data (e.g., ICOS). This expedition was supported by the Helmholtz Research Programme "Changing Earth – Sustaining our Future" Topic 6, Subtopic 6.2 and 6.3, Topic 2, Subtopic 2.1. In all publications based on this expedition, the **Grant No. AWI_PS148_03** will be quoted and the following publication will be cited:

Alfred-Wegener-Institut Helmholtz-Zentrum für Polar- und Meeresforschung (2017) Polar Research and Supply Vessel POLARSTERN Operated by the Alfred-Wegener-Institute. Journal of large-scale research facilities, 3, A119. http://dx.doi.org/10.17815/jlsrf-3-163.

References

Becker S, Aoyama M, Woodward E M S, Coverly S, Mahaffey C, Tanhua T (2020) GO-SHIP Repeat Hydrography Nutrient Manual: the precise and accurate determination of dissolved inorganic nutrients in seawater, using continuos flow analysis methods. Frontiers in Marine Science 7:581790. https://doi.org/10.3389/fmars.2020.581790

Hydes D, Aoyama M, Aminot A, Bakker K, Becker S (2010) Recommendations for the determination of nutrients in seawater to high levels of precision and inter-comparability using continuos flow auotoanalysers. The GO-SHIP repeat hydrography manual: a collection of expert reports and guidelines.

Langdon C (2010) Determination of dissolved oxygen in seawater by Winkler titration using the amperometric technique. The GO-SHIP Repeat Hydrography Manual: A Collection of Expert Reports and Guidelines. IOCCP Report No. 14, ICPO Publication Series No. 134.

Sakamoto CM, Johnson KS, Coletti LJ (2009) Improved Algorithm for the Computation of nitrate concentrations in seawater using an in situ Ultraviolet Spectrophotometer. Limnology and Oceanography: Methods 7:132–143.

6. ALONGATE: A LONG-TERM OBSERVATORY OF THE NORTH ATLANTIC GATEWAY TO THE ARCTIC

Saskia Brix*[1,2], Carolin Uhlir[1,2], Logan Heath[1], Franziska Iwan[1], Katrin Linse[3], Yvonne Schulze-Tenberge[4]
not on board: Bodil Bluhm[5]
*sbrix@senckenberg.de

[1]DE.SENCKENBERG
[2]DE.UHH
[3]UK.BAS
[4]DE.AWI
[5]NO.UiT

Grant-No. AWI_PS148_05 / AWI_PS148_06

Outline

Iceland sits at the top of an underwater mountain chain (Greenland-Iceland-Scotland Ridge: GIS Ridge), which creates an important oceanographic barrier at the border of the North Atlantic to the Arctic Ocean. This ridge system produces „overflow regions“ in the Denmark Strait and between Iceland and the Faroe Islands and its influence in faunal composition and ocean chemistry can be observed as North as Svalbard, Norway (Mauritzen 1996; Puerta et al. 2020; Semper et al. 2020). Known as the “North Atlantic Gateway to the Arctic Ocean” (Jöst et al. 2019), the influence of the North Atlantic water inflow in this Subarctic boundary region demarcates a distinct ecoregion with a unique fauna (Brix et al. 2018a,b, 2022; Uhlir et al. 2021). The ALONGate North-South transect focuses on biodiversity change and connects data from previous established projects around Iceland (BIOICE: Benthic Invertebrates of Icelandic waters 1992 - 2004 and IceAGE: Icelandic marine Animals: Genetics and Ecology since 2011) and additional new samples from *Polarstern*, which transits every year from Germany north to the HAUSGARTEN LTER site in Fram Strait. While a huge amount of biodiversity data is available for this area, the accumulation of data in frequently sampled regions shows clear sampling gaps especially in deep and remote regions (Ramirez-Llodra et al. 2010, 2024). This project fills a critical geographic gap that leverages substantial power from these other recent and ongoing studies. The new lander deployment adds on an intersection of a North-South transect across the North Atlantic Gateway Area complementing the HAUSGARTEN data obtained on PS136 in 2023 and PS143/1 in 2024.

Objectives

The main objective of ALONGate 1 during PS148 is to close sampling and data gaps on the latitudinal transect between Iceland (IceAGE stations) and the LTER HAUSGARTEN (Fig. 6.1). During PS148, the ALONGate-project involves the deployment of a deep-sea benthic lander system in the abyssal plain of the Norwegian Sea at AG-5, which is planned to be recovered in 2026 during the next upcoming FRAM expedition PS155.

The following scientific questions are approached:

1. Do the sampled stations along the latitudinal transect (N/S in the North Atlantic Gateway Area) differ regarding the composition and diversity of the studied benthic species?
2. Are distinct faunal communities in terms of taxonomic composition/species diversity/abundances discernible at the different WAs?
3. Are there potential endemic or widely distributed species present?

Selected specimens collected by benthic sampling are integrated into the British interdisciplinary 5-year NERC programme BIOPOLE (https://biopole.ac.uk/) with the goal to examine biogeochemical processes and ecosystem function in polar ecosystems. It addresses a fundamental aspect of the earth system – how nutrients in polar waters drive the global carbon cycle and primary productivity. The oceans play a vital role in absorbing atmospheric CO2, mitigating large amounts of manmade carbon emissions. Katrin Linse as part of workpackage 2 (WP2) focuses on how biological processes alter carbon:nutrient ratios in polar environments, including focus on parametrising biological processes of the lipid pump.

Research questions to be addressed are:

1. Do benthic animals increase the efficiency of the lipid pump by consuming overwintering zooplankton, especially calanoid copepods, at depth?
2. How can we represent the stoichiometric consequences of the polar lipid pump in a biogeochemical model?

The benthic and copepod samples collected will be used to link benthic biodiversity and productivity patterns to inputs from the upper ocean and in particular to diapausing zooplankton via modelling work within WP2, which aims to improve parameterisation and quantification of the lipid pump within the polar oceans.

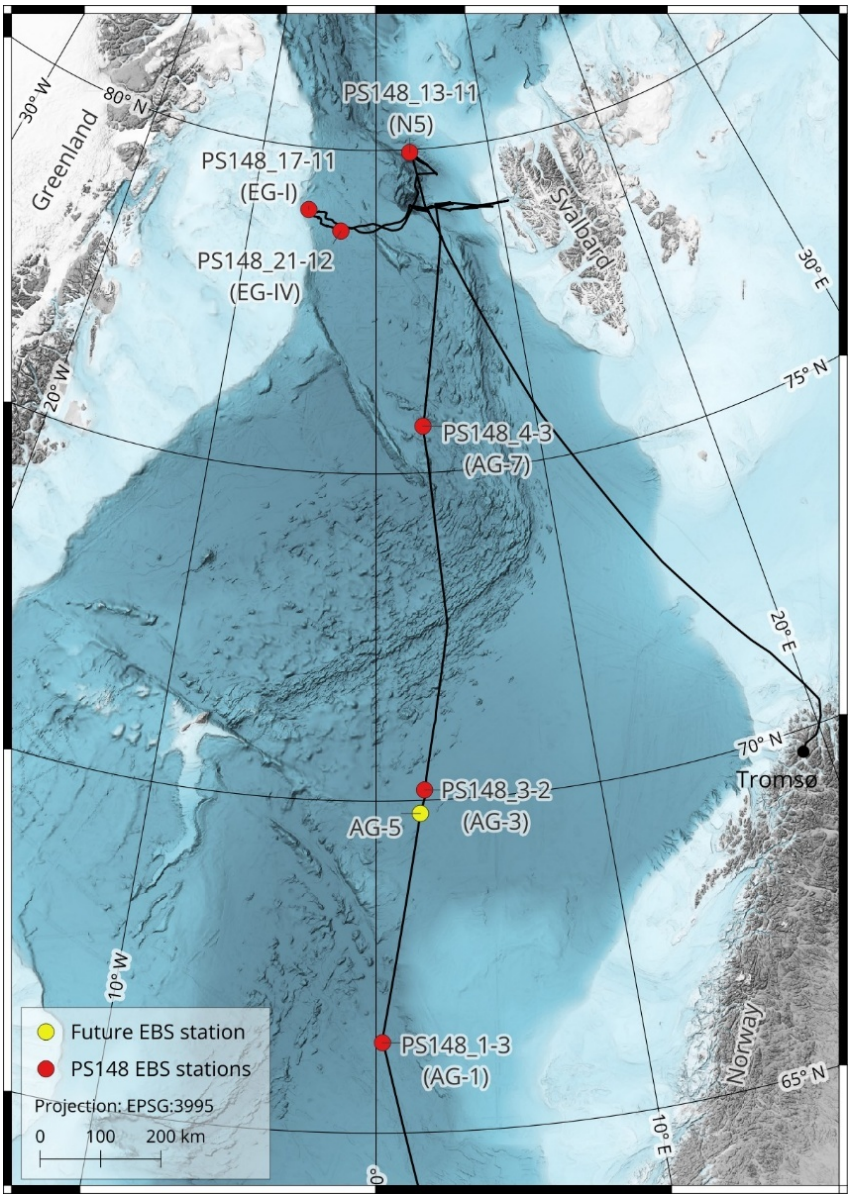

Fig. 6.1: ALONGate transect map with ALONGate (AG) Working Areas (WAs: AG-1,-3,-5 and -7) and deployments within the HAUSGARTEN area (EG-I, EG-IV, N5)

Work at sea

Benthic sampling was conducted across four Working Areas (WAs: AG-1, AG-3, AG-5, AG-7) on the transect from Bremerhaven to Fram Strait (Fig. 6.1). Within the HAUSGARTEN area, gear deployments were prioritized at eastern (EG-I and EG-IV) and northern (N5) stations. Gear deployment in each WA started with a deep CTD to measure conductivity, temperature, chlorophyll concentration, O2 from the water column, and to act as reference for multibeam mapping via a sound velocity profile; Multibeam echosounder (MBES) surveys were performed in each area prior to station work to decide on the exact position of Epibenthic Sledge (EBS, Brenke 2005) deployment. Afterwards, the EBS was deployed for sampling of macro-epifauna. The programme at AG-5 on the transect included the deployment of an Ocean Floor Observation Bathymetry System (OFOBS) to study megafaunal communities, a short-term deep-sea profiling lander as well as a long-term lander equipped with a benthic chamber and

imaging system, allowing us to collect invaluable in-situ observations and measurements to fill this critical knowledge void.

Hydroacoustics

During cruise PS148, bathymetric surveys were conducted with the hull-mounted MBES Teledyne Reson HYDROSWEEP DS3 (HSDS3). The Hydrosweep is a deep-water system for continuous mapping with the full swath potential. It operates on a frequency of ~14 kHz. On *Polarstern*, the MBES transducer arrays are arranged in a Mills cross configuration of 3 m (transmit unit) by 3 m (receive unit). The combined motion, position (Trimble GNSS), and time data comes from an iXBlue Hydrins system and the signal is directly transferred into the Control Module (CM) of the MBES to carry out real-time motion compensation in Pitch, Roll and Yaw. With a combination of phase and amplitude detection algorithms the CM computes the water depth from the returning backscatter signal. The system can cover a sector of up to 140° with 70° per side. In the deep sea, an angle of ~50° to both sides could be achieved.

En route data acquisition was carried out throughout the entire cruise between Bremerhaven and Tromsø where permitted. In addition, four areas with each a radius of around 5 nmi were surveyed for the EBS deployment (see Tab. 6.1). For the surveys, the ship's speed was reduced to approx. 6 kn, to achieve higher swath density. The MBES was operated with Sonar UI and for online data visualization, Teledyne PDS was used. The collected bathymetry was stored in S7K raw files. Subsequent data processing was performed using Caris HIPS and SIPS. For generating maps, the data were exported to QGIS in the GeoTIFF raster format.

For best survey results and to correct the Hydrosweep depths for changes of the sound velocity (SV) in the water column, SV proviles were generated from CTD data that were collected and provided by the physical oceanographic group, see more details about the CTD in chapter 4. SV correlates with the density of a water mass and is thus depending on pressure, temperature and salinity of the seawater in a given location at a given depth. Wrong or outdated SV profiles lead to refraction errors, reduced data quality and faulty depth measurements. In areas where no CTD was operated, synthetic SV profiles were generated with data from the World Ocean Atlas 2018 (Boyer et al. 2018; Locarnini et al. 2019; Zweng et al. 2019) using HydrOffice's Sound Speed Manager. During PS148, a total of 37 SV profiles were applied to the MBES, including 25 profiles from CTD data and 12 synthetic profiles. The CTD-derived SV profiles were also used to calibrate POSIDONIA, which was attached to the EBS.

All bathymetry related stations are listed in Tab. 6.1. For a complete station list that includes the CTD casts, see appendix A.4.

Tab. 6.1: List of bathymetry related stations during PS148

Station Number	Area	Device	Action	Event Time [UTC]	Latitude	Longitude
PS148_0_ Underway-7		HSDS3	profile start	2025-05-30 18:25	57.9771	4.58961
PS148_0_ Underway-7		HSDS3	profile end	2025-06-28 23:48	70.7390	19.8513
PS148_1-2	AG-1	HSDS3	profile start	2025-06-01 23:22	66.371672	0.260782
PS148_1-2	AG-1	HSDS3	profile end	2025-06-02 01:38	66.404624	0.303766
PS148_2-3	AG-5	HSDS3	profile start	2025-06-03 05:50	69.802559	1.948266
PS148_2-3	AG-5	HSDS3	profile end	2025-06-03 08:43	69.839994	1.866767

Station Number	Area	Device	Action	Event Time [UTC]	Latitude	Longitude
PS148_3-1	AG-3	HSDS3	profile start	2025-06-03 19:57	70.112835	2.239526
PS148_3-1	AG-3	HSDS3	profile end	2025-06-03 22:29	70.163857	2.067542
PS148_4-2	AG-7	HSDS3	profile start	2025-06-05 13:28	75.674586	2.936266
PS148_4-2	AG-7	HSDS3	profile end	2025-06-05 16:14	75.658096	2.64177

In addition to the multibeam echosounder, the sub-bottom profiling or sediment echosounding system Teledyne Parasound P70 was used to image the upper tens of meters of the ocean floor's subsurface throughout the entire cruise between Bremerhaven and Tromsø where permitted.

Sub-bottom profiles were recorded with the hull-mounted Deep-Sea Sediment Echosounder PARASOUND (Teledyne Reson, Bremen, Germany) system PS3-P70. This system generates two primary, high-frequency acoustic signals with slightly differing frequencies selectable in a range of 18-24 kHz (PLF, PHF). Due to the non-linear acoustic behaviour of water, the so-called "Parametric Effect", two secondary harmonic frequencies (SLF, SHF) are generated in the water column of which one is the difference (SLF) and the other the sum (SHF), respectively. As a result of the longer wavelength, the secondary low frequency signal (SLF) is able to penetrate the sediment column as deep as for example a 4 kHz signal (up to 100 m depending on sediment conditions), with a vertical resolution of about some decimeters in sediments. With the primary high frequency-signal (PHF), a higher lateral resolution can be achieved, and imaging of small-scale structures on the seafloor is superior to conventional systems. (The secondary high frequency (SHF) can be used for detection of bubbles in the water column, but was not applied on this cruise.) The primary signals are emitted in a narrow beam of 4.5°, but at high power. That has the advantage that the sediment-penetrating SLF pulse is generated within the narrow beam of the primary frequencies, and thereby providing a very high lateral resolution. The system, however, has limitations in imaging rough sea floor topographies or submarine ridges with slopes steeper than 4°. Here, the signal energy reflected from the small inclined footprint on the seafloor is scattered out of the lateral range of the receiving transducers in the hull of the vessel. As a consequence, only few reflections from the seafloor are recorded, i.e., even fewer from the sub-bottom.

During expedition PS148, a 22 kHz setting was used as the PHF, to avoid interferences with the Hydrosweep echosounder system. The SLF was set to 4 kHz. Depending on the properties of the sea-floor surface and sediments, the settings enabled an imaging of the sub-bottom down to more than 100 m, and with a vertical resolution of about 30 cm. The combined signal has a beam width of ~4.5°. The resulting beam's footprint on the sea bottom is about 7 % of the water depth. The system was controlled using the programme Hydromap Control. Live data visualization and data storage was performed with the Parastore software. Data was stored in the file formats ASD and PS3.

Data acquisition took place *en route* and during station work (see Tab. 6.2). The system ran most of the time unobserved due to limited workforce. As a result, system crashes and incorrect settings were often only noticed at a late stage, leading to data gaps. Data conversion and post-processing were not possible and will be done later.

Tab. 6.2: List of sub-bottom profiling related stations during PS148

Station Number	Device	Action	Event Time [UTC]	Latitude	Longitude
PS148_0_ Underway-8	P70	profile start	2025-06-02 16:44:00	68.0957	1.0618
PS148_0_ Underway-8	P70	profile end	2025-06-28 23:40:00	70.7614	19.8155

Benthic macrofauna

The position of the EBS deployments were chosen to complete the station network in the HAUSGARTEN area bulding up on the EBS deployement during PS136 (2023) and PS143/1 (2024) to allow a biodiversity comparison of the qualitative box corer sampling to the semi-qualitative EBS deployment over a larger distance. Deployments took between 2.5 and 3.5 hours and measured trawling distance varied between approx. 300 and 500 m (see Tab. 6.3). The trawled distances were planned to be either parallel or in min. 1 nm distance to the OFOBS transect lines to enable a collection of reference specimens next to a visual description of the sampled area by still and video imagery (see Tab. 2.2). The EBS was deployed via the A-frame of *Polarstern* (Fig. 6.2) following a standard protocol in ice-free areas and an adapted “flexible” protocol to allow sampling with the ice drift in ice covered areas:

1. *Polarstern* holding on start position (in sea-ice drifting with the ice)
2. Lower with 0.5 m/s (max. 0.8 m/s) to 300 m over ground (in sea-ice conditions depending on the drift speed)
3. Winch speed reduced to 0.3 m/s to stop swinging of EBS and letting the gear flowing behind the vessel in the right direction in the water column
4. *Polarstern* moving forward with 1 kt over ground, while lowering with 0.5 m/s until 500 m cable length over water depth or cable length depending on space of free water between the ice floats. The winch speed on stations in the ice depended on the speed of the ice drift as well as the position holding or letting *Polarstern* drifting with the ice during deployment
5. Winch stopped
6. *Polarstern* stopped (step omitted in sea ice conditions or vessel operating against the drift to secure the wire)
7. Heave with 0.3 m/s (max. 0.4) until EBS leaves seafloor
8. Raise heaving speed to 1.0 m/s until deck
9. On deck the EBS will be secured in a hanging position to enable cleaning of nets prior to removal of cod ends and empty of sediment in nets into rectangular rubber tubs.

Landing of the EBS on ground and lift off ground were monitored by the vessels tension meter system digitally and on paper. The trawl lengths were determined by measuring the distance between landing and off-ground position of imbedded POSIDONIA coordinates in QGIS. As the POSIDONIA system crashed at station PS148_13-11, the trawling distance for this station was calculated based on the vessel’s ActionLog coordinates and subtracted by the mean deviation of POSIDONIA and vessel distance at the other five stations.

Fig. 6.2: Deployment of the Epibenthic Sledge ‘BERTA’ *during the ALONGate transect on PS148*

Upon arrival on deck, the cod ends were retrieved from the nets and immediately transported to the cooling container (+2°C). Here, samples were sieved in pre-cooled filtered seawater over a 300 µm mesh. Organisms visible to the eye were removed from the sieve for live sorting and photography of all representative invertebrate taxa and subsequently fixed in undenatured 96 % ethanol. The remaining samples from the cod ends were bulk fixed in pre-cooled denaturated 96 % ethanol and kept at -20°C for 48 h.

When available, net supernatant was sieved on deck at the sieving table with filtered seawater over stacked 1,000 µm, 500 µm and 300 µm sieves. Organisms visible to the eye were removed from the sieve for photography. The remaining samples per sieving fraction were bulk fixed in denatured 96% ethanol.

The decanted fraction of the sieves was caught via a small plankton sieve to focus on copepod crustaceans in collaboration with the BIOPOLE programme. These were sorted independently from the live picked samples and frozen for biochemical analyses. For the macrofauna live picked specimens, if > 3 specimens were found of the same morphotype, one was fixed in 96 % undenatured ethanol, one was frozen at -80°C and one preserved in RNA later, to enable additional transcriptome and genome studies as well as lipid analyses (BIOPOLE: responsible

person Katrin Linse). If less than three specimens per morphospecies were found, the first specimen was fixed in ethanol, the second in RNAlater or frozen. All these specimens were catalogued in the DZMB sample database and documented photographically. Specific samples were given out to cooperating scientists and participants directly on board (potential parasites associated with hosting macrofauna to Sonja Rückert; nematodes to Christiane Hasemann).

During the first 12 h, bulk samples were gently moved every three hours to avoid freezing of the samples. After 24 h the ethanol concentration was measured and the sorting process could be started when 90 % was exceeded. Samples with ethanol concentration lower than 85 % were re-fixed to keep ethanol at high concentrations. All samples were sorted to higher taxon level (phylum, class, order) and selected groups (isopods, cumaceans, pycnogonids, bivalves, gastropods) to family, genus and in some cases to species level.

Tab. 6.3: EBS stations during PS148 based on the vessel's ActionLog. Trawling distances were determined based on POSIDONIA start and end trawling coordinates in QGIS

Area	Station	Date	degLat	degLong	Depth [m]	Gear ActionLog	Trawling Distance [m]
AG-1	PS148_1-3	02.06.2025	66.353076 66.356166	0.244119 0.242887	3108-3118	EBS start EBS end	226
AG-3	PS148_3-2	04.06.2025	70.156326 70.156547	2.172294 2.187242	3215-3216	EBS start EBS end	300
AG-7	PS148_4-3	05.06.2025	75.71764 75.721866	2.931271 2.921763	3117-3123	EBS start EBS end	258
N5	PS148_13-11	12.06.2025	79.956556 79.961869	3.004177 2.98345	2536-2537	EBS start EBS end	506*
EG-I	PS148_17-11	16.06.2025	79.035232 79.040932	-5.465958 -5.483588	999-1002	EBS start EBS end	798
EG-IV	PS148_21-12	18.06.2025	78.738272 78.737275	-2.779475 -2.779714	2560-2561	EBS start EBS end	195

** no POSIDONIA data, calculated based on ActionLog coordinates and subtracted by mean deviation of POSIDONIA trawling and vessel's ActionLog distance of the other stations.*

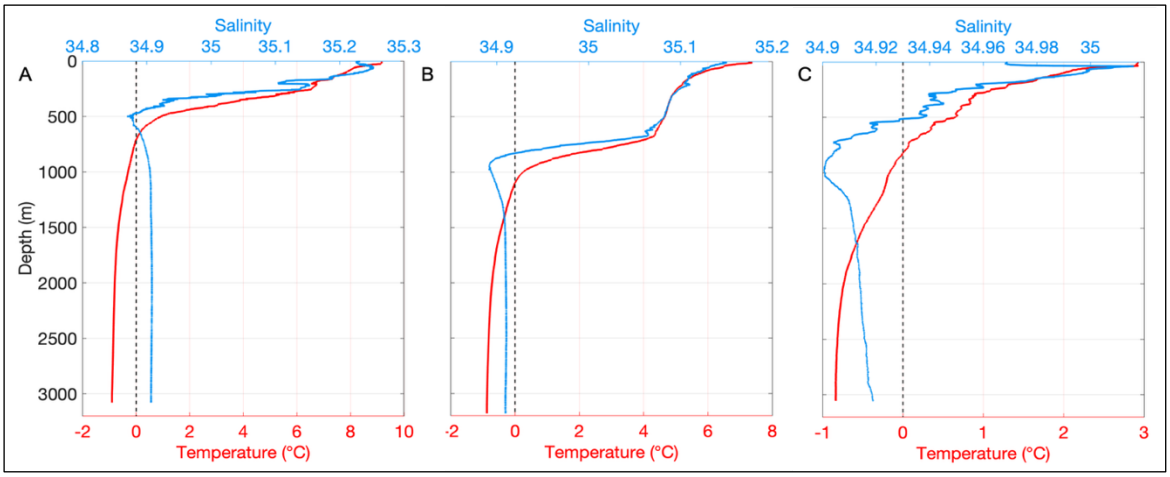

Fig. 6.3: Temperature and salinity data from CTD profiles during EBS deployments at working areas (A) AG-1 (station PS148_1-1), (B) AG-5 (PS148_2-2), and (C) AG-7 (PS148_4-1).

Preliminary results

Hydrography

The CTD profiles (AG-1, AG-5, AG-7) highlight the regional variability of water masses in the Norwegian Sea (Fig 6.3). The profiles at AG-1 and AG-5 show a surface layer of warm (> 2°C) and saline Atlantic Water (AW) overlaying colder, fresher water below 1,000 m. AW temperatures are surface-intensified, up to 8°C, and decrease with depth, though remain relatively constant at approximately -1°C below 1,000 m towards maximum depths below 3,000 m. This is indicative of the Norwegian Atlantic Front Current that transports warm AW northwards from the North Atlantic towards Fram Strait. It forms the offshore branch of the West Spitsbergen Current; half of which recirculates westward in Fram Strait while the rest enters the Arctic Ocean. The AG-7 station is still characterised by a surface layer of warm AW but the temperatures are much lower, reaching a maximum of 3°C. This decrease in AW temperature and its site to the west of the Knipovitch Ridge suggests this is not a continuation of the northwards flowing boundary current but part of the recirculation branch that transports AW westwards towards Greenland. From an oceanographic view it would be anticipated that the benthic communities at stations AG-1 and AG-5 would have similarities, but disparate to the communities at site AG-7.

Hydroacoustics

During approx. 29 days, bathymetric data was surveyed along a track of ~2,854 nmi (~5,286 km) by the swath bathymetry system. Fig. 6.4 shows the generated bathymetry grid over the transit and study area.

In total ~2,078 nmi (~3,849 km) of sub-bottom profiles were acquired during approx. 26 days of operation.

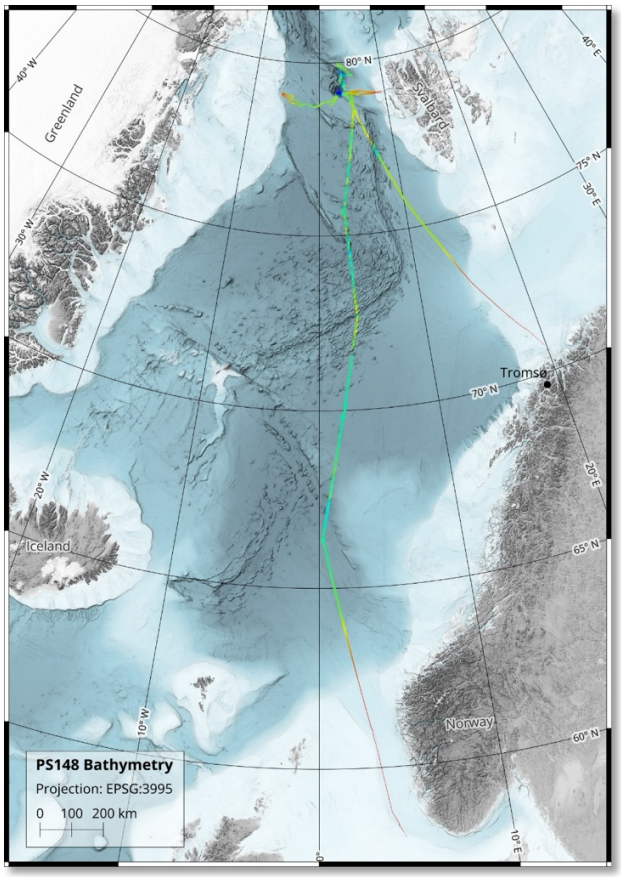

Fig. 6.4: Overview of the bathymetric data acquired during PS148. Background map: AWI Basemap based on the GEBCO 2024 grid (GEBCO Bathymetric Compilation Group 2024 2024)

Benthic macrofauna

A total of 18 samples were taken by EBS in a depth range of 999 – 3,216 m. All samples were sorted directly on board, resulting in 9,437 macrobenthic specimens on higher taxonomic levels. The top ten taxa with the highest number of individuals were Polychaeta (1,742 specimens), Holothuroidea (1,474), Bivalvia (1,325), Isopoda (1,000), Copepoda (772), Cumacea (580), Porifera (525), Mysidacea (504), Tanaidacea (409) and Nematoda (324). To obtain the best possible results for further genetic analyses of the fresh material, the DNA of selected taxa was extracted on board, resulting in a total of 119 voucher specimens (Isopoda: 97 specimens; Cumacea: 25; Pycnogonida: 5; Decapoda: 1; Polychaeta: 1). Live photography documented 51 different morphospecies belonging to 18 higher taxa (selection in Fig. 6.5). For the BIOPOLE programme, 126 macrobenthic specimens (17 Polychaeta, 24 Amphipoda, 2 Cumacea, 4 Decapoda, 9 Isopoda, 21 Mysidacea, 1 Ostracoda, 3 Tanaidacea, 1 Ostracoda, 7 Holothuroidea, 18 Chaetognatha, 2 Cnidaria, 3 Bivalvia, 1 Gastropod, 6 Pycnogonida, 6 Porifera, 3 Pisces), 13 calanoid copepod samples (10 *Calanus hyperboreus*, 3 *Calanus finmarchicus*) and 12 sediment samples were selected and frozen at -80°C for lipid biomarker and bulk stable isotope analyses to study the biological carbon pump and the Fram Strait food web.

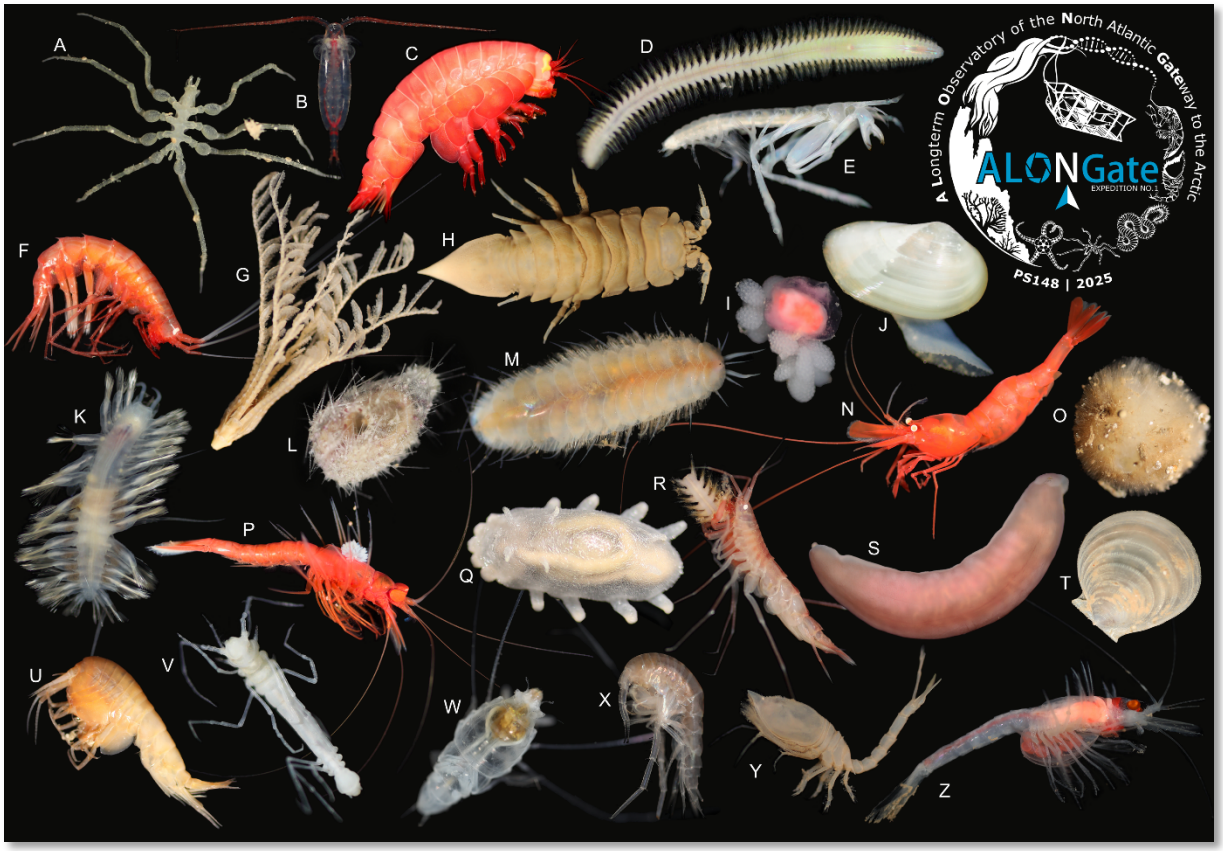

Fig. 6.5: Selection of live photographed morphospecies on PS148 ALONGate-1 transect and in the HAUSGARTEN survey area. A. Pycnogonida (Ascorhynchidae), B. Copepoda (Calanoida), C. Amphipoda (Lysianassidae), D. Polychaeta (Nephtyidae), E. Tanaidacea (Sphyrapodidae), F. Amphipoda (Calliopiidae), G. Crinoidea (Bathycrinidae), H. Isopoda (Chaetiliidae), I. Copepoda (parasitic), J. Bivalvia (Yoldiidae), K. Polychaeta, L. Echinoidea (Pourtalesiidae), M. Polychaeta (Polynoidae), N. Decapoda (Bythocarididae), O. Porifera, P. Mysida with parasitic copepods, Q. Holothuroidea (Elpidiidae), R. Amphipoda with Polychaeta, S. Nemertea, T. Bivalvia (Pectinidae), U. Amphipoda, V. Isopoda (Ischnomesidae), W. Isopoda (Munnopsidae), X. Amphipoda, Y. Cumacea (Diastylidae), Z. Mysida.

Data management

All benthic samples by EBS are curated at the German Center for Marine Biodiversity (DZMB) in Hamburg and Wilhelmshaven, Germany. Specimens assigned to the BIOPOLE programme will be stored until the destructive biomarker and bulk isotope analyses at the British Antarctic Survey (BAS) in Cambridge, United Kingdom. All samples were sorted directly on board to higher taxa level. Specific groups will be handed over to taxonomic experts for further identification. Molecular DNA and RNA data will be archived, published and disseminated within the publicly accessible repositories GenBank (https://www.ncbi.nlm.nih.gov/genbank/) and BOLD (https://www.boldsystems.org/index.php). After successful identification, records will be uploaded to the Ocean Biodiversity Information System (OBIS. https://obis.org) and the Global Biodiversity Information Facility (GBIF, https://www.gbif.org).

Environmental data will be archived, published and disseminated according to international standards by the World Data Center PANGAEA Data Publisher for Earth & Environmental Science (https://www.pangaea.de) within two years after the end of the expedition at the latest. By default, the CC-BY license will be applied.

Any other data will be submitted to an appropriate long-term archive that provides unique and stable identifiers for the datasets and allows open online access to the data.

This expedition was supported A) by the Leibniz program for women professors under grant P150/2023, B) by the Helmholtz Research Programme “Changing Earth – Sustaining our Future” Topic 2, Subtopic 2 and 3, and the BIOPOLE National Capability Multicentre Round 2 funding from the Natural Environment Research Council (grant no. NE/W004933/1)

In all publications based on this expedition, the **Grant No. AWI_PS148_05** and **AWI_PS148_06** will be quoted and the following publication will be cited:

Alfred-Wegener-Institut Helmholtz-Zentrum für Polar- und Meeresforschung (2017) Polar Research and Supply Vessel POLARSTERN Operated by the Alfred-Wegener-Institute. Journal of large-scale research facilities. 3. A119. http://dx.doi.org/10.17815/jlsrf-3-163.

References

Boyer TP, García HE, Locarnini RA, Zweng MM, Mishonov AV, Reagan JR, Weathers KA, Baranova OK, Paver CR, Seidov D, Smolyar IV (2018) World Ocean Atlas.

Brenke N (2005) An epibenthic sledge for operations on marine soft bottom and bedrock. Marine Technology Society Journal 39:11–21.

Brix S, Lörz AN, Jazdzewska AM, Hughes L, Tandberg AH, Pabis K, Stransky B, Krapp-Schickel T, Sorbe JC, Hendrycks E, Vader W (2018a) Amphipod family distributions around Iceland. ZooKeys 731:1.

Brix S, Stransky B, Malyutina M, Pabis K, Svavarsson J, Riehl T (2018b) Distributional patterns of isopods (Crustacea) in Icelandic and adjacent waters. Marine Biodiversity 48:783–811.

Brix S, Kaiser S, Lörz A, Le Saout M, Schumacher M, Bonk F, Egilsdottir H, Olafsdottir SH, Tandberg AHS, Taylor J, Tewes S, Xavier JR, Linse K (2022) Habitat variability and faunal zonation at the Ægir Ridge, a canyon-like structure in the deep Norwegian Sea. PeerJ 10:e13394. https://doi.org/10.7717/peerj.13394

GEBCO Bathymetric Compilation Group 2024 (2024) The GEBCO_2024 Grid - a continuous terrain model of the global oceans and land. https://doi.org/10.5285/1C44CE99-0A0D-5F4F-E063-7086ABC0EA0F

Jöst AB, Yasuhara M, Wei CL, Okahashi H, Ostmann A, Martinez Arbizu P, Mamo B, Svavarsson J, Brix S (2019) North Atlantic gateway: Test bed of deep-sea macroecological patterns. Journal of Biogeography 46:2056–2066.

Locarnini RA, Mishonov AV, Baranova OK, Boyer TP, Zweng MM, Garcia HE, Reagan JR, Seidov D, Weathers KW, Paver CR, Smolyar IV (2019) World Ocean Atlas 2018, Volume 1: Temperature. Mishonov AV (ed) NOAA Atlas NESDIS 81, 52 pp. https://doi.org/10.25923/e5rn-9711

Mauritzen C (1996) Production of dense overflow waters feeding the North Atlantic across the Greenland-Scotland Ridge. Part 1: Evidence for a revised circulation scheme. Deep Sea Research Part I: Oceanographic Research Papers 43:769–806.

Puerta P, Johnson C, Carreiro-Silva M, Henry LA, Kenchington E, Morato T, Kazanidis G, Rueda JL, Urra J, Ross S, Wei CL, Gonzalez-Irusta JM, Arnaud-Haond S, Orejas C (2020) Influence of water masses on the biodiversity and biogeography of deep-sea benthic ecosystems in the North Atlantic. Frontiers in Marine Science 7:239.

Ramirez-Llodra E, Brandt A, Danovaro R, De Mol B, Escobar E, German CR, Levin LA, Martinez Arbizu P, Menot L, Buhl-Mortensen P, Narayanaswamy BE, Smith CR, Tittensor DP, Tyler PA, Vanreusel A, Vecchione M (2010) Deep, diverse and definitely different: Unique attributes of the world's largest ecosystem. Biogeosciences 7:2851–2899.

Ramirez-Llodra E, Meyer HK, Bluhm BA, Brix S, Brandt A, Dannheim J, Downey RV, Egilsdottir H, Eilertsen MH, Gaudron SM, Gebruk A, Golikov A, Hasemann C, Hilario A, Jørgensen LL, Kaiser S, Korfhage SA, Kürzel K, Lörz AN, Buhl-Mortensen P, Ólafsdóttir SH, Piepenburg D, Purser A, Ribeiro PA, Sen A, Soltwedel T, Stratmann T, Steger J, Svavarsson J, Tandberg AHS, Taylor J, Theising FI, Uhlir C, Waller RG, Xavier JR, Zhulay I, Saaedi H (2024) The emerging picture of a diverse deep Arctic Ocean seafloor: From habitats to ecosystems. Elementa: Science of the Anthropocene 12:e00140. https://doi.org/10.1525/elementa.2023.00140

Semper S, Pickart RS, Våge K, Larsen KMH, Hátún H, Hansen B (2020) The Iceland-Faroe Slope Jet: A conduit for dense water toward the Faroe Bank Channel overflow. Nature Communications 11:5390. https://doi.org/10.1038/s41467-020-19049-5

Uhlir C, Schwentner M, Meland K, Kongsrud JA, Glenner H, Brandt A, Thiel R, Svavarsson J, Lörz A, Brix S (2021) Adding pieces to the puzzle: Insights into diversity and distribution patterns of Cumacea (Crustacea: Peracarida) from the deep North Atlantic to the Arctic Ocean. PeerJ 9:e12379. https://doi.org/10.7717/peerj.12379

Zweng MM, Reagan JR, Seidov D, et al. (2019) World Ocean Atlas 2018. Volume 2: Salinity. https://doi.org/10.25923/9pgv-1224

7. BIOGEOCHEMISTRY AND MICROBIAL ECOLOGY AT LTER HAUSGARTEN AND THE MOLLOY DEEP

Johannes Maring[1], Leonie Buchele[1], Frank Wenzhöfer[1,2], Lisbeth Fürst Sørensen[2], Hannah Sophie Mihm[2]

*frank.wenzhoefer@awi.de

[1]DE.AWI
[2]DK.SDU

Grant-No. AWI_PS148_07

Outline

Benthic communities are strictly dependent on carbon supply through the water column, which is determined by temporal and spatial variations in the vertical export flux from the euphotic zone but also lateral supply from shelf areas. Most organic carbon is recycled in the pelagic, but a significant fraction of the organic material ultimately reaches the seafloor, where it is either re-mineralized or retained in the sediment record. One of the central questions is to what extent sea-ice cover controls primary production and subsequent export of carbon to the seafloor on a seasonal and interannual scale. Benthic oxygen fluxes provide the best and integrated measurement of the metabolic activity of surface sediments. They quantify benthic carbon mineralization rates and thus can be used to evaluate the efficiency of the biological pump. In order to link long-term variations in surface and sea-ice productivity and consequently in export flux to the seafloor, detailed investigation of the temporal variations in benthic oxygen consumption rates would be very valuable. Yearly measurements with benthic lander provide information on the interannual variations. Benthic crawler, mobile seafloor platforms capable to perform weekly oxygen gradient measurements for a 12-month period, provide information on the seasonal variations. In addition, long-term benthic lander systems equipped with sediment traps and cameras for time-lapse imaging of the seafloor record the supply of organic material throughout the year. Many areas of the deep sea are still little explored. Deep-sea (or hadal) trenches, for example, only account for less than 2% of the global seabed area, but could via sediment focusing act as regionally important but unexplored traps for organic material (Glud et al. 2013, 2021). Benthic mineralization is mainly driven by vast numbers of bacteria and archaea, with direct or indirect contributions by viruses, fungi, protists, and meiofauna. Currently, even the most basic information on abundance and distribution of microbes and small eukaryotes in deep sea and trench sediments are missing. We want to use the Molloy Deep (5.5 km) as a model area to quantify the carbon mineralization-efficiency of sediments in and at adjacent shallower reference sites, identify the key players for the processing and compare process rates and microbial communities with other deep sea and trench ecosystems.

Objectives

Benthic flux study:

Seafloor carbon mineralization was studied in-situ at sites with varying sea-ice conditions (AG-5, HG-IV, N4) using a benthic lander system (Hoffmann et al. 2018). The benthic O_2 uptake is commonly used measure for the benthic mineralization rate (Wenzhöfer et al. 2016). We measured benthic oxygen consumption rates at different spatial and temporal scales. The benthic lander was equipped with two different profiling instruments to investigate the oxygen penetration and distribution as well as the benthic oxygen uptake of Arctic deep-sea sediments: i) electrode-microprofiler, for high-resolution pore water profiles (O_2, resistivity) across the sediment-water interface, and ii) a deep optode-profiler, to measure the entire oxygen penetration depth. From the measured profiles, the oxygen consumption is calculated from which the carbon turnover rates are determined.

Quantification of the pelagic export and benthic mineralization of organic carbon:

Using state-of-the-art lander technology, we measured in situ benthic oxygen consumption rates within and around the Molloy Deep. The data provided a unique assessment of the regional benthic carbon mineralization rates and filled data gaps in the current global data base. The involved diagenetic pathways were quantified from porewater profiles and the distribution of solid-state iron and manganese, and dissolved inorganic nitrogen as well as onboard measurements of sulfate reduction, denitrification, and anammox. The site-specific turn-over rates are going to be linked to the pelagic activity and sedimentation rates derived from the distribution of natural radionuclides but also linked to long-term assessments of pelagic productivity at the respective sites estimated from remote sensing (Jørgensen et al. 2022). Thereby we are aiming to assess the quantitative link between surface primary production and underlying benthic activity and evaluate the potential importance of horizontal transport of organic material in the complex benthic seascape of the region.

Exploring the biogeochemical function and community composition in the deep sea:

The proposed studies are essential for understanding carbon and nitrogen cycling, pelagic-benthic coupling and benthic community structures in this very important region of the Arctic Ocean. However, the work should also be seen in the context of a wider ambition of exploring life and biogeochemical function of the deep sea. The proposed work in the productive region of the Molloy Deep within the Fram Strait greatly complemented investigations on hadal systems of different biogeographic provinces. The combined data provided generic insights on the biogeochemical function and life in deep-sea and hadal trench systems underlying different productivity regimes. The analysis on community structures will explore the extent by which deep basins and trench systems act as isolated biogeographic habitats dominated by unique co-evolving communities or if they represent interconnected extreme environments. To assess the effect of hydrostatic pressure on marine microbes, on-board pressure tank experiments were carried out. Rates of benthic microbial processes like aerobic respiration, nitrification, denitrification, anammox, and sulfate reduction were measured at different pressure levels.

Work at sea

We investigated key ecosystem functions such as benthic respiration, remineralization, matter transport, and microbial and meiofaunal biodiversity in the Molloy Deep (5,500 m) and the surrounding abyssal and bathyal sediments of the Arctic Ocean. Our primary focus was on in-situ benthic flux measurements, microbial process rates, and sediment sampling. These measurements contributed to the limited existing dataset on deep-sea and hadal environments.

A benthic lander system was used to investigate benthic oxygen uptake rates, oxygen distribution, and penetration depths at various spatial resolutions within the sediment. The

lander was used to obtain multiple vertical oxygen profiles across the sediment–water interface. Equipped with up to nine oxygen electrodes, a conductivity sensor, and a temperature sensor, it measured concentration profiles along a 50 cm horizontal transect with 100 µm vertical resolution over depths of 15 - 25 cm. These data were used to quantify diffusive oxygen uptake (DOU), attributed to microbial respiration. The benthic lander was deployed at stations AG-5, HG-IX, HG-IV, and N4.

At HG-IV a benthic crawler system (Crawler-III), which was deployed in 2024 (PS143/1), was recovered after its 12-month mission. The crawler system was pre-programmed to perform >50 measurements along a ca 1.0 km transect. Crawler-III (similar with crawler NOMAD; Lemburg et al. 2018) used oxygen optodes to measure vertical concentration profiles across the sediment-water interface (one set of profiles each week). Additionally, the crawler was equipped with benthic chambers and a seafloor imaging and scanning camera system to take images of the seafloor combined with a laser scan. From this information we were able to reconstruct the sediment surface at high resolution. When seafloor images and topography scans were overlaid, we were able to identify hot spots of intensified organic matter accumulation. These two seafloor observations were performed during the 10 m long transect at the beginning of each measuring cycle. At the end of each transect, oxygen concentration profiles were measured and benthic chamber incubations were performed. From these data oxygen consumption rates could be obtained which provided information on carbon mineralization. These cycles were repeated every week for a period of 12-month.

A multicorer (MUC) was used to retrieve intact and undisturbed sediment cores from our two focus stations: HG-IX (the Molloy Deep) and HG-IV (used as a reference station). Sediments from these stations underwent a wide range of (bio)geochemical analyses (Tab. 7.1). Cores were sectioned into 1 cm slices from 0 to 10 cm depth, followed by 2.5 cm slices down to the bottom of the core. All sediment samples were preserved accordingly for further analysis at the University of Southern Denmark. Additional onboard measurements included porewater analysis and microbial rate assessments. The importance of hydrostatic pressure for microbial processes was investigated using state-of-the-art (self-made) pressure cylinders. Pressure effects on key microbial processes; anammox, denitrification (using ^{15}N tracer combinations), and sulfate reduction (using ^{35}S radiotracers) in sediments from the Molloy Deep were determined through pressure time series experiments conducted at 0.1, 20, 40, 55, 80, and 100 MPa. The data obtained from these experiments will contribute to an existing dataset on pressure effects on microbial rates in sediments retrieved from shallow to deep-sea environments. In addition to sampling at the two focus stations, sediment was collected for trace metal, mercury, and methylmercury analyses at stations S3, N5, N4, N3, EG-IV, HG-VI, and HG-I. Surface water (0-500 m) and hand-net samples for phytoplankton and water were sampled at HG-IX, HG-IV, S3, and N4 for analysis of mercury and methylmercery. Bottom water (50 m above seafloor) was sampled at HG-IX for further experiments at the University of Southern Denmark.

Tab. 7.1: Overview measured and to be measured parameters on sampled sediment on board.

Geochemistry	Porosity, density, grainsize, organic carbon content, C/N, core photo, trace metals, mercury and methylmercury, microplastics.
Biogeochemistry	Porewater profiles: O_2, NO_2^-, NO_3^-, NH_4^+, SO_4^{2-}, PO_4^{3-}, Fe^{2+}, Mn^{2+}, DIC. Solid state profiles: Fe and Mn.
Biology	DNA sequencing (metagenomics), Diatom
Microbial process rates	Sulfate reduction, denitrification, anammox at different hydrostatic pressures.

Preliminary (expected results

In situ work:

In-situ oxygen profiles from Lander deployments were completed at several stations (Tab. 7.2). Unfortunately, Crawler III, deployaed at HG-IV, only worked for approximately five weeks; after that, the mission was aborted due to a technical error. In-situ high-resolution microprofiles in the top sediment layer were performed at all stations and are used to calculate the oxygen uptake (DOU) across the sediment-water interface using the linear gradient in the diffusive boundary layer (DBL) above the sediment.

Tab. 7.2: Overview of in-situ devices

Station	Device Operation	Description	Event Time	Action	Latitude	Longitude	Depth (m)
AG-5	PS148_2-1	Flux-Lander	03.06.25 02:47	deployed	69° 47,642' N	001° 57,617' E	3218
AG-5	PS148_2-6	LT-Lander_AlonGate	03.06.25 15:54	deployed	69° 49,742' N	001° 58,453' E	3225
HG-IV	PS148_6-8	Flux-Lander Deployment	08.06.25 11:27	deployed	79° 04,837' N	004° 05,332' E	2448
HG-IV	PS148_6-9	Crawler-III	08.06.25 12:09	information	79° 04,671' N	004° 05,694' E	2445
HG-IV	PS148_8-4	Crawler-III	09.06.25 13:21	information	79° 04,867' N	004° 04,394' E	2445
HG-IV	PS148_8-5	Lander-Crawler	09.06.25 16:51	deployed	79° 04,840' N	004° 05,473' E	2446
N-4	PS148_14-1	Flux-Lander	12.06.25 23:56	deployed	79° 44,236' N	004° 29,537' E	2645
EG-IV	PS148_21-1	Lander-Crawler	17.06.25 22:32	deployed	78° 45,806' N	002° 46,395' W	2552
HG-IX	PS148_22-1	Flux-Lander	19.06.25 18:12	deployed	79° 08,559' N	002° 45,620' E	5552
HG-IX	PS148_22-3	Hadal-Mooring	20.06.25 11:51	deployed	79° 08,304' N	002° 47,131' E	5553
HG-IV	PS148_25-2	LT-Lander_2024	21.06.25 07:22	released	79° 03,465' N	004° 14,898' E	2415
HG-IV	PS148_25-3	OFOBS-Crawler	21.06.25 12:46	in water	79° 04,727' N	004° 07,598' E	2427
HG-IV	PS148_25-3	OFOBS-Crawler	21.06.25 15:40	information	79° 04,631' N	004° 06,164' E	2446
HG-IV	PS148_25-3	OFOBS-Crawler	21.06.25 18:33	off water	79° 04,536' N	004° 06,272' E	2449
HG-IV	PS148_33-1	OFOBS-Crawler	24.06.25 17:38	in the water	79° 04,514' N	004° 07,257' E	2438
HG-IV	PS148_33-1	OFOBS-Crawler	24.06.25 19:15	recovered	79° 04,648' N	004° 06,207' E	2444
HG-IV	PS148_33-1	OFOBS-Crawler	24.06.25 22:10	off water	79° 04,719' N	004° 05,723' E	2449
HG-IV	PS148_33-2	LT-Lander_2025	24.06.25 22:49	deployed	79° 01,902' N	004° 13,558' E	2534

Laboratory work:

Core photos of the collected sediments from sites HG-IV and HG-IX revealed clear differences in sediment characteristics. HG-IV sediments were brown to orange in color with a mixed composition, indicating well-oxidized conditions and the presence of iron oxides. In contrast, the deeper site HG-IX displayed laminated sediments with black to grey layers, likely reflecting the accumulation of iron sulfides due to sulfate reduction. Onboard measurements of porewater NH_4^+ showed distinct vertical profiles at each site. At HG-IX, elevated NH_4^+ concentrations below the oxygen penetration depth (5.5 cm) suggested high rates of organic carbon mineralization. The consistently low NH_4^+ concentrations at HG-IV indicated more oxidized conditions and lower rates of organic matter breakdown (Fig. 7.1). These findings are consistent with NH_4^+ measurements recorded from PS143/1 expedition in 2024.

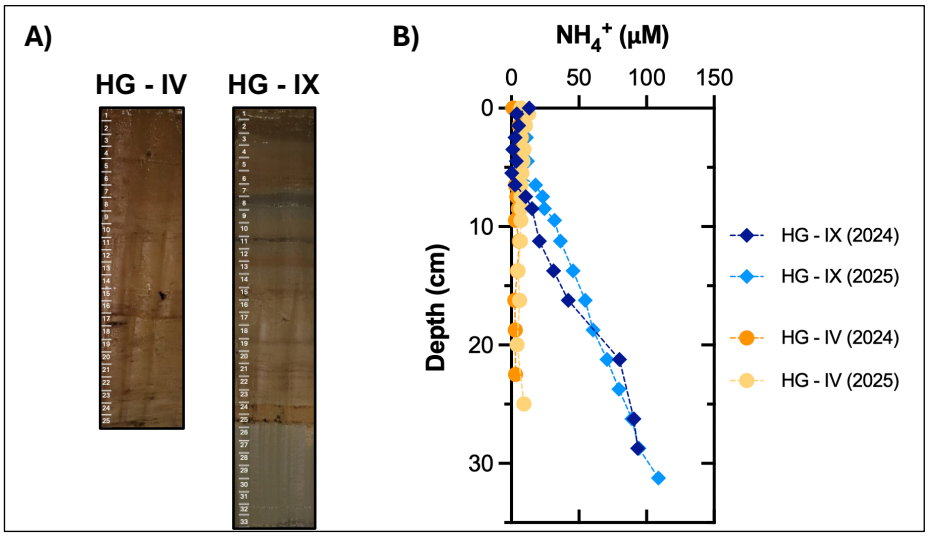

Fig. 7.1: A) Photos of vertically splitted sediment cores from HG-IV and HG-IX. B) NH_4^+ Porewater concentration at HG-IV (2400 m) and HG-IV (5500 m) from PS142/1 in 2024 and from this cruise, 2025

Data management

Environmental data will be archived, published and disseminated according to international standards by the World Data Center PANGAEA Data Publisher for Earth & Environmental Science (https://www.pangaea.de) within two years after the end of the expedition at the latest. By default, the CC-BY license will be applied.

Molecular data (DNA and RNA data) will be archived, published and disseminated within one of the repositories of the International Nucleotide Sequence Data Collaboration (INSDC, www.insdc.org) comprising of EMBL-EBI/ENA, GenBank and DDBJ).

Any other data will be submitted to an appropriate long-term archive that provides unique and stable identifiers for the datasets and allows open online access to the data.

This expedition was supported by the Helmholtz Research Programme “Changing Earth – Sustaining our Future” Topic 6, Subtopic 3; and the Center of Excellence; “Danish Center for Hadal Research – HADAL (DNRF145)”.

In all publications based on this expedition, the **Grant No. AWI_ PS148_07** will be quoted and the following publication will be cited:

Alfred-Wegener-Institut Helmholtz-Zentrum für Polar- und Meeresforschung (2017) Polar Research and Supply Vessel POLARSTERN Operated by the Alfred-Wegener-Institute. Journal of large-scale research facilities, 3, A119. http://dx.doi.org/10.17815/jlsrf-3-163..

References

Hoffmann R, Braeckman U, Hasemann C, Wenzhöfer F (2018) Deep-sea benthic communities and oxygen fluxes in the Arctic Fram Strait controlled by sea-ice cover and water depth. Biogeosciences 15:4849–4869.

Lemburg J, Wenzhöfer F, Hofbauer M, Färber P, Meyer V (2018) Benthic crawler NOMAD – Increasing payload by low-density design. Proceedings OCEANS 2018 MTS/IEEE Kobe, Japan, 279–285.

Glud RN, Berg P, Thamdrup B, Larsen M, Stewart HA, Jamieson AJ, Glud A, Oguri K, Sanei H, Rowden AA, Wenzhöfer F (2021) Hadal trenches are dynamic hotspots for early diagenesis in the deep-sea. Commun Earth Environ 2:21. https://doi.org/10.1038/s43247-020-00087-2

Glud RN, Wenzhöfer F, Middelboe M, Oguri K, Turnewitsch R, Canfield DE, Kitazato H (2013) High rates of benthic microbial activity at 10.900 meters depth: Results from the Challenger Deep (Mariana Trench), Nature Geoscience 6:284–288. https://doi.org/10.1038/NGEO1773

Jørgensen BB, Wenzhöfer F, Egger M, Glud RN (2022) Sediment oxygen consumption: Role in the global marine carbon cycle. Earth-Science Reviews 228:103987. https://doi.org/10.1016/j.earscirev.2022.103987

Wenzhöfer F, Oguri K, Middelboe M, Turnewitsch R, Toyofuku T, Kitazato H, Glud RN (2016) Benthic carbon mineralizationin hadal trenches: Assessment by *in situ* O_2 microprofile measurements. Deep Sea Res I 116:276–286.

APPENDIX

A.1 TEILNEHMENDE INSTITUTE / PARTICIPATING INSTITUTES

A.2 FAHRTTEILNEHMER:INNEN / CRUISE PARTICIPANTS

A.3 SCHIFFSBESATZUNG / SHIP‘S CREW

A.4. STATIONSLISTE / STATION LIST PS148

A.1 TEILNEHMENDE INSTITUTE / PARTICIPATING INSTITUTES

Affiliation	Address
DE.AWI	Alfred-Wegener-Institut Helmholtz-Zentrum für Polar- und Meeresforschung Postfach 120161 27515 Bremerhaven Germany
DE.CAU	Christian-Albrechts-Universität zu Kiel Christian-Albrechts-Platz 4 24118 Kiel Germany
DE.DRF	DRF Luftrettung gAG Laval Avenue E312 77836 Rheinmünster Germany
DE.DWD	Deutscher Wetterdienst Frankfurter Strasse 135 63067 Offenbach am Main Germany
DE.GEOMAR	GEOMAR Helmholtz-Zentrum für Ozeanforschung Wischofstr. 1-3 24148 Kiel Germany
DE.HS-Bremerhaven	Hochschule Bremerhaven An der Karlstadt 8 27568 Bremerhaven Germany
DE.NHC	Northern HeliCopter GmbH Gorch-Fock-Str. 103 26721 Emden Germany
DE.SENCKENBERG	Senckenberg Forschungsinstitut und Naturmuseum Martin-Luther-King-Platz 3 20146 Hamburg Germany
DE.UNI-Bremen	Universität Bremen Leobener Straße, NW2a Otto-Hahn-Allee 1 28359 Bremen Germany

Affiliation	Address
DE.UNI-DUE	Universität Duisburg-Essen Universitätsstraße 2/5 45141 Essen Germany
DE.UNI-Oldenburg	Carl von Ossietzky Universität Oldenburg Carl-von-Ossietzky-Strasse 9-11 26130 Oldenburg Germany
DK.SDU	University of Southern Denmark Campusvej 55 5230 Odense Denmark
UK.BAS	British Antarctic Survey Hich Cross CB3 0ET Cambridge United Kingdom
Not on board / Not in the field	
NO.UiT	UiT The Arctic University of Norway PO Box 6050 Stakkevollan N-9037 Tromsø Norway

A.2 FAHRTTEILNEHMER:INNEN / CRUISE PARTICIPANTS

Name/ Last name	Vorname/ First name	Institut/ Institute	Beruf/ Profession	Fachrichtung/ Discipline
Barz	Jakob	DE.AWI	Technician	Chemistry
Becker	Luise	DE.UNI-Bremen	Student (Master)	Physics
Bienhold	Christina Andrea	DE.AWI	Scientist	Biology
Brauer	Jens	DE.NHC	Pilot	Helicopter Service
Brenner	Claudia	DE.UNI-Bremen	Student (Bachelor)	Biology
Bretinger	Jan Paul	DE.UNI-DUE	Student (Master)	Biology
Brix-Elsig	Saskia Bianca	DE.SENCKENBERG	Scientist	Biology
Buchele	Leonie	DE.AWI	Engineer	Engineering Sciences
Buchholz	Stine Margritli	DE.AWI	HiWi	Biology
Busack	Michael	DE.AWI	Engineer	Engineering Sciences
Claver	Miriam Christina	DE.UNI-Oldenburg	Student (Master)	Biology
Dannheim	Jennifer	DE.AWI	Scientist	Biology
Dolinkiewicz	Magdalena Ewa	DE.AWI	PhD student	Biology
Dörmbach	Barbara	DE.AWI	PhD student	Biology
Gorniak	Rebecca	DE.UNI-Bremen	Student (Bachelor)	Biology
Handelmann	Nils	DE.AWI	Engineer	Engineering Sciences
Hasemann	Christiane Margarete Elisabeth	DE.AWI	Scientist	Biology
Hausen	Robert	DE.DWD	Scientist	Meteorology
Heath	Logan	DE.SENCKENBERG	Student (Master)	Biology
Hoge	Ulrich	DE.AWI	Engineer	Engineering Sciences
Hölzer	Martin	DE.DRF	Technician	Helicopter Service
Iwan	Franziska	DE.SENCKENBERG	Technician	Biology
Kistrup	Katharina	DE.UNI-Bremen	Student (Bachelor)	Biology
Kluever	Tania	DE.GEOMAR	Technician	Biology
Knüppel	Nadine	DE.AWI	Technician	Biology
Kohlenbach	Katharina	DE.AWI	PhD student	Biology
Köhler	Raphael Harry	DE.AWI	Scientist	Meteorology
Lehmenhecker	Sascha Bernd Peter	DE.AWI	Engineer	Engineering Sciences
Linder	Samira Sarojani	DE.CAU	Student (Master)	Oceanography
Linse	Katrin	UK.BAS	Scientist	Biology
Lochthofen	Normen	DE.AWI	Engineer	Engineering Sciences

Name/ Last name	Vorname/ First name	Institut/ Institute	Beruf/ Profession	Fachrichtung/ Discipline
Ludszuweit	Janine	DE.AWI	Technician	Biology
Maring	Johannes	DE.AWI	Technician	Engineering Sciences
Markus	Johannes	DE.AWI	Student (Bachelor)	Engineering Sciences
McPherson	Rebecca	DE.AWI	Scientist	Oceanography
Metfies	Katja	DE.AWI	Scientist	Biology
Mihm	Hannah Sofie	DK.SDU	Scientist	Earth Sciences
Pein	Carla Marlene	DE.GEOMAR	PhD student	Biology
Purser	Autun	DE.AWI	Scientist	Biology
Rode	Jörg	DE.DRF	Engineer	Helicopter Service
Rückert	Sonja	DE.UNI-DUE	Scientist	Biology
Schewe	Ingo	DE.AWI	Scientist	Biology
Schmidt	Ina	DE.AWI	Technician	Physics
Scholz	Daniel Alexander	DE.AWI	Engineer	Chemistry
Schulze Tenberge	Yvonne	DE.AWI	Scientist	Geophysics
Soerensen	Lisbeth Fürst	DK.SDU	PhD student	Biology
Uhlir	Carolin Diana	DE.SENCKENBERG	PhD student	Biology
Vaupel	Lars	DE.NHC	Pilot	Helicopter Service
Wenzhoefer	Frank	DE.AWI	Scientist	Biology
Westphal	Matthias	DE.HS-Bremerhaven	Student (Bachelor)	Biology
Zeising	Moritz	DE.AWI	PhD student	Oceanography

A.3 SCHIFFSBESATZUNG / SHIP'S CREW

No	Dienstgrad	Rank	Nachname / Last name	Vorname / First name
1	Kapitän	Master	Schwarze	Stefan
2	1. Offizier	Chief Mate	Strauss	Erik
3	1. Offizier Ladung	Chief Mate Cargo	Eckenfels	Hannes
4	2. Offizier	2nd Mate	Stelljes	Daniel
5	2. Offizier	2nd Mate	Peine	Lutz
6	Schiffsarzt	Doctor	Guba	Klaus
7	Leitender Ingenieur	Chief Engineer	Ziemann	Olaf
8	2. Ingenieur	2nd Engineer	Ehrke	Tom
9	2. Ingenieur	2nd Engineer	Krinfeld	Oleksandr
10	2. Ingenieur	2nd Engineer	Rusch	Torben
11	Schiffselektrotechniker Maschine	Ship Electrotechnical Officer Engine	Pommerencke	Bernd
12	Elektroniker Winden	Electrotechnical Engineer Winches	Krüger	Lars
13	Elektroniker Netzwerk/Brücke	Electrotechnical Engineer Network/Bridge	Hofmann	Jörg
14	Elektroniker Labor	Electrotechnical Engineer Labor	Ejury	René
15	Elektroniker System	Electrotechnical Engineer System	Winter	Andreas
16	Bootsmann	Bosun	Meier	Jan
17	Zimmermann	Carpenter	Keller	Jürgen
18	Schiffsmechaniker Deck	Multi Purpose Rating Deck	Buchholz	Joscha
19	Schiffsmechaniker Deck	Multi Purpose Rating Deck	Möller	Falko
20	Schiffsmechaniker Deck	Multi Purpose Rating Deck	Mahlmann	Oliver Karl-Heinz
21	Schiffsmechaniker Deck	Multi Purpose Rating Deck	Schade	Tom
22	Schiffsmechaniker Deck	Multi Purpose Rating Deck	Siegel	Kilian

No	Dienstgrad	Rank	Nachname / Last name	Vorname / First name
23	Schiffsmechaniker Deck	Multi Purpose Rating Deck	Deutschbein	Felix Maximilian
24	Schiffsmechaniker Deck	Multi Purpose Rating Deck	Siemon	Leon Anton
25	Decksmann/Matrose	Able Seaman	Niebuhr	Tim
26	Lagerhalter	Storekeeper	Plehn	Marco Markus
27	Schiffsmechaniker Maschine	Multi Purpose Rating Engine	Schröder	Paul
28	Schiffsmechaniker Maschine	Multi Purpose Rating Engine	Probst	Lorenz
29	Schiffsmechanikerin Maschine	Multi Purpose Rating Engine	Stubenrauch	Paula
30	Schiffsmechaniker Maschine	Multi Purpose Rating Engine	Buchholz	Karl Erik
31	Schiffsmechanikerin Maschine	Multi Purpose Rating Engine	Töben	Carlotta
32	1. Koch	1st Cook	Skrzipale	Mitja
33	2. Köchin	2nd Cook	Fehrenbach	Martina
34	2. Koch	2nd Cook	Loibl	Patrick
35	1. Stewardess	1st Stewardess	Witusch	Petra Gertrud Ramona
36	2. Stewardess	2nd Stewardess	Stocker	Eileen Sigourney
37	2. Steward	2nd Steward	Golla	Gerald
38	2. Stewardess	2nd Stewardess	Holl	Claudia
39	2. Stewardess / Krankenschwester	2nd Stewardess / Nurse	Ilk	Romy
40	2. Steward / Wäscherei	2nd Steward / Laundry	Shi	Wubo
41	2. Steward / Wäscherei	2nd Steward / Laundry	Chen	Jirong
42	2. Steward / Wäscherei	2nd Steward / Laundry	Chen	Quanlun
43	Auszubildender Schiffsmechaniker	Apprentice Multi Purpose Rating (in Funktion SM Deck)	Glawe	Jonathan Elias

A.4 STATIONSLISTE / STATION LIST PS148

Station list of expedition PS148 from Bremerhaven – Tromsø; the list details the action log for all stations along the cruise track.
See https://www.pangaea.de/expeditions/events/PS148 to display the station (event) list for expedition PS148.
This version contains Uniform Resource Identifiers for all sensors listed under https://sensor.awi.de. See https://www.awi.de/en/about-us/service/computing-centre/data-flow-framework.html for further information about AWI's data flow framework from sensor observations to archives (O2A).

Event label	Optional label	Date/Time	Latitude	Longitude	Depth [m]	Gear	Action	Comment *
PS148-track		2025-05-29T00:00:00	53.56750	8.55480		CT	Station start	Bremerhaven - Tromsø
PS148-track		2025-06-29T00:00:00	69.67800	18.98980		CT	Station end	Bremerhaven - Tromsø
PS148_0_Underway-1		2025-05-29T14:00:00	53.55787	8.55969	2.2	SWEAS	Station start	
PS148_0_Underway-1		2025-06-29T06:17:00	69.74732	19.14245	12.7	SWEAS	Station end	
PS148_0_Underway-2		2025-05-29T18:54:00	54.16575	7.50597	26.6	FBOX	Station start	
PS148_0_Underway-2		2025-06-28T20:03:00	71.36477	18.75074	239.7	FBOX	Station end	

Event label	Optional label	Date/Time	Latitude	Longitude	Depth [m]	Gear	Action	Comment *
PS148_0_Underway-3		2025-05-29T18:57:00	54.17275	7.50003	26.1	pCO2	Station start	
PS148_0_Underway-3		2025-06-28T20:02:00	71.36690	18.74557	236.9	pCO2	Station end	
PS148_0_Underway-4		2025-05-29T18:57:00	54.17472	7.49832	26.3	ADCP	Station start	
PS148_0_Underway-4		2025-06-28T20:01:00	71.36865	18.74131	239.7	ADCP	Station end	
PS148_0_Underway-5		2025-05-29T18:58:00	54.17638	7.49690	26.1	TSG	Station start	
PS148_0_Underway-5		2025-06-28T20:01:00	71.36977	18.73862	238.7	TSG	Station end	
PS148_0_Underway-6		2025-05-29T18:59:00	54.17929	7.49451	26.1	TSG	Station start	
PS148_0_Underway-6		2025-06-28T20:00:00	71.37162	18.73391	239.8	TSG	Station end	
PS148_0_Underway-7		2025-05-30T18:57:04	58.06250	4.50627	85.9	MBES	Station start	Event shows start/end point (date/time & coordinates) of first/last data record using Atlas Hydrographic Hydrosweep DS 3 multibeam…

Event label	Optional label	Date/Time	Latitude	Longitude	Depth [m]	Gear	Action	Comment *
PS148_0_Underway-7		2025-06-28T23:46:56	70.74210	19.84600	169.9	MBES	Station end	Event shows start/end point (date/time & coordinates) of first/last data record using Atlas Hydrographic Hydrosweep DS 3 multibeam…
PS148_0_Underway-8		2025-06-02T16:40:00	68.08397	1.05584	2978.2	PS	Station start	
PS148_0_Underway-8		2025-06-28T23:42:00	70.75601	19.82383	170.4	PS	Station end	
PS148_1-1		2025-06-01T21:25:00	66.37286	0.26308	3089.7	CTD-RO	max depth	
PS148_1-2		2025-06-01T23:22:00	66.37167	0.26078	3087.6	MBES	Station start	
PS148_1-2		2025-06-02T01:38:00	66.40462	0.30377	3125.0	MBES	Station end	
PS148_1-3		2025-06-02T02:06:00	66.34909	0.24746	3131.5	EBS	Station start	
PS148_1-3		2025-06-02T06:15:00	66.35451	0.24305	3111.7	EBS	Station end	
PS148_2-1		2025-06-03T02:30:00	69.79347	1.96242	3219.1	B_LANDER	Station start	
PS148_2-1		2025-06-03T18:01:00	69.81422	1.97224		B_LANDER	Station end	

Event label	Optional label	Date/Time	Latitude	Longitude	Depth [m]	Gear	Action	Comment *
PS148_2-2		2025-06-03T04:17:00	69.80234	1.94921	3219.5	CTD-RO	max depth	
PS148_2-3		2025-06-03T05:49:00	69.80255	1.94847	3222.0	MBES	Station start	
PS148_2-3		2025-06-03T08:43:00	69.83999	1.86677	3227.8	MBES	Station end	
PS148_2-4		2025-06-03T10:26:00	69.80221	1.94988	3224.9	OFOBS	Station start	
PS148_2-4		2025-06-03T13:00:00	69.82619	1.96650	3226.5	OFOBS	Station end	
PS148_2-5		2025-06-03T14:32:00	69.82666	1.97058	3225.7	LIGHT	Station start	
PS148_2-5		2025-06-03T15:27:00	69.82866	1.97438	3225.7	LIGHT	Station end	
PS148_2-6		2025-06-03T15:33:00	69.82891	1.97459	3225.4	B_LANDER	Station start	
PS148_2-6		2025-06-03T15:55:00	69.82904	1.97419		B_LANDER	Station end	
PS148_3-1		2025-06-03T19:57:00	70.11230	2.23917	3214.5	MBES	Station start	
PS148_3-1		2025-06-03T22:29:00	70.16427	2.06787	3218.4	MBES	Station end	
PS148_3-2		2025-06-03T22:52:00	70.15737	2.16040	3214.8	EBS	Station start	

Event label	Optional label	Date/Time	Latitude	Longitude	Depth [m]	Gear	Action	Comment *
PS148_3-2		2025-06-04T02:46:00	70.15749	2.20799	3214.6	EBS	Station end	
PS148_4-1		2025-06-05T11:40:00	75.67426	2.93125	3084.4	CTD-RO	max depth	
PS148_4-2		2025-06-05T13:28:00	75.67459	2.93627	3088.2	MBES	Station start	
PS148_4-2		2025-06-05T16:14:00	75.65810	2.64177	2938.4	MBES	Station end	
PS148_4-3		2025-06-05T16:54:00	75.71345	2.94301	3121.8	EBS	Station start	
PS148_4-3		2025-06-05T20:56:00	75.72475	2.91092	3113.4	EBS	Station end	
PS148_5-2		2025-06-06T13:42:00	78.60887	5.06120	2278.4	HN	Station start	
PS148_5-2		2025-06-06T13:57:00	78.60802	5.06142	2281.1	HN	Station end	
PS148_5-1		2025-06-06T13:44:00	78.60876	5.06089	2280.4	CTD-RO	max depth	
PS148_5-4		2025-06-06T15:13:00	78.60961	5.06578	2280.0	OOSS	Station start	
PS148_5-4		2025-06-06T15:25:00	78.60968	5.06750	2280.6	OOSS	Station end	
PS148_5-3		2025-06-06T15:36:00	78.61010	5.06721	2280.0	CTD-RO	max depth	

Event label	Optional label	Date/Time	Latitude	Longitude	Depth [m]	Gear	Action	Comment *
PS148_5-5		2025-06-06T16:45:00	78.60984	5.06829	2279.6	LIGHT	Station start	
PS148_5-5		2025-06-06T17:56:00	78.60906	5.06583	2279.4	LIGHT	Station end	
PS148_5-6		2025-06-06T17:57:00	78.60894	5.06590	2279.4	LOKI	Station start	
PS148_5-6		2025-06-06T19:43:00	78.60979	5.06812	2281.3	LOKI	Station end	
PS148_5-7		2025-06-06T19:48:00	78.60969	5.06925	2279.1	MSN	Station start	
PS148_5-7		2025-06-06T21:24:00	78.60965	5.06854	2280.6	MSN	Station end	
PS148_5-8		2025-06-06T21:25:00	78.60963	5.06857	2278.3	MSN	Station start	
PS148_5-8		2025-06-06T23:34:00	78.60951	5.06832	2280.0	MSN	Station end	
PS148_5-9		2025-06-07T00:55:00	78.61032	5.06559	2278.8	GKG	max depth	
PS148_5-10		2025-06-07T03:06:00	78.60970	5.06705	2278.0	TVMUC	max depth	
PS148_5-11		2025-06-07T04:50:00	78.61034	5.06649	2277.8	GKG	max depth	
PS148_5-12		2025-06-07T06:00:00	78.61007	5.06766	2281.3	AUV_lab	Station start	

Event label	Optional label	Date/Time	Latitude	Longitude	Depth [m]	Gear	Action	Comment *
PS148_5-12		2025-06-07T11:35:00	78.60840	5.05740	2284.9	AUV_lab	Station end	
PS148_5-13		2025-06-07T12:22:00	78.61549	5.14435	2293.4	OFOBS	max depth	
PS148_6-1		2025-06-07T18:36:00	79.06404	4.18185	2410.5	LOKI	Station start	
PS148_6-1		2025-06-07T20:03:00	79.06543	4.18017	2408.2	LOKI	Station end	
PS148_6-2		2025-06-07T20:04:00	79.06539	4.17992	2404.9	MSN	Station start	
PS148_6-2		2025-06-07T21:35:00	79.06531	4.18036	2407.6	MSN	Station end	
PS148_6-3		2025-06-07T21:36:00	79.06531	4.18027	2405.4	MSN	Station start	
PS148_6-3		2025-06-07T23:36:00	79.06563	4.17654	2407.8	MSN	Station end	
PS148_6-4		2025-06-08T00:43:00	79.06582	4.17851	2406.0	CTD-RO	max depth	
PS148_6-5		2025-06-08T03:45:00	79.06466	4.18110	2410.1	MUC	max depth	
PS148_6-6		2025-06-08T05:50:00	79.06482	4.18214	2405.3	MUC	max depth	
PS148_6-7		2025-06-08T07:28:00	79.00151	4.32013	2553.5	MOOR	Station start	recovery

Event label	Optional label	Date/Time	Latitude	Longitude	Depth [m]	Gear	Action	Comment *
PS148_6-7		2025-06-08T09:58:00	79.02346	4.28458	2532.5	MOOR	Station end	recovery
PS148_6-8		2025-06-08T10:38:00	79.07981	4.09331	2448.3	B_LANDER	Station start	
PS148_6-8		2025-06-08T11:28:00	79.08077	4.08797	2448.0	B_LANDER	Station end	
PS148_6-9		2025-06-08T11:43:00	79.07767	4.10052	2446.7	BCRAWL_III	Station start	
PS148_6-9		2025-06-08T13:37:00	79.07340	4.13162		BCRAWL_III	Station end	
PS148_6-10		2025-06-08T13:55:00	79.08042	4.08795		AUV_lab	Station start	
PS148_6-10		2025-06-08T15:09:00	79.08315	4.10929	2426.6	AUV_lab	Station end	
PS148_6-11		2025-06-08T15:26:00	79.06643	4.17676	2406.4	LIGHT	Station start	
PS148_6-11		2025-06-08T16:08:00	79.06495	4.18100	2406.7	LIGHT	Station end	
PS148_6-12		2025-06-08T16:08:00	79.06494	4.18099	2406.2	OOSS	Station start	
PS148_6-12		2025-06-08T16:21:00	79.06491	4.18256	2404.8	OOSS	Station end	
PS148_6-14		2025-06-08T16:27:00	79.06491	4.18224	2405.1	HN	Station start	

Event label	Optional label	Date/Time	Latitude	Longitude	Depth [m]	Gear	Action	Comment *
PS148_6-14		2025-06-08T16:58:00	79.06516	4.18126	2406.9	HN	Station end	
PS148_6-13		2025-06-08T16:59:00	79.06513	4.18133	2404.8	CTD-RO	max depth	
PS148_6-15		2025-06-08T19:08:00	79.06485	4.18264	2405.9	GKG	max depth	
PS148_6-16		2025-06-08T20:57:00	79.06477	4.18275	2405.0	MUC	max depth	
PS148_6-17		2025-06-08T22:44:00	79.06491	4.18144	2404.4	GKG	max depth	
PS148_7-2		2025-06-09T00:28:00	79.10871	4.59584	1858.8	HN	Station start	
PS148_7-2		2025-06-09T00:31:00	79.10862	4.59587	1859.1	HN	Station end	
PS148_7-1		2025-06-09T01:05:00	79.10810	4.59644	1874.7	CTD-RO	max depth	
PS148_7-3		2025-06-09T02:19:00	79.10771	4.59984	1881.6	MSN	Station start	
PS148_7-3		2025-06-09T04:51:00	79.10772	4.60217	1883.1	MSN	Station end	
PS148_7-4		2025-06-09T04:51:00	79.10768	4.60236	1881.2	LIGHT	Station start	
PS148_7-4		2025-06-09T06:06:00	79.10807	4.60055	1864.7	LIGHT	Station end	

Event label	Optional label	Date/Time	Latitude	Longitude	Depth [m]	Gear	Action	Comment *
PS148_8-1		2025-06-09T07:00:00	79.06780	4.19093	2394.9	AUV_lab	Station start	
PS148_8-1		2025-06-09T07:24:00	79.07011	4.19301	2385.5	AUV_lab	Station end	
PS148_8-2		2025-06-09T08:17:00	79.00017	4.33150	2543.1	MOOR	Station start	deployment
PS148_8-2		2025-06-09T11:12:00	78.99985	4.33207	2542.1	MOOR	Station end	deployment
PS148_8-3		2025-06-09T12:01:00	79.07309	4.11132	2451.3	B_LANDER	Station start	
PS148_8-3		2025-06-09T13:07:00	79.08383	4.07747		B_LANDER	Station end	
PS148_8-4		2025-06-09T13:19:00	79.08147	4.07237		BCRAWL_III	Station start	
PS148_8-4		2025-06-09T13:58:00	79.07958	4.11836		BCRAWL_III	Station end	
PS148_8-5		2025-06-09T14:37:00	79.08066	4.08683	2449.0	TRAMPER	Station start	crawler fully recovered
PS148_8-5		2025-06-11T16:29:00	79.08338	4.05884	2462.7	TRAMPER	Station end	crawler fully recovered
PS148_9-2		2025-06-09T19:00:00	79.13360	2.84165	5540.4	HN	Station start	
PS148_9-2		2025-06-09T19:24:00	79.13363	2.84202	5543.4	HN	Station end	

Event label	Optional label	Date/Time	Latitude	Longitude	Depth [m]	Gear	Action	Comment *
PS148_9-1		2025-06-09T19:35:00	79.13344	2.84227	5540.4	CTD-RO	max depth	
PS148_9-3		2025-06-09T20:52:00	79.13343	2.84255	5542.4	LOKI	Station start	
PS148_9-3		2025-06-09T22:20:00	79.13338	2.84022	5543.3	LOKI	Station end	
PS148_9-4		2025-06-09T22:32:00	79.13328	2.84183	5541.6	MSN	Station start	
PS148_9-4		2025-06-09T23:21:00	79.13320	2.84264	5541.1	MSN	Station end	
PS148_9-5		2025-06-09T23:28:00	79.13340	2.84413	5542.2	MSN	Station start	
PS148_9-5		2025-06-10T01:20:00	79.13326	2.84381	5539.7	MSN	Station end	
PS148_9-6		2025-06-10T03:23:00	79.13353	2.83968	5542.5	CTD-RO	max depth	
PS148_9-7		2025-06-10T05:35:00	79.13389	2.84114	5540.8	OOSS	Station start	
PS148_9-7		2025-06-10T05:49:00	79.13375	2.84253	5540.5	OOSS	Station end	
PS148_9-8		2025-06-10T08:00:00	79.13386	2.84158	5545.4	LIGHT	Station start	
PS148_9-8		2025-06-10T08:41:00	79.13388	2.84050	5546.6	LIGHT	Station end	

Event label	Optional label	Date/Time	Latitude	Longitude	Depth [m]	Gear	Action	Comment *
PS148_9-9		2025-06-10T10:43:00	79.13317	2.84435	5544.3	MUC	max depth	
PS148_9-10		2025-06-10T14:22:00	79.13340	2.84233	5545.7	GKG	max depth	
PS148_9-11		2025-06-10T18:13:00	79.13300	2.84444	5542.6	MUC	max depth	
PS148_10-1		2025-06-10T21:00:00	79.06377	3.33657	5065.6	LIGHT	Station start	
PS148_10-1		2025-06-10T21:48:00	79.06431	3.33605	5071.9	LIGHT	Station end	
PS148_10-3		2025-06-10T21:59:00	79.06433	3.33534	5064.8	OOSS	Station start	cancelled due to bad optical condition (clouds)
PS148_10-3		2025-06-10T22:00:00	79.06429	3.33549	5072.1	OOSS	Station end	cancelled due to bad optical condition (clouds)
PS148_10-4		2025-06-10T22:00:00	79.06432	3.33537	5075.7	HN	Station start	
PS148_10-4		2025-06-10T22:03:00	79.06414	3.33601	5073.6	HN	Station end	
PS148_10-2		2025-06-10T22:30:00	79.06405	3.33215	5087.6	CTD-RO	max depth	
PS148_11-2		2025-06-11T01:07:00	79.05992	3.47556	4029.9	OOSS	max depth	cancelled due to bad optical condition (clouds)
PS148_11-3		2025-06-11T01:08:00	79.06002	3.47514	4033.5	HN	Station start	

Event label	Optional label	Date/Time	Latitude	Longitude	Depth [m]	Gear	Action	Comment *
PS148_11-3		2025-06-11T01:12:00	79.06036	3.47405	4023.7	HN	Station end	
PS148_11-1		2025-06-11T01:43:00	79.05978	3.47548	4026.7	CTD-RO	max depth	
PS148_11-4		2025-06-11T03:19:00	79.06004	3.47533	4018.4	LIGHT	Station start	
PS148_11-4		2025-06-11T04:14:00	79.05988	3.47470	4048.7	LIGHT	Station end	
PS148_11-5		2025-06-11T04:15:00	79.05988	3.47473	4039.5	MUC	max depth	
PS148_11-6		2025-06-11T08:38:00	79.06085	3.47629	4035.0	GKG	Station start	
PS148_11-6		2025-06-11T08:43:00	79.06083	3.47585	4030.8	GKG	Station end	
PS148_12-2		2025-06-11T10:41:00	79.06376	3.65251	3109.8	HN	Station start	
PS148_12-2		2025-06-11T10:44:00	79.06381	3.65309	3112.8	HN	Station end	
PS148_12-1		2025-06-11T11:16:00	79.06384	3.65499	3101.8	CTD-RO	max depth	
PS148_12-3		2025-06-11T11:57:00	79.06301	3.65652	3093.8	OOSS	max depth	cancelled due to bad optical condition (clouds)
PS148_12-4		2025-06-11T12:45:00	79.06358	3.65258	3109.5	LIGHT	Station start	

Event label	Optional label	Date/Time	Latitude	Longitude	Depth [m]	Gear	Action	Comment *
PS148_12-4		2025-06-11T13:27:00	79.06344	3.65091	3121.8	LIGHT	Station end	
PS148_13-1		2025-06-11T21:40:00	79.94371	3.11858	2506.6	LOKI	Station start	
PS148_13-1		2025-06-11T22:57:00	79.94433	3.12091	2501.4	LOKI	Station end	
PS148_13-2		2025-06-11T23:00:00	79.94418	3.11957	2501.8	MSN	Station start	
PS148_13-2		2025-06-11T23:50:00	79.94379	3.11697	2504.9	MSN	Station end	
PS148_13-3		2025-06-11T23:59:00	79.94380	3.11411	2503.8	MSN	Station start	
PS148_13-3		2025-06-12T01:47:00	79.94459	3.11972	2502.3	MSN	Station end	
PS148_13-5		2025-06-12T02:13:00	79.94452	3.11926	2500.8	HN	Station start	
PS148_13-5		2025-06-12T02:33:00	79.94408	3.12020	2501.7	HN	Station end	
PS148_13-4		2025-06-12T02:39:00	79.94404	3.11997	2501.4	CTD-RO	max depth	
PS148_13-6		2025-06-12T04:39:00	79.94370	3.11949	2504.1	OOSS	Station start	cancelled due to bad optical condition (clouds)
PS148_13-6		2025-06-12T04:40:00	79.94371	3.11948	2505.0	OOSS	Station end	cancelled due to bad optical condition (clouds)

Event label	Optional label	Date/Time	Latitude	Longitude	Depth [m]	Gear	Action	Comment *
PS148_13-7		2025-06-12T04:41:00	79.94371	3.11949	2502.8	LIGHT	Station start	
PS148_13-7		2025-06-12T05:39:00	79.94396	3.12054	2504.9	LIGHT	Station end	
PS148_13-8		2025-06-12T06:43:00	79.94455	3.11897	2501.5	GKG	max depth	
PS148_13-9		2025-06-12T08:35:00	79.94446	3.11994	2500.7	MUC	max depth	
PS148_13-10		2025-06-12T10:22:00	79.94569	3.12134	2504.4	GKG	max depth	
PS148_13-11		2025-06-12T11:38:00	79.95555	3.04238	2520.9	EBS	Station start	
PS148_13-11		2025-06-12T14:51:00	79.96252	2.98329	2536.0	EBS	Station end	
PS148_13-12		2025-06-12T14:53:00	79.96343	2.98489	2533.7	AUV_lab	Station start	
PS148_13-12		2025-06-12T22:13:00	79.87564	3.26479	2510.4	AUV_lab	Station end	
PS148_13-13		2025-06-12T16:02:00	79.93864	3.11725	2516.4	OFOBS	max depth	
PS148_14-1		2025-06-12T23:53:00	79.73754	4.49276	2633.5	B_LANDER	Station start	
PS148_14-1		2025-06-13T14:29:00	79.73776	4.51007	2684.2	B_LANDER	Station end	

Event label	Optional label	Date/Time	Latitude	Longitude	Depth [m]	Gear	Action	Comment *
PS148_14-3		2025-06-13T00:11:00	79.73636	4.49246	2659.2	HN	Station start	
PS148_14-3		2025-06-13T00:14:00	79.73638	4.49285	2662.8	HN	Station end	
PS148_14-2		2025-06-13T00:49:00	79.73567	4.49378	2675.8	CTD-RO	max depth	
PS148_14-4		2025-06-13T02:27:00	79.73584	4.49371	2671.0	LOKI	Station start	
PS148_14-4		2025-06-13T03:47:00	79.73582	4.49417	2673.2	LOKI	Station end	
PS148_14-5		2025-06-13T03:48:00	79.73582	4.49423	2673.6	MSN	Station start	
PS148_14-5		2025-06-13T04:51:00	79.73560	4.49780	2686.1	MSN	Station end	
PS148_14-6		2025-06-13T04:51:00	79.73559	4.49777	2688.9	MSN	Station start	
PS148_14-6		2025-06-13T06:51:00	79.73584	4.49403	2674.6	MSN	Station end	
PS148_14-7		2025-06-13T06:52:00	79.73585	4.49451	2672.5	LIGHT	Station start	
PS148_14-7		2025-06-13T07:40:00	79.73554	4.49787	2694.5	LIGHT	Station end	
PS148_14-9		2025-06-13T07:53:00	79.73573	4.49630	2681.9	HN	max depth	

Event label	Optional label	Date/Time	Latitude	Longitude	Depth [m]	Gear	Action	Comment *
PS148_14-10		2025-06-13T08:34:00	79.73597	4.49798	2681.6	OOSS	Station start	
PS148_14-10		2025-06-13T08:51:00	79.73572	4.49591	2687.3	OOSS	Station end	
PS148_14-8		2025-06-13T08:51:00	79.73572	4.49587	2684.2	CTD-RO	max depth	
PS148_14-11		2025-06-13T11:56:00	79.73452	4.50086	2700.3	MUC	max depth	
PS148_15-1		2025-06-13T17:42:00	79.92148	3.06694	2546.6	OFOBS	Station start	
PS148_15-1		2025-06-13T21:01:00	79.93895	3.15479	2498.4	OFOBS	Station end	
PS148_16-1		2025-06-14T01:55:00	79.60366	5.16901	2729.0	OFOBS	Station start	
PS148_16-1		2025-06-14T04:45:00	79.57811	5.23689	2607.9	OFOBS	Station end	
PS148_16-3		2025-06-14T07:05:00	79.60411	5.17191	2726.9	HN	Station start	
PS148_16-3		2025-06-14T07:09:00	79.60416	5.17154	2726.4	HN	Station end	
PS148_16-4		2025-06-14T07:22:00	79.60410	5.17168	2725.0	OOSS	Station start	
PS148_16-4		2025-06-14T07:54:00	79.60416	5.17165	2724.1	OOSS	Station end	

Event label	Optional label	Date/Time	Latitude	Longitude	Depth [m]	Gear	Action	Comment *
PS148_16-2		2025-06-14T07:41:00	79.60410	5.17227	2725.1	CTD-RO	max depth	
PS148_16-5		2025-06-14T09:03:00	79.60383	5.17202	2727.8	LIGHT	Station start	
PS148_16-5		2025-06-14T09:45:00	79.60391	5.17296	2725.8	LIGHT	Station end	
PS148_16-6		2025-06-14T11:58:00	79.60405	5.17241	2727.7	GKG	max depth	
PS148_16-7		2025-06-14T14:00:00	79.60330	5.17544	2725.9	MUC	max depth	
PS148_17-2		2025-06-15T12:33:00	78.97957	-5.45195	926.5	HN	Station start	
PS148_17-2		2025-06-15T12:36:00	78.98009	-5.45456	925.2	HN	Station end	
PS148_17-1		2025-06-15T12:54:00	78.98381	-5.47166	922.3	CTD-RO	max depth	
PS148_17-3		2025-06-15T13:42:00	78.99448	-5.52349	906.8	OOSS	max depth	cancelled due to bad optical condition (clouds)
PS148_17-4		2025-06-15T13:48:00	78.99553	-5.53072	904.8	LIGHT	Station start	
PS148_17-4		2025-06-15T14:27:00	79.00525	-5.56611	890.4	LIGHT	Station end	
PS148_17-5		2025-06-15T14:28:00	79.00536	-5.56649	890.3	LOKI	Station start	

Event label	Optional label	Date/Time	Latitude	Longitude	Depth [m]	Gear	Action	Comment *
PS148_17-5		2025-06-15T15:35:00	79.02190	-5.61117	880.1	LOKI	Station end	
PS148_17-6		2025-06-15T15:36:00	79.02202	-5.61144	879.7	MSN	Station start	
PS148_17-6		2025-06-15T16:54:00	79.04133	-5.64955	879.3	MSN	Station end	
PS148_17-7		2025-06-15T16:54:00	79.04140	-5.64968	878.9	MSN	Station start	
PS148_17-7		2025-06-15T18:20:00	79.06104	-5.69193	883.5	MSN	Station end	
PS148_17-8		2025-06-15T18:22:00	79.06126	-5.69250	883.9	WP2	Station start	
PS148_17-8		2025-06-15T18:43:00	79.06549	-5.70367	883.3	WP2	Station end	
PS148_17-9		2025-06-15T21:23:00	79.00696	-5.41518	1004.3	GKG	max depth	
PS148_17-10		2025-06-15T22:20:00	79.01337	-5.45893	979.1	MUC	max depth	
PS148_17-11		2025-06-15T23:37:00	79.02935	-5.45787	998.8	EBS	Station start	
PS148_17-11		2025-06-16T01:06:00	79.04534	-5.50380	992.9	EBS	Station end	
PS148_17-12		2025-06-16T02:27:00	79.02536	-5.45109	995.9	GKG	max depth	

Event label	Optional label	Date/Time	Latitude	Longitude	Depth [m]	Gear	Action	Comment *
PS148_18-1		2025-06-16T03:19:00	79.03738	-5.49196	983.6	CTD-RO	max depth	
PS148_18-2		2025-06-16T03:34:00	79.04154	-5.50133	986.1	HN	Station start	
PS148_18-2		2025-06-16T03:37:00	79.04224	-5.50274	986.5	HN	Station end	
PS148_18-3		2025-06-16T04:45:00	79.00226	-5.36074	1029.3	MOOR	Station start	recovery
PS148_18-3		2025-06-16T06:29:00	79.01656	-5.44614	990.4	MOOR	Station end	recovery
PS148_18-4		2025-06-16T12:44:00	79.03450	-5.39148	1056.0	MOOR	Station start	deployment
PS148_18-4		2025-06-16T14:22:00	79.05083	-5.46876	1027.8	MOOR	Station end	deployment
PS148_18-5		2025-06-16T15:24:00	79.06372	-5.53376	996.6	CTD-RO	max depth	
PS148_19-2		2025-06-16T18:16:00	78.92801	-4.67918	1470.3	HN	Station start	
PS148_19-2		2025-06-16T18:21:00	78.92756	-4.68046	1470.0	HN	Station end	
PS148_19-3		2025-06-16T18:26:00	78.92730	-4.68178	1468.3	OOSS	Station start	
PS148_19-3		2025-06-16T18:43:00	78.92668	-4.68452	1465.2	OOSS	Station end	

Event label	Optional label	Date/Time	Latitude	Longitude	Depth [m]	Gear	Action	Comment *
PS148_19-1		2025-06-16T18:49:00	78.92642	-4.68466	1465.2	CTD-RO	max depth	
PS148_19-4		2025-06-16T20:24:00	78.93195	-4.63384	1509.2	LIGHT	Station start	
PS148_19-4		2025-06-16T21:15:00	78.92603	-4.65458	1485.2	LIGHT	Station end	
PS148_19-5		2025-06-16T21:16:00	78.92593	-4.65494	1485.5	MSN	Station start	
PS148_19-5		2025-06-16T22:29:00	78.91859	-4.69591	1447.0	MSN	Station end	
PS148_19-6		2025-06-16T23:14:00	78.92850	-4.61934	1512.5	MSN	Station start	
PS148_19-6		2025-06-17T01:13:00	78.90788	-4.68858	1425.4	MSN	Station end	
PS148_19-7		2025-06-17T01:45:00	78.93989	-4.62071	1530.0	WP2	Station start	
PS148_19-7		2025-06-17T02:14:00	78.93630	-4.64079	1512.3	WP2	Station end	
PS148_19-8		2025-06-17T03:03:00	78.93159	-4.67115	1483.7	MUC	max depth	
PS148_20-2		2025-06-17T06:38:00	78.80405	-3.90936	1919.3	HN	Station start	
PS148_20-2		2025-06-17T06:53:00	78.80475	-3.91609	1913.6	HN	Station end	

Event label	Optional label	Date/Time	Latitude	Longitude	Depth [m]	Gear	Action	Comment *
PS148_20-1		2025-06-17T07:12:00	78.80575	-3.92519	1906.1	CTD-RO	max depth	
PS148_20-3		2025-06-17T08:39:00	78.80909	-3.96707	1873.7	LIGHT	Station start	
PS148_20-3		2025-06-17T09:12:00	78.81019	-3.97244	1870.4	LIGHT	Station end	
PS148_20-4		2025-06-17T09:35:00	78.80182	-3.85576	1953.9	LOKI	Station start	
PS148_20-4		2025-06-17T10:54:00	78.80436	-3.89741	1929.5	LOKI	Station end	
PS148_20-5		2025-06-17T11:04:00	78.80436	-3.90299	1924.6	MSN	max depth	
PS148_20-6		2025-06-17T14:11:00	78.80303	-3.88889	1936.7	GKG	max depth	
PS148_20-7		2025-06-17T15:48:00	78.80339	-3.89080	1935.2	MUC	max depth	
PS148_20-8		2025-06-17T17:20:00	78.80326	-3.89501	1932.3	GKG	max depth	
PS148_21-1		2025-06-17T20:50:00	78.76717	-2.76624	2550.9	TRAMPER	Station start	deployment Lander Crawler; Lander + Crawler + Mooring Releaser

Event label	Optional label	Date/Time	Latitude	Longitude	Depth [m]	Gear	Action	Comment *
PS148_21-1		2025-06-19T09:16:00	78.75238	-2.80576	2555.5	TRAMPER	Station end	deployment Lander Crawler; Lander + Crawler + Mooring Releaser
PS148_21-2		2025-06-17T23:31:00	78.75620	-2.78796	2551.6	CTD-RO	max depth	
PS148_21-3		2025-06-18T01:14:00	78.75729	-2.73019	2561.2	LOKI	Station start	
PS148_21-3		2025-06-18T02:36:00	78.74710	-2.74733	2564.9	LOKI	Station end	
PS148_21-4		2025-06-18T02:37:00	78.74710	-2.74707	2564.0	MSN	Station start	
PS148_21-4		2025-06-18T04:36:00	78.73934	-2.77949	2559.9	MSN	Station end	
PS148_21-5		2025-06-18T04:36:00	78.73981	-2.77645	2560.7	WP2	Station start	
PS148_21-5		2025-06-18T05:19:00	78.74554	-2.73803	2566.5	WP2	Station end	
PS148_21-6		2025-06-18T04:49:00	78.74622	-2.73224	2567.5	HN	Station start	
PS148_21-6		2025-06-18T04:52:00	78.74617	-2.73225	2568.3	HN	Station end	
PS148_21-7		2025-06-18T04:52:00	78.74614	-2.73232	2568.0	OOSS	Station start	

Event label	Optional label	Date/Time	Latitude	Longitude	Depth [m]	Gear	Action	Comment *
PS148_21-7		2025-06-18T05:04:00	78.74584	-2.73318	2568.0	OOSS	Station end	
PS148_21-8		2025-06-18T05:19:00	78.74554	-2.73823	2566.7	LIGHT	Station start	
PS148_21-8		2025-06-18T06:17:00	78.73854	-2.75858	2563.3	LIGHT	Station end	
PS148_21-9		2025-06-18T07:29:00	78.74694	-2.75545	2563.2	GKG	max depth	
PS148_21-10		2025-06-18T09:22:00	78.74528	-2.78230	2558.7	MUC	max depth	
PS148_21-11		2025-06-18T11:31:00	78.75105	-2.73358	2563.4	GKG	max depth	
PS148_21-12		2025-06-18T13:09:00	78.74973	-2.79710	2556.0	EBS	Station start	
PS148_21-12		2025-06-18T16:30:00	78.72499	-2.79300	2552.3	EBS	Station end	
PS148_21-13		2025-06-18T18:10:00	78.76263	-2.74179	2557.6	OFOBS	max depth	
PS148_21-14		2025-06-19T04:39:00	78.75299	-2.76824	2560.8	CTD-RO	max depth	
PS148_22-1		2025-06-19T18:09:00	79.14272	2.76016	5553.3	B_LANDER	Station start	
PS148_22-1		2025-06-20T08:14:00	79.13851	2.78747	5552.1	B_LANDER	Station end	

Event label	Optional label	Date/Time	Latitude	Longitude	Depth [m]	Gear	Action	Comment *
PS148_22-2		2025-06-19T21:09:00	79.10484	3.27200	5334.0	OFOBS	Station start	
PS148_22-2		2025-06-20T03:15:00	79.09367	3.43764	4494.3	OFOBS	Station end	
PS148_22-3		2025-06-20T08:15:00	79.13851	2.78750	5555.3	MOOR	Station start	deployment
PS148_22-3		2025-06-20T12:10:00	79.13414	2.78520	5546.5	MOOR	Station end	deployment
PS148_23-1		2025-06-20T13:24:00	79.06018	3.58974	3445.6	CTD-RO	max depth	
PS148_23-2		2025-06-20T13:28:00	79.06014	3.58801	3456.3	HN	Station start	
PS148_23-2		2025-06-20T13:30:00	79.05988	3.58674	3463.8	HN	Station end	
PS148_23-3		2025-06-20T14:33:00	79.06257	3.58802	3450.1	OOSS	max depth	cancelled due to bad optical condition (clouds)
PS148_23-4		2025-06-20T16:33:00	79.05951	3.58325	3466.2	LIGHT	max depth	
PS148_23-5		2025-06-20T17:40:00	79.05994	3.58020	3486.9	MUC	max depth	
PS148_24-1		2025-06-20T21:04:00	79.06389	3.65828	3103.1	GKG	max depth	
PS148_24-2		2025-06-20T23:14:00	79.06422	3.66281	3079.2	MUC	max depth	

Event label	Optional label	Date/Time	Latitude	Longitude	Depth [m]	Gear	Action	Comment *
PS148_25-1		2025-06-21T03:21:00	79.03501	4.17222	2563.9	OFOBS	Station start	
PS148_25-1		2025-06-21T06:46:00	79.05997	4.26737	2387.5	OFOBS	Station end	
PS148_25-2		2025-06-21T07:22:00	79.05777	4.24840	2414.0	B_LANDER	Station start	
PS148_25-2		2025-06-21T08:30:00	79.03149	4.22896	2530.6	B_LANDER	Station end	
PS148_25-3		2025-06-21T08:58:00	79.07768	4.12354	2432.2	BCRAWL_III	Station start	
PS148_25-3		2025-06-21T18:45:00	79.08147	4.16531	2383.5	BCRAWL_III	Station end	
PS148_26-1		2025-06-21T21:33:00	79.10841	4.59659	1860.9	GKG	max depth	
PS148_26-2		2025-06-21T23:11:00	79.10843	4.59758	1861.3	MUC	max depth	
PS148_26-3		2025-06-22T01:23:00	79.10852	4.59776	1861.2	GKG	max depth	
PS148_27-2		2025-06-22T05:07:00	79.01158	6.03255	1717.8	HN	Station start	
PS148_27-2		2025-06-22T05:16:00	79.01165	6.03472	1716.1	HN	Station end	
PS148_27-1		2025-06-22T05:12:00	79.01169	6.03440	1716.1	CTD-RO	max depth	

Event label	Optional label	Date/Time	Latitude	Longitude	Depth [m]	Gear	Action	Comment *
PS148_27-3		2025-06-22T05:55:00	79.01151	6.03269	1718.0	OOSS	Station start	
PS148_27-3		2025-06-22T06:07:00	79.01194	6.03414	1714.7	OOSS	Station end	
PS148_27-4		2025-06-22T06:38:00	79.01176	6.03270	1716.9	CTD-RO	max depth	
PS148_27-5		2025-06-22T08:01:00	79.01179	6.03367	1713.5	LIGHT	Station start	
PS148_27-5		2025-06-22T09:00:00	79.01199	6.03373	1712.8	LIGHT	Station end	
PS148_27-6		2025-06-22T09:00:00	79.01199	6.03373	1713.6	LOKI	Station start	
PS148_27-6		2025-06-22T10:19:00	79.01192	6.03252	1714.9	LOKI	Station end	
PS148_27-7		2025-06-22T10:30:00	79.01147	6.03701	1715.9	MSN	Station start	
PS148_27-7		2025-06-22T12:20:00	79.01254	6.03141	1710.7	MSN	Station end	
PS148_27-8		2025-06-22T12:21:00	79.01264	6.03083	1710.5	WP2	Station start	
PS148_27-8		2025-06-22T12:49:00	79.01372	6.04095	1695.4	WP2	Station end	
PS148_27-10		2025-06-22T14:09:00	79.01535	6.99293	1236.5	MOOR	Station start	recovery

Event label	Optional label	Date/Time	Latitude	Longitude	Depth [m]	Gear	Action	Comment *
PS148_27-10		2025-06-22T16:43:00	79.01096	6.94766	1212.8	MOOR	Station end	recovery
PS148_27-9		2025-06-22T14:15:00	79.01499	6.99448	1236.0	CTD-RO	max depth	
PS148_27-11		2025-06-22T17:00:00	79.00941	7.03240	1232.3	MOOR	Station start	recovery
PS148_27-11		2025-06-22T19:21:00	79.01285	6.97149	1226.1	MOOR	Station end	recovery
PS148_28-2		2025-06-22T23:45:00	79.02869	10.81569		HN	Station start	
PS148_28-2		2025-06-22T23:51:00	79.02842	10.81532		HN	Station end	
PS148_28-1		2025-06-22T23:49:00	79.02846	10.81534		CTD-RO	max depth	
PS148_28-3		2025-06-23T01:06:00	79.03103	10.81438		CTD-RO	max depth	
PS148_28-4		2025-06-23T01:44:00	79.03067	10.81321		OOSS	max depth	cancelled due to bad optical condition (clouds)
PS148_28-5		2025-06-23T01:45:00	79.03062	10.81320		LIGHT	Station start	
PS148_28-5		2025-06-23T02:36:00	79.02985	10.81057		LIGHT	Station end	
PS148_28-6		2025-06-23T02:36:00	79.02986	10.81052		LOKI	Station start	

Event label	Optional label	Date/Time	Latitude	Longitude	Depth [m]	Gear	Action	Comment *
PS148_28-6		2025-06-23T03:10:00	79.03018	10.81101		LOKI	Station end	
PS148_28-7		2025-06-23T03:10:00	79.03018	10.81098		MSN	Station start	
PS148_28-7		2025-06-23T03:55:00	79.03053	10.81111		MSN	Station end	
PS148_28-8		2025-06-23T03:56:00	79.03053	10.81111		WP2	Station start	
PS148_28-8		2025-06-23T04:30:00	79.03045	10.81001	320.6	WP2	Station end	
PS148_29-1		2025-06-23T10:10:00	79.01159	7.03690	1237.7	AUV_lab	max depth	no end action defined in Dship
PS148_29-2		2025-06-23T11:16:00	79.01181	7.03410	1237.8	MOOR	Station start	deployment
PS148_29-2		2025-06-23T13:39:00	79.01161	7.03458	1236.6	MOOR	Station end	deployment
PS148_29-3		2025-06-23T14:18:00	79.01263	6.97059	1225.9	MOOR	Station start	deployment
PS148_29-3		2025-06-23T15:25:00	79.01179	6.96500	1222.1	MOOR	Station end	deployment
PS148_29-4		2025-06-23T15:48:00	79.01316	6.93674	1216.1	CTD-RO	max depth	
PS148_29-5		2025-06-23T16:29:00	79.02076	6.81185	1194.6	AUV_lab	Station start	

Event label	Optional label	Date/Time	Latitude	Longitude	Depth [m]	Gear	Action	Comment *
PS148_29-5		2025-06-23T18:33:00	79.01726	7.00997	1243.7	AUV_lab	Station end	
PS148_29-6		2025-06-23T19:14:00	79.01803	7.00453	1244.5	CTD-RO	max depth	
PS148_30-1		2025-06-23T21:34:00	79.00071	8.24835	872.5	CTD-RO	max depth	
PS148_30-2		2025-06-23T21:41:00	79.00076	8.24805	871.9	HN	Station start	
PS148_30-2		2025-06-23T21:48:00	79.00093	8.25022	870.2	HN	Station end	
PS148_30-3		2025-06-23T22:25:00	79.00056	8.24721	872.2	OOSS	Station start	
PS148_30-3		2025-06-23T22:39:00	79.00040	8.24534	872.9	OOSS	Station end	
PS148_30-4		2025-06-23T23:02:00	79.00009	8.24198	874.9	LIGHT	max depth	no end action defined in Dship
PS148_31-2		2025-06-24T01:26:00	78.97821	9.50326	213.6	HN	Station start	
PS148_31-2		2025-06-24T01:28:00	78.97813	9.50379	213.8	HN	Station end	
PS148_31-1		2025-06-24T01:35:00	78.97803	9.50542	213.3	CTD-RO	max depth	
PS148_31-3		2025-06-24T01:37:00	78.97804	9.50554	213.2	OOSS	Station start	

Event label	Optional label	Date/Time	Latitude	Longitude	Depth [m]	Gear	Action	Comment *
PS148_31-3		2025-06-24T01:45:00	78.97818	9.50470	212.5	OOSS	Station end	
PS148_31-4		2025-06-24T02:14:00	78.97897	9.50213	212.7	LIGHT	Station start	
PS148_31-4		2025-06-24T03:00:00	78.97920	9.50636	211.7	LIGHT	Station end	
PS148_32-1		2025-06-24T07:01:00	79.13303	6.09172	1240.8	AUV_lab	Station start	
PS148_32-1		2025-06-24T14:45:00	79.10487	6.31719	1220.5	AUV_lab	Station end	
PS148_32-3		2025-06-24T08:45:00	79.13293	6.09476	1238.9	HN	Station start	
PS148_32-3		2025-06-24T08:48:00	79.13276	6.09605	1239.5	HN	Station end	
PS148_32-2		2025-06-24T09:06:00	79.13115	6.10067	1241.3	OFOBS	Station start	
PS148_32-2		2025-06-24T12:26:00	79.11736	6.17051	1229.7	OFOBS	Station end	
PS148_32-4		2025-06-24T09:22:00	79.12978	6.11007	1236.4	OOSS	Station start	
PS148_32-4		2025-06-24T09:35:00	79.12861	6.11375	1231.9	OOSS	Station end	
PS148_33-1		2025-06-24T17:15:00	79.07549	4.12568	2435.0	BCRAWL_III	Station start	

Event label	Optional label	Date/Time	Latitude	Longitude	Depth [m]	Gear	Action	Comment *
PS148_33-1		2025-06-24T22:11:00	79.07867	4.09538	2449.6	BCRAWL_III	Station end	
PS148_33-2		2025-06-24T22:47:00	79.03188	4.22718	2531.2	B_LANDER	Station start	
PS148_33-2		2025-06-24T22:51:00	79.03142	4.22731	2532.4	B_LANDER	Station end	
PS148_34-1		2025-06-25T00:33:00	79.06085	3.58382	3471.9	CTD-RO	max depth	
PS148_34-2		2025-06-25T00:37:00	79.06094	3.58527	3471.6	OOSS	max depth	cancelled due to bad optical condition (clouds)
PS148_34-3		2025-06-25T02:09:00	79.05944	3.57411	3538.1	LIGHT	Station start	
PS148_34-3		2025-06-25T03:03:00	79.05957	3.57228	3537.0	LIGHT	Station end	
PS148_35-1		2025-06-25T11:20:00	79.13047	6.10350	1241.0	LOKI	Station start	
PS148_35-1		2025-06-25T12:31:00	79.13381	6.09911	1243.1	LOKI	Station end	
PS148_35-2		2025-06-25T12:42:00	79.13281	6.09081	1239.4	MSN	Station start	
PS148_35-2		2025-06-25T14:00:00	79.13470	6.09050	1240.4	MSN	Station end	
PS148_35-3		2025-06-25T14:01:00	79.13470	6.09062	1241.5	MSN	Station start	

Event label	Optional label	Date/Time	Latitude	Longitude	Depth [m]	Gear	Action	Comment *
PS148_35-3		2025-06-25T15:44:00	79.13326	6.09350	1239.3	MSN	Station end	
PS148_35-4		2025-06-25T15:47:00	79.13329	6.09290	1240.4	WP2	Station start	
PS148_35-4		2025-06-25T16:18:00	79.13365	6.09428	1239.3	WP2	Station end	
PS148_35-5		2025-06-25T17:07:00	79.13344	6.09557	1238.9	CTD-RO	max depth	
PS148_35-6		2025-06-25T18:03:00	79.13333	6.09519	1239.9	LIGHT	Station start	
PS148_35-6		2025-06-25T19:18:00	79.13304	6.09036	1238.2	LIGHT	Station end	
PS148_35-7		2025-06-25T19:48:00	79.13306	6.09027	1239.0	GKG	max depth	
PS148_35-8		2025-06-26T00:13:00	79.13405	6.09274	1241.2	MUC	max depth	
PS148_35-9		2025-06-26T01:13:00	79.13402	6.09647	1242.9	GKG	max depth	
PS148_36-2		2025-06-26T03:22:00	79.13030	4.90277	1506.1	HN	Station start	
PS148_36-2		2025-06-26T03:24:00	79.13037	4.90263	1506.4	HN	Station end	
PS148_36-1		2025-06-26T03:56:00	79.13058	4.90199	1506.3	CTD-RO	max depth	

Event label	Optional label	Date/Time	Latitude	Longitude	Depth [m]	Gear	Action	Comment *
PS148_36-3		2025-06-26T04:10:00	79.13052	4.90154	1505.2	OOSS	Station start	
PS148_36-3		2025-06-26T04:30:00	79.13013	4.90251	1507.9	OOSS	Station end	
PS148_36-4		2025-06-26T05:06:00	79.13065	4.89780	1508.7	LIGHT	Station start	
PS148_36-4		2025-06-26T06:13:00	79.13023	4.90127	1506.3	LIGHT	Station end	
PS148_36-5		2025-06-26T06:59:00	79.12990	4.90185	1508.3	GKG	max depth	
PS148_36-6		2025-06-26T08:14:00	79.12986	4.90354	1507.5	MUC	max depth	
PS148_36-7		2025-06-26T09:22:00	79.12978	4.90227	1510.2	GKG	max depth	
PS148_37-1		2025-06-26T14:26:00	78.61689	5.00844	2301.8	OFOBS	Station start	
PS148_37-1		2025-06-26T17:03:00	78.61713	5.12163	2280.6	OFOBS	Station end	
PS148_37-2		2025-06-26T18:11:00	78.61727	5.13246	2287.1	CTD-RO	max depth	

**Comments are limited to 130 characters. See https://www.pangaea.de/expeditions/events/PS148 to show full comments in conjunction with the station (event) list for expedition PS148.*

Abbreviation	Method/Device
ADCP	Acoustic Doppler Current Profiler
AUV_lab	Autonomous underwater vehicle PAUL
BCRAWL_III	Autonomous benthic crawler system CRAWLER-III
B_LANDER	Bottom lander
CT	Underway cruise track measurements
CTD-RO	CTD/Rosette
EBS	Epibenthic sledge
FBOX	FerryBox
GKG	Giant box corer
HN	Hand net
LIGHT	Light profiler
LOKI	Light frame on-sight keyspecies investigation
MBES	Multibeam echosounder
MOOR	Mooring
MSN	Multiple opening/closing net
MUC	MultiCorer
OFOBS	Ocean Floor Observation and Bathymetry System
OOSS	Ocean optics spectrometer system
PS	ParaSound
SWEAS	Ship Weather Station
TRAMPER	TRAMPER
TSG	Thermosalinograph
TVMUC	Multicorer with television
WP2	WP-2 towed closing plankton net
pCO2	pCO2 sensor

Die **Berichte zur Polar- und Meeresforschung** (ISSN 1866-3192) werden beginnend mit dem Band 569 (2008) als Open-Access-Publikation herausgegeben. Ein Verzeichnis aller Bände einschließlich der Druckausgaben (ISSN 1618-3193, Band 377-568, von 2000 bis 2008) sowie der früheren **Berichte zur Polarforschung** (ISSN 0176-5027, Band 1–376, von 1981 bis 2000) befindet sich im electronic Publication Information Center **(ePIC)** des Alfred-Wegener-Instituts, Helmholtz-Zentrum für Polar- und Meeresforschung (AWI); see https://epic.awi.de. Durch Auswahl “Reports on Polar- and Marine Research“ (via “browse”/”type”) wird eine Liste der Publikationen, sortiert nach Bandnummer, innerhalb der absteigenden chronologischen Reihenfolge der Jahrgänge mit Verweis auf das jeweilige pdf-Symbol zum Herunterladen angezeigt.

The **Reports on Polar and Marine Research** (ISSN 1866-3192) are available as open access publications since 2008. A table of all volumes including the printed issues (ISSN 1618-3193, Vol. 377-568, from 2000 until 2008), as well as the earlier **Reports on Polar Research** (ISSN 0176-5027, Vol. 1–376, from 1981 until 2000) is provided by the electronic Publication Information Center **(ePIC)** of the Alfred Wegener Institute, Helmholtz Centre for Polar and Marine Research (AWI); see URL https://epic.awi.de. To generate a list of all Reports, use the URL http://epic.awi.de and select “browse”/”type” to browse ”Reports on Polar and Marine Research”. A chronological list in declining order will be presented, and pdf-icons displayed for downloading.

Zuletzt erschienene Ausgaben:

Recently published issues:

803 (2025) The Expedition PS148 of the Research Vessel POLARSTERN to the Arctic Ocean in 2025. Edited by Jennifer Dannheim with contributions of the participants.

802 (2025) Arctic Land Expeditions in Permafrost Research in 2024. Edited by Anne Morgenstern, Lutz Schirrmeister and Milena Gottschalk with contributions of the participants.

801 (2025) The Expedition PS143/2 of the Research Vessel POLARSTERN to the Arctic Ocean in 2024. Edited by Katja Metfies with contributions of the participants.

800 (2025) The Expedition PS143/1 of the Research Vessel POLARSTERN to the Arctic Ocean in 2024. Edited by Frank Wenzhöfer with contributions of the participants.

799 (2025) The Expeditions PS147/1 and PS147/2 of the Research Vessel POLARSTERN to the Atlantic Ocean in 2025. Edited by Yvonne Schulze Tenberge and Björn Fiedler with contributions of the participants.

798 (2025) The Expedition PS146 of the Research Vessel POLARSTERN to the Weddell Sea in 2024/2025. Edited by Olaf Boebel with contributions of the participants.

797 (2025) Arctic Land Expeditions in Permafrost Research in 2023. Edited by Anne Morgenstern and Milena Gottschalk with contributions of the participants.

796 (2025) Expeditions to Antarctica: ANT-Land 2023/24 NEUMAYER STATION III, Kohnen Station and Field Campaigns. Edited by Julia Regnery, Tim Heitland and Christine Wesche with contributions of the participants.

795 (2025) The Expeditions PS145/1 and PS145/2 of the Research Vessel POLARSTERN to the Atlantic Ocean in 2024, edited by Claudia Hanfland and Natalie Cornish with contributions of the participants.

ALFRED-WEGENER-INSTITUT
HELMHOLTZ-ZENTRUM FÜR POLAR-
UND MEERESFORSCHUNG

BREMERHAVEN

Am Handelshafen 12
27570 Bremerhaven
Telefon 0471 4831-0
Telefax 0471 4831-1149
www.awi.de

HELMHOLTZ